



Review

Monitoring Water Diversity and Water Quality with Remote Sensing and Traits

Angela Lausch^{1,2,3,4,*} , Lutz Bannehr⁴, Stella A. Berger⁵ , Erik Borg^{6,7} , Jan Bumberger^{8,9,10} , Jorg M. Hacker^{11,12} , Thomas Heege¹³, Michael Hupfer^{14,15}, András Jung¹⁶ , Katja Kuhwald¹⁷ , Natascha Oppelt¹⁷ , Marion Pause⁴ , Franziska Schrodt¹⁸, Peter Selsam⁸ , Fabian von Trentini¹³, Michael Vohland^{10,19} and Cornelia Glässer³

- ¹ Department of Computational Landscape Ecology, Helmholtz Centre for Environmental Research-UFZ, Permoserstr. 15, D-04318 Leipzig, Germany
- ² Landscape Ecology Lab, Geography Department, Humboldt-Universität zu Berlin, Unter den Linden 6, D-10099 Berlin, Germany
- ³ Department of Physical Geography and Geoecology, Martin Luther University Halle-Wittenberg, Von-Seckendorff-Platz 4, D-06120 Halle, Germany; cornelia.glaesser@geo.uni-halle.de
- ⁴ Department of Architecture, Facility Management and Geoinformation, Institute for Geo-Information and Land Surveying, Anhalt University of Applied Sciences, Seminarplatz 2a, D-06846 Dessau, Germany; l.bannehr@afg.hs-anhalt.de (L.B.); marion.pause@hs-anhalt.de (M.P.)
- ⁵ Department of Plankton and Microbial Ecology, Leibniz Institute of Freshwater Ecology and Inland Fisheries, Zur alten Fischerhütte 2, D-16775 Stechlin, Germany; stella.berger@igb-berlin.de
- ⁶ German Aerospace Center, German Remote Sensing Data Center, National Ground Segment, Kalkhorstweg 53, D-17235 Neustrelitz, Germany; erik.borg@dlr.de
- ⁷ Faculty of Landscape Sciences and Geoinformatics, University of Applied Sciences, Brodaer Str. 2, D-17033 Neubrandenburg, Germany
- ⁸ Department of Monitoring and Exploration Technologies, Helmholtz Centre for Environmental Research-UFZ, Permoserstr. 15, D-04318 Leipzig, Germany; jan.bumberger@ufz.de (J.B.); peter.selsam@ufz.de (P.S.)
- ⁹ Research Data Management—RDM, Helmholtz Centre for Environmental Research-UFZ, Permoserstr. 15, D-04318 Leipzig, Germany
- ¹⁰ German Centre for Integrative Biodiversity Research (iDiv) Halle-Jena-Leipzig, Puschstraße 4, D-04103 Leipzig, Germany; michael.vohland@uni-leipzig.de
- ¹¹ College of Science and Engineering, Flinders University, Adelaide, SA 5000, Australia
- ¹² Airborne Research Australia (ARA), Parafield Airport, Adelaide, SA 5106, Australia; jorg.hacker@airborneresearch.org.au
- ¹³ EOMAP GmbH & Co KG, Schlosshof 4a, D-82229 Seefeld, Germany; heege@eomap.de (T.H.); trentini@eomap.de (F.v.T.)
- ¹⁴ Department of Ecohydrology and Biogeochemistry, Leibniz Institute of Freshwater Ecology and Inland Fisheries, Müggelseedamm 301, D-12587 Berlin, Germany; michael.hupfer@igb-berlin.de
- ¹⁵ Department of Aquatic Ecology, Brandenburg Technical University Cottbus-Senftenberg, Seestr. 45, D-15526 Bad Saarow, Germany
- ¹⁶ Faculty of Informatics, Institute of Cartography and Geoinformatics, Eötvös Loránd University, Pázmány Péter sétány 1/A, H-1117 Budapest, Hungary; jung@inf.elte.hu
- ¹⁷ Department of Geography, Christian-Albrechts-University of Kiel, Ludewig-Meyn-Str. 8, D-24098 Kiel, Germany; katja.kuhwald@geographie.uni-kiel.de (K.K.); oppelt@geographie.uni-kiel.de (N.O.)
- ¹⁸ School of Geography, University of Nottingham, University Park, Nottingham NG7 2RD, UK; franziska.schrodt1@nottingham.ac.uk
- ¹⁹ Geoinformatics and Remote Sensing, Institute of Geography, University of Leipzig, Johannisallee 19a, D-04103 Leipzig, Germany
- * Correspondence: angela.lausch@ufz.de; Tel.: +49-341-235-1961; Fax: +49-341-235-1939



Citation: Lausch, A.; Bannehr, L.; Berger, S.A.; Borg, E.; Bumberger, J.; Hacker, J.M.; Heege, T.; Hupfer, M.; Jung, A.; Kuhwald, K.; et al. Monitoring Water Diversity and Water Quality with Remote Sensing and Traits. *Remote Sens.* **2024**, *16*, 2425. <https://doi.org/10.3390/rs16132425>

Academic Editor: Hatim Sharif

Received: 27 May 2024

Revised: 23 June 2024

Accepted: 27 June 2024

Published: 1 July 2024



Copyright: © 2024 by the authors. Licensee MDPI, Basel, Switzerland. This article is an open access article distributed under the terms and conditions of the Creative Commons Attribution (CC BY) license (<https://creativecommons.org/licenses/by/4.0/>).

Abstract: Changes and disturbances to water diversity and quality are complex and multi-scale in space and time. Although in situ methods provide detailed point information on the condition of water bodies, they are of limited use for making area-based monitoring over time, as aquatic ecosystems are extremely dynamic. Remote sensing (RS) provides methods and data for the cost-effective, comprehensive, continuous and standardised monitoring of characteristics and changes in characteristics of water diversity and water quality from local and regional scales to the scale of entire continents. In order to apply and better understand RS techniques and their derived spectral indicators in monitoring water diversity and quality, this study defines five characteristics of water

diversity and quality that can be monitored using RS. These are the diversity of water traits, the diversity of water genesis, the structural diversity of water, the taxonomic diversity of water and the functional diversity of water. It is essential to record the diversity of water traits to derive the other four characteristics of water diversity from RS. Furthermore, traits are the only and most important interface between in situ and RS monitoring approaches. The monitoring of these five characteristics of water diversity and water quality using RS technologies is presented in detail and discussed using numerous examples. Finally, current and future developments are presented to advance monitoring using RS and the trait approach in modelling, prediction and assessment as a basis for successful monitoring and management strategies.

Keywords: water diversity; water quality; traits; earth observation; remote sensing; water trait diversity; water genesis diversity; water structural diversity; water taxonomic diversity; water functional diversity

1. Introduction

The sea, inland waters and rivers are crucial to the life and survival of all individuals and fulfil central functions in our aquatic and wider ecosystems [1]. They provide habitats and critical niches for a wide range of species and are essential components of water, carbon and nutrient cycles [2]. However, land use intensity (LUI), climate change, urbanisation and tourism are leading to major changes and even the complete destruction of the ecological functions and resilience of water bodies due to multiple interacting stress factors [3,4]. Local to global changes in the world's freshwater ecosystems are already apparent due to physical, chemical and biological changes [5], such as the biotic homogenisation of algae in watersheds (i.e., the decreasing differences in taxonomic and functional characteristics of algal communities) [6], the influence of microplastics [7,8], the effect in antibiotics [9], the increase in browning [10] or the increase in eutrophication and excess nitrogen in water bodies [11]. Many studies assume that the productivity of aquatic ecosystems will increase as a result of global warming [12–15] due to increased nutrient inputs and the intensification of internal nutrients. However, changes in stratification due to warming can also lead to (longer) interruptions to internal nutrient cycling. It is also evident that species respond very differently to, for example, heat stress in water bodies [16]. This requires a well-founded differentiation of species and knowledge of phylogeny, the entire aquatic ecosystem and its influencing factors in order to better understand the responses of organisms and ecosystems to environmental change.

Numerous national and international guidelines have been developed, such as the Water Framework Directive in Europe (https://environment.ec.europa.eu/topics/water/water-framework-directive_en, accessed on 26 June 2024), the US Clean Water Act (<https://www.epa.gov/sites/default/files/2017-08/documents/federal-water-pollution-control-act-508full.pdf>, accessed on 26 June 2024), the National Water Management Strategy of Australia and New Zealand (<https://www.waterquality.gov.au/sites/default/files/documents/nwqms-charter.pdf>, accessed on 26 June 2024), the Canada Water Act (<https://laws-lois.justice.gc.ca/eng/acts/c-11/>, accessed on 26 June 2024), and the International Initiative on Water Quality (IIWQ) of UNESCO's International Hydrological Programme (IHP) (<https://www.unesco.org/en/iwp>, accessed on 26 June 2024), which aim to maintain and sustainably improve the ecological status of water bodies. Improving water quality is one of the world's greatest societal challenges and is, therefore, a key issue in the UN 2030 Agenda for Sustainable Development Goal 6: "Ensure availability and sustainable management of water and sanitation for all". Strategies and actions to achieve this goal require the coherent measurement, analysis and visualisation of water quality from regional to global scales. The GlobeWQ project (<https://www.globewq.info/>, accessed on 26 June 2024) is embedded in the World Water Quality Alliance, led by the UN Environment Programme, with the challenging task of producing a World Water Quality Assessment of current and

future freshwater quality. A common goal of these guidelines is to improve water quality by identifying pollutants and implementing sustainable management strategies that can be achieved through continuous monitoring of all water bodies [17–19]. Current monitoring programmes use labour-intensive, costly and time-consuming in situ methods such as distributed sampling, analysis, point measurements or other comparable methods. Although these provide detailed information on the physical, chemical and biological status of water bodies, their local and selective monitoring and low temporal resolution can lead to inaccurate assessments and, consequently, a false categorisation of water quality [20,21]. The temporal and spatial variability of phenomena and ongoing processes and changes, as well as disturbances caused by, for example, short-lived cyanobacteria or phytoplankton blooms in water bodies, cannot be sufficiently monitored by infrequent in situ point sampling measurements [22,23].

To gain an ecosystem-level understanding of water bodies and the role of lakes “as sentinels, integrators and regulators of climate change” [24], there is an urgent global need for long-term monitoring approaches that can capture standardised and transferable spatio-temporal monitoring of water status, quality and change [21]. Ecologists have repeatedly proposed the use of remote sensing (RS) for monitoring water diversity and water quality and coupling it with locally conducted in situ measurements to take advantage of both area-scale RS information and local measurements [25]. Complementary approaches such as the synergistic use of innovative RS technologies, in situ sensors and measurements, databases and modelling approaches are required to provide an assessment of the ecosystem integrity of water status and its health [25,26].

RS techniques are already being used to successfully monitor, model and assess terrestrial ecosystem properties such as vegetation diversity [27,28], geodiversity [29–31], geomorpho-diversity [32] and hydrology [33] to assess the quality and support the sustainable management of marine and coastal protected areas [34]. For some time now, various water characteristics and water quality indicators have been used, such as turbidity, chlorophyll-a, harmful algal bloom indicators and total absorption (IIWQ World Water Quality Information and Capacity Building Portal, <https://www.eomap.com/world-water-quality/about-iiwq-portal/>, accessed on 26 June 2024), which have been merged as global datasets based on different RS time series from RS missions such as Landsat and Copernicus or hyperspectral RS satellites (e.g., EnMAP and PRISMA) (<https://climate.esa.int/en/projects/lakes/>, accessed on 26 June 2024). Recent technological developments and satellite missions such as the DLR Earth Sensing Imaging Spectrometer (DESI, [35]), the hyperspectral Environmental Mapping and Analysis Programme (EnMap, [36]) and the first space-based GEDI Ecosystem LiDAR [37] or ICESat-2 [38] are now available and largely free of charge. They help us to gain a deeper understanding of the processes and to specifically monitor water heat, water properties, processes and interactions. NASA’s future Surface Biology and Geology (SBG) missions (<https://sbg.jpl.nasa.gov/>, accessed on 26 June 2024) with the Hyperspectral Infrared Imager (HyspIRI) will be particularly important for RS-based monitoring of water quality, as the sensor combination of hyperspectral and the Thermal Infrared RS (TIR) will simultaneously record and continuously monitor various water quality characteristics as well as additional vegetation and geodiversity characteristics on local to global scales [39].

The basic reason why RS can capture changes in water quality characteristics is that the spectral reflectance and absorption of pixels in an optical RS image is the result of complex interactions between light (the atmosphere); the water surface; the genesis; and optical, biochemical–biophysical, morphological, physiological, phenotypical, structural, taxonomic and functional characteristics of water and its constituents, such as phytoplankton [40] and water quality [41], vegetation [42], geodiversity [30,32] and their interactions [43]. The basis of the trait approach is the Spectral Variation Hypothesis (SVH) approach [44]. The Spectral Variation Hypothesis states that the pixel-to-pixel variability of the spectral response in an RS image is determined by several factors, such as environmental diversity, the diversity of biochemical and structural characteristics, e.g., leaf

and canopy properties, as well as functional vegetation properties and their responses through interactions with the topography, soil and geodiversity as an expression of the integrability of the spectral signal and its changes [44]. RS can capture traits and trait variations. Therefore, traits are crucial indicators and proxies of terrestrial and aquatic status, opportunities, disturbances and resource limitations. They are also a crucial link between in situ and RS monitoring approaches [45]. Therefore, RS and the traits approach are appropriate for assessing changes to water diversity and water quality.

The traits approach for water has already been mentioned by numerous studies in the past, but they mainly refer to in situ measurements [41,46–51]. The traits approach is crucial for a better understanding of why organisms live where they do and how they respond to environmental change [52]. To date, trait approaches with RS have only been in the context of terrestrial vegetation diversity [45,53,54], forest health [55–57], geodiversity (soil characteristics [31], geomorphology, [32], urban intensity [58] or social-ecological systems [59].

Therefore, the aims of this paper are as follows: (i) to apply the RS-based traits approach to aquatic and marine systems for the first time. For this purpose, five characteristics of aquatic diversity have been defined, namely: the diversity of water traits, the diversity of water genesis, the structural diversity of water, the taxonomic diversity of water and the functional diversity of water; (ii) to illustrate how RS technologies can monitor these five traits of water diversity; (iii) to summarise the characteristics of water diversity; and (iv) to discuss the future opportunity of an integrative approach and application of traits and RS to integrate a more focused RS and trait approach into water quality assessment and sustainable management.

2. Definition and Standards of Water Quality and Water Characteristics

The assessment of water quality is based on a set of definitions and standards established by various organisations. Monitoring of water quality and water characteristics is often conducted by in situ measurements, but the specific tests and measurements used will depend on the water's intended use for rivers, lakes, groundwater or drinking water. Here are some of the key parameters and definitions that are commonly used:

Physical characteristics: These relate to parameters such as light (Photosynthetically Available Radiation—PAR), temperature (thermal stratification), conductivity, transparency, colour, turbidity (clarity) and total suspended solids. The presence of suspended materials such as clay, silt, fine organic material, plankton and other inorganic materials in water is referred to as turbidity, which is a measure of water clarity. For example, the oxygen saturation in water depends on the temperature, and a higher level of turbidity can indicate pollution (Environmental Protection Agency (EPA), https://www.epa.ie/pubs/advice/water/quality/Water_Quality.pdf, accessed on 26 June 2024).

Chemical characteristics: These include parameters such as pH; hardness; alkalinity; salinity; nutrients; dissolved organic carbon; anions such as chloride and sulphate; and cations such as calcium, sodium, magnesium, iron and manganese and the concentration of dissolved oxygen. Nutrients such as nitrogen, phosphorus and silicon are measured to estimate the eutrophication level [60]. The presence and concentration of chemicals that can be harmful to humans or ecosystems are also included, such as heavy metals or persistent organic pollutants (US Geological Survey, <https://www.usgs.gov/>, accessed on 26 June 2024).

Biological characteristics: These refer to the microbial quality of water, such as the presence and quantities of bacteria, viruses, microalgae, fungi and other microorganisms. Certain types of bacteria (e.g., *Escherichia coli*) are used as indicators of water pollution, especially from faecal sources (World Health Organization, <https://www.who.int/publications/i/item/9789241549950>, accessed on 26 June 2024).

Ecological characteristics/bioindicators: Certain species of animals (insect larvae, snails, mussels, amphibians and fish) and/or plants (cyanobacteria, microalgae, submerged macrophytes and reeds) serve as bioindicators of the state of an ecosystem. The presence or

absence of species and changes in their populations can provide important information on the condition and changes to the water body and its environmental conditions and anthropogenic influences [60].

Standards and Guidelines

The recording of water quality and water properties is based on various standards and guidelines that are defined by several international organisations and frameworks. These organisations and guidelines significantly shape the way in which water properties and water quality are recorded and assessed worldwide. They provide frameworks to protect and promote both environmental impacts and human health. Here are some of the most important organisations and their associated guidelines:

3. Definition of Water Diversity Using Remote Sensing

The recording of water quality and thus water constituents is one of the most frequently requested RS applications. Due to the immense scale of the area to be monitored worldwide, the integration of RS technologies into a water monitoring system was not put into practice until the early 1980s [61]. However, RS approaches represent a target-oriented approach to monitor the properties and changes to water quality based on the following criteria:

RS can capture the traits and trait variations of water characteristics and water quality as well as those of plants, vegetation, geodiversity, geomorphology and land use intensity. Consequently, RS-based water quality monitoring can monitor not only water quality traits but also the terrestrial compartments of geodiversity and vegetation diversity and take into account the process interactions and drivers of water quality. The spectral reflectance and absorption of pixels are the result of interactions between light (the atmosphere), phylogenetic/genesis, biophysical, biochemical, physical, morphological, physiological, phenotypic, structural, taxonomic and functional traits of the captured characteristics of water, vegetation and geodiversity, as well as their interactions between vegetation diversity and geodiversity [42,43].

The traits approach forms the basis for the in situ monitoring [41] and RS monitoring of water quality and is therefore a crucial link between the two monitoring approaches [45]. Therefore, in the context of monitoring water diversity and water quality using RS, a new definition of monitoring water diversity and quality is required.

Water diversity can be described by its five characteristics, namely: the diversity of water traits, the diversity of water genesis, the structural diversity of water, the taxonomic diversity of water and the functional diversity of water (modified after Lausch et al. [62]). These five characteristics of water diversity exist on all spatial and temporal scales and can be defined as follows (modified after Lausch et al. [32]):

- (I) The diversity of water traits, which represents the diversity of the biochemical-, physical, optical, morphological-, structural-, textural- and functional characteristics of water traits that affect, interact with or are influenced by their genesis-, taxonomic-, structural- and functional diversity;
- (II) The diversity of water genesis, which refers to the diversity of the length of evolutionary pathways associated with a particular set of water traits, taxa, structures and functions of water diversity. Therefore, groups of water traits, water taxa, water structures and water functions that maximise the accumulation of functional diversity of water diversity are identified;
- (III) The structural diversity of water, namely, the diversity of the composition and configuration of water characteristics;
- (IV) The taxonomic diversity of water, representing the diversity of water components that differ from a taxonomic perspective;
- (V) The functional diversity of water, which is the diversity of water functions and processes, as well as their intra- and interspecific interactions.

A clear separation and assignment of the five characteristics of water diversity monitored by RS is not always possible but nevertheless helps to monitor, assign and assess the

various indicators derived with RS, as well as to understand the links between in situ and RS approaches [62].

4. Approaches for Monitoring Water Diversity and Water Quality

There are two methods for monitoring water characteristics and water diversity, as well as its properties, health and changes. These are in situ/field observations and the RS approach (see Figure 1).

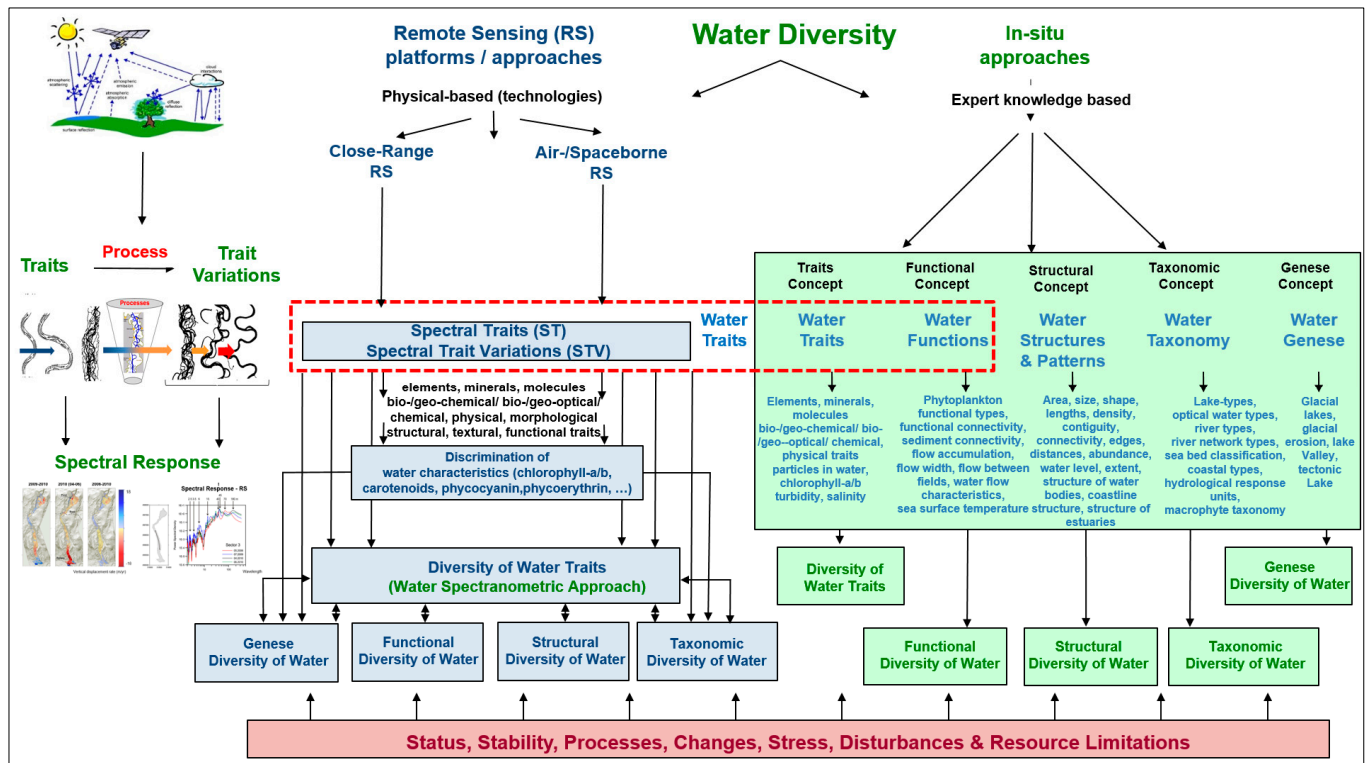


Figure 1. In situ and remote-sensing approaches and the five characteristics of water diversity (diversity of water traits, diversity of water genesis, structural diversity of water, taxonomic diversity of water and functional diversity of water). Diversity of water traits is the most important link between in situ and RS monitoring approaches (modified after Lausch et al. [32]).

4.1. In Situ Approaches

In situ monitoring refers to the direct expert recording, identification and monitoring of changes to water characteristics (traits), their diversity and health. Alexander von Humboldt was one of the first to adopt a holistic and standardised approach to in situ monitoring, in which the traits and processes of hydro-, geo- and biodiversity were observed, compared and evaluated, and their interactions and feedback mechanisms were recorded [63–65]. Organisations and guidelines (see Table 1) have a decisive influence on the way in which water properties and water quality are recorded and evaluated in a standardised manner worldwide (see Table A1, Appendix A).

In situ water quality monitoring is based on sampling and on-site observations. Increasingly, however, in situ measurements are also supported by reagent-free, low-maintenance, autonomous and continuous monitoring sensors and aquatic wireless sensor networks (WSN) ([66–68], such as the GLEON network (Global Lake Ecological Observatory Network) <https://gleon.org/> accessed on 26 June 2024). Furthermore, low-cost automated GPS, electrical conductivity and temperature sensing devices and Android platforms for water quality monitoring are also used [69]. Recently, trait-based approaches have also been increasingly used for in situ monitoring to investigate and evaluate, e.g., short- and long-term phytoplankton dynamics and the establishment of phytoplankton communities

in freshwater and marine research. There are some image-based efforts for more automated plankton analyses (see [70]). These are based on trait-based approaches, which are currently spreading rapidly [41,46,71].

Table 1. Standards and guidelines, recognised organisations and frameworks for monitoring water properties and water quality.

Organisation	Guidelines	Link
World Health Organisation (WHO):	<ul style="list-style-type: none"> ○ The WHO sets guidelines for drinking water quality, which include standards for microbiological, chemical and radiological parameters. ○ These guidelines serve as the basis for national legislation and standards for drinking water quality worldwide. 	https://www.who.int/publications/i/item/9789241549950 , accessed on 26 June 2024
U.S. Environmental Protection Agency (EPA):	<ul style="list-style-type: none"> ○ The EPA provides extensive regulations and standards for water quality in the U.S., including the Safe Drinking Water Act and the Clean Water Act. ○ These include limit values for impurities in drinking water and standards for surface water. 	https://www.epa.ie/pubs/advice/water/quality/Water_Quality.pdf , accessed on 26 June 2024
European Union (EU):	<ul style="list-style-type: none"> ○ The EU Water Framework Directive (WFD) is a key document that aims to bring all bodies of water (rivers, lakes, coastal waters and groundwater) to a “good status”. ○ The EU also lays down specific guidelines for drinking water and bathing water. 	https://environment.ec.europa.eu/topics/water/water-framework-directive_en , accessed on 26 June 2024
International Organisation for Standardisation (ISO):	<ul style="list-style-type: none"> ○ ISO offers various standards for water quality, including methods for testing and analysing water. ○ Examples include ISO 14046 for the water footprint and various ISO standards for analysing specific contaminants. 	https://www.iso.org/home.html , accessed on 26 June 2024
American Public Health Association (APHA):	<ul style="list-style-type: none"> ○ APHA publishes the “Standard Methods for the Examination of Water and Wastewater”, a comprehensive manual containing standardised laboratory procedures for the analysis of water quality. 	https://www.apha.org/ , accessed on 26 June 2024
European Union (EU) Water Framework Directive (WFD)	<ul style="list-style-type: none"> ○ Citizens, nature and industry all need healthy rivers and lakes, groundwater and bathing waters. The Water Framework Directive (WFD) focuses on ensuring good qualitative and quantitative health, i.e., on reducing and removing pollution and on ensuring that there is enough water to support wildlife at the same time as human needs. ○ Finland is one of the few countries to have switched to RS-based national monitoring. 	https://environment.ec.europa.eu/topics/water/water-framework-directive_en , accessed on 26 June 2024

Despite the increasing amount of in situ data and the development of water quality databases such as GEMStat (<https://gemstat.org>, accessed on 26 June 2024), as well as the increasing free availability of these data, the spatial and temporal continuous resolution of in situ data has so far been insufficient to provide comprehensive information and assessments of water quality from the local to the regional and the global scale [25]. Monitoring programmes or in situ buoys are often at one location in a lake, i.e., the point where the

lake is deepest. This should then represent the whole lake, which is often not the case. Furthermore, these are often conducted in low-income countries and in regions known for their lack of policies for permanent in situ monitoring. The inclusion of areal RS data, as well as water quality modelling that provides relationships between water quality status and its influencing factors, such as agricultural practices and/or the discharge of untreated municipal wastewater, can close this gap [25].

In order to optimally incorporate airborne and spaceborne RS data for monitoring water quality, RS data must be validated by standardised in situ monitoring networks to monitor bio-geo-optical traits and the diversity of inland and coastal waters. For example, the GLObal Reflectance Community Dataset for Imaging and Optical Sensing of Aquatic Environments (GLORIA) provides an important dataset of 7572 local hyperspectral RS reflectance measurements, which were measured in 1 nm intervals in the wavelength range from 350 to 900 nm and distributed globally. In this dataset, in addition to spectral measurements, at least one measurement of water quality (chlorophyll-a, total suspended solids, dissolved solids absorption and Secchi depth) is also monitored and provided [72].

The optical complexity of coastal and inland waters with different trophic states is challenging for RS, especially for the retrieval of phytoplankton functional or pigment groups, and therefore requires additional in situ and laboratory measurements for validation [73]. The LakeLab, a large-scale experimental research facility in Lake Stechlin (NE Germany, Figure 2), provides such a unique opportunity for collaboration between aquatic ecologists and remote sensing experts for validation and calibration. The LakeLab is an experimental platform for studying the effects of climate change on aquatic organisms, their interactions and ecological processes in lake ecosystems [74,75]. It consists of a large central enclosure (30 metres in diameter) and 24 experimental units (enclosures), each 9 metres in diameter. All 24 enclosures of the LakeLab and 4 additional stations in Lake Stechlin are equipped with in situ sensors (YSI EXO, LiCor PAR) mounted on automatic profiling systems and provide continuous data from different water depths, including chlorophyll, phycocyanin, phycoerythrin, temperature, oxygen, conductivity, pH and light as PAR. Measurements such as HPLC-based chlorophyll-a and other pigments, image-based flow cytometry (FlowCam, MDPI, Amnis Image Stream) for plankton organisms, nutrients and carbon fractions are performed in the nearby laboratories of the Department of Plankton and Microbial Ecology of the IGB in Stechlin. Several international collaborations with measurement campaigns in the LakeLab have been carried out to characterise key optical properties of water and to understand the formation of the remote sensing signal, to compare and validate remote sensing data (multi- or hyperspectral cameras on satellites, aeroplanes, drones and handheld) with in situ and laboratory measurements in optically diverse and complex water bodies created in the LakeLab (Figure 2), supported by the AQUACOSM project.

4.2. Remote Sensing Approach

All RS technologies are contactless and detect traits and trait variations on and in the water at a distance of a few millimetres to thousands of kilometres. The sensors are used on different RS platforms such as aquatic wireless sensor networks (WSN), underwater cameras on submarines and robots, buoys, ships, drones, and airborne and spaceborne platforms, which use different RS technologies (RGB/photography, multispectral, hyperspectral, thermal, laser, radio/radar, acoustic, and LiDAR (Light Detection and Ranging) installed to monitor water diversity, water quality and traits of geodiversity such as bathymetry and depth of the basic composition of water bodies (see Figure 3). There is already extensive literature describing methodological and sensor technology for recording and monitoring water quality and water characteristics [1,76]; therefore, they are not the subject of this paper.

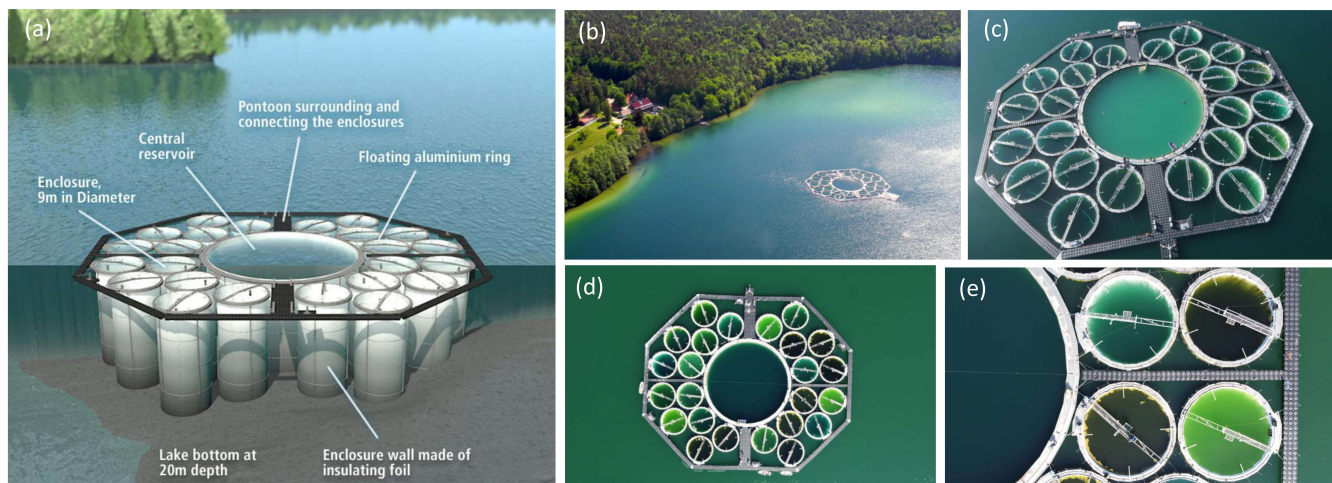


Figure 2. The IGB LakeLab in Stechlin Lake is a large-scale experimental research facility with 24 lake water basins (enclosures), each 9 metres in diameter and approximately 20 metres deep, isolated from the lake by a cylindrical watertight membrane extending from the surface to the natural bottom. The LakeLab can be used to simulate future environmental scenarios and study their effects on lake ecosystems. The LakeLab is well equipped with in-situ sensor profiling systems and is located in close proximity to the IGB laboratories of the Department of Plankton and Microbial Ecology, Stechlin, Germany. The IGB LakeLab also serves as a platform for validation and calibration of in-situ and laboratory measurements with remote sensing products. Graphic (a) shows the 24 enclosures around the central reservoir (Credit: IGB); Aerial photo (b) shows the LakeLab in Lake Stechlin and the laboratories of the Department of Plankton and Microbial Ecology on the shore next to the Federal Weather Station (Credit: Dr. Peter Casper); Drone photo (c) illustrates the size of the LakeLab with people standing on the ring of the central reservoir (Credit: Dr Carmen Cillero, 3edata); Drone photos (d,e) illustrate replicated enclosures treated in four different ways (control, cDOM, nutrients, nutrients + cDOM) and the resulting colours after the additions and the response of the plankton community (credit: Prof. Andreas Jechow).

However, the monitoring of water bodies and their quality using RS poses a challenge compared to terrestrial RS for several reasons: (I) Light absorption and scattering in the water: water absorbs light, especially in deeper layers. This limits the penetration depth of the light and therefore the ability of the sensors to obtain information from deeper water layers. Water also scatters the light, which makes it more difficult to interpret the data recorded by the sensors. (II) Complex reflection patterns: The surface of water bodies can exhibit a variety of reflection patterns caused by waves, sediments, organic materials and other factors. These patterns can affect the accuracy of RS data. (III) Influence of the atmosphere: when passing through the atmosphere, RS signals are altered by water vapour, aerosols and other atmospheric components. All these factors make it difficult to obtain precise information about water quality. Globally consistent and harmonised water quality data from various different sensors can be ensured with physics-based approaches due to their relation to the absorption and scattering properties of water constituents. Other factors should also be considered, namely:

- The spatial and temporal resolution of RS data: many bodies of water change rapidly both spatially and temporally. Sensors with insufficient spatial or temporal resolution may therefore not be able to provide accurate or up-to-date data.
- The heterogeneity of water bodies: water bodies are often heterogeneous in their composition. Different areas of a water body can have different characteristics, which complicates the analysis and interpretation of RS data.
- The spectral signature of substances: various substances in water (such as chlorophyll, dissolved organic matter and sediments) have specific spectral signatures. The precise

identification and quantification of these substances require specialised sensors and complex analysis methods.

- Technical limitations: the available technology, in particular the spectral and spatial resolution of the sensors, as well as the limited availability of validation data sets, limits what can be recorded and analysed.
- Interdisciplinary challenges: the correct interpretation of RS data with regard to water quality often requires a deep understanding of different scientific disciplines, including limnology, oceanography and environmental sciences.

Due to these challenges, the monitoring of water bodies using RS is a complex endeavour that requires ongoing research and development in the fields of sensor technology, data analysis and environmental science. Therefore, as a first step, a new definition of the five characteristics for monitoring water diversity is needed to better understand the RS-based trait approach (see Chapter 3). RS can use proxies to directly or indirectly monitor the different indicators of the five characteristics of water diversity (see Figure 4).

However, to gain a basic understanding of the potential and limitations of RS techniques, the suitability for monitoring the five characteristics of water diversity is discussed in the following chapters.

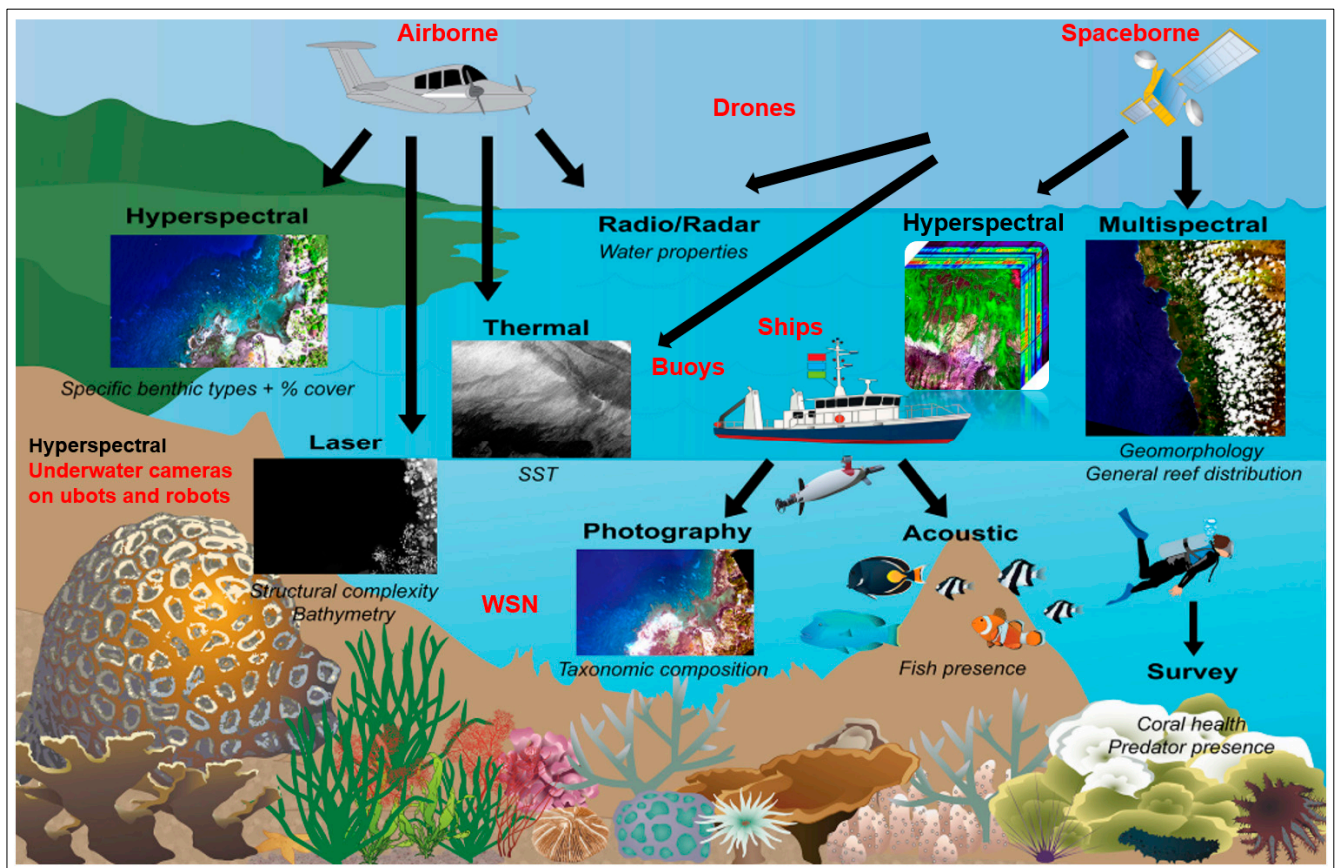


Figure 3. Different RS platforms; aquatic wireless sensor networks (WSN); underwater cameras on submarines and robots, buoys, ships, drones and airborne and spaceborne platforms; and RS technologies (RGB/photography, multispectral, hyperspectral, thermal, laser, radio/radar, acoustic and LiDAR) to capture water quality, water diversity and traits of geodiversity like aquatic geomorphology (bathymetry, depth, basic composition of waters) (from Foo and Asner [77]).

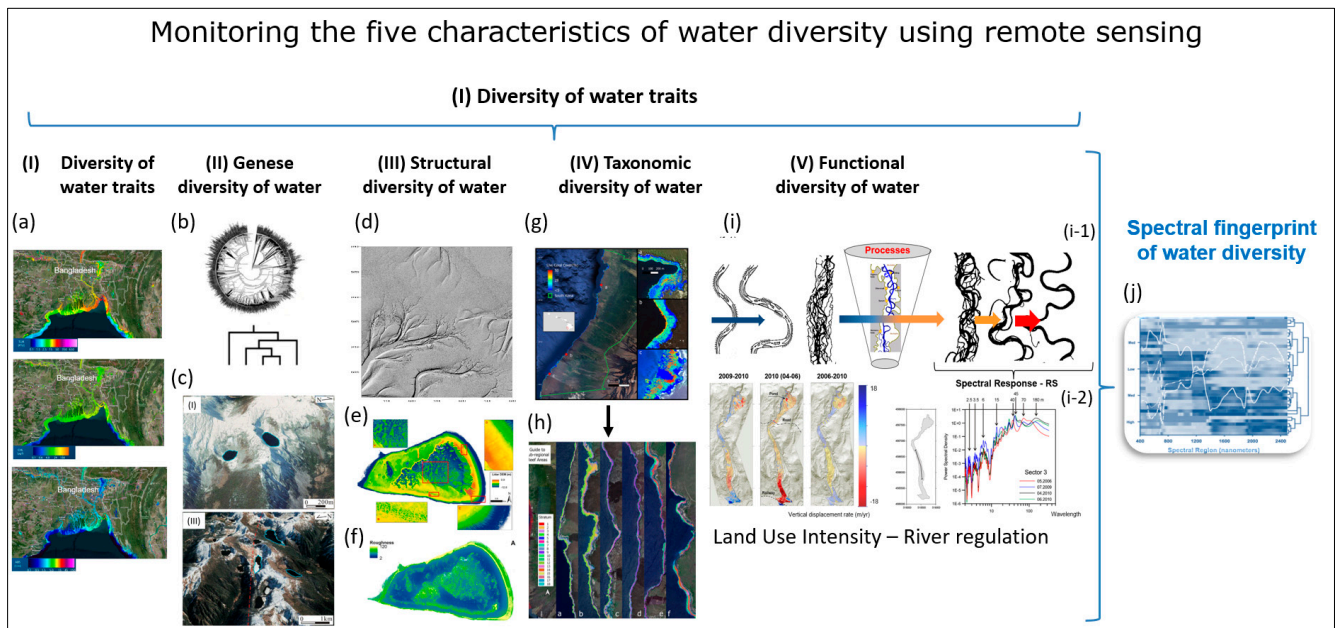


Figure 4. Remote sensing monitoring of the five characteristics of water diversity (see Chapter 3): (I) Diversity of water traits: spectral traits of water diversity monitored with remote-sensing approaches. (a) Monitoring of turbidity, chlorophyll content, ABS Indicator, Bangladesh, India, (<https://aqua.eoapp.de>, accessed on 26 June 2024). (II) Diversity of water genesis: (b) Geological genesis leads to the formation and shaping of different lakes. (c) Classification of glacial lakes based on Landsat TM/OLI and Aster DGM data (I) Glacial erosion lakes and (III) Tectonic lakes (from Weit et al. [78]). (III) Structural diversity of water: (d) Tideways in the Weser River, northeast of Wilhelmshaven, Germany monitored by airborne LiDAR (from Lausch et al. [62]). (e) The LiDAR-derived digital elevation model (DEM) (0.25 m cell-size) for One Tree Reef showing some key features (complex patch reef structure in the deep lagoon) that could not be quantified in the past using a coarse DEM and single beam echo-sounder surveys. (f) Indicator for the maximum roughness magnitude with LiDAR DEM. Figure (e,f) (from Harris et al. [79]). (IV) Water taxonomic diversity: (g) The location of the South Kona District is shown in the green lines on the left, with live coral cover mapped along the coast based on airborne hyperspectral data in 2019 and 2020. Example areas of live coral cover are shown at Honaunau Bay, Papa Bay and Okoe-Kapua Bay (from Asner et al. [80]). (h) The final 18-stratum map of coral reef conditions for the South Kona District coast was derived from the airborne hyperspectral data. The far-left panel indicates the location of each sub-regional zoom image (a–h) shown in the remaining panels. Each colour indicates the location of each ecological layer in the reef system (from Asner et al., [80]). (V) The functional diversity of water: (i) Different processes during the geological genesis lead to the formation of specific morphometric fluvial traits—the meanders. (i-1) The entire river system is characterised by these meanders. Processes/drivers such as land use intensity, river regulations or barrages lead to changes in structural and functional fluvial traits (fluvial trait variations) (i-2). These fluvial trait variations lead to spectral responses in the remote sensing signal. Example of monitoring temporal changes to fluvial traits—vertical displacement rate of the river system from 2006 to 2010 with remote sensing technologies (LiDAR). From Ventura et al. [81], reprinted with permission from Ventura et al. [81], 2021, Elsevier. license No. 5816961386058 (from Lausch et al. [32]). (j) Based on the five characteristics of water diversity, the spectral fingerprint, also known as the spectranometric approach, could be determined for water bodies.

4.2.1. Monitoring the Diversity of Water Traits Using Remote Sensing

“The diversity of water traits, which represents the diversity of the biochemical, physical, optical, morphological-, structural-, textural-, and functional characteristics of water

traits, that affect, interact with, or are influenced by their genesis, taxonomic-, structural-, and water functional diversity” (see Chapter 3, modified after Lausch et al. [32]).

RS records the biochemical, physical, optical, morphological, structural, textural and functional characteristics (traits) of water, ranging from abiotic elements and molecular structures to individuals, populations and communities of aquatic plants to the entire aquatic ecosystem and its connectivity and interactions to components of geological and vegetation diversity. Furthermore, RS records water traits, as well as the trait variations altered by various processes or drivers. For example, river straightening due to the intensification of shipping leads to straightening and alteration of the meandering, which leads to changes in water structure, flow velocity and ecological self-purification. These trait variations can be recorded using RS.

In contrast to in situ approaches carried out by an expert, RS approaches (close-range, airborne and spaceborne RS) are not able to capture all characteristics and trait variations of and within the water column (see limitations, Chapter 4.2). We therefore speak of “spectral water traits” (properties that can be captured by RS) as opposed to “water traits” (total set of water properties) [55]. The reasons why far fewer water traits can be measured using RS are manifold and have already been addressed in Chapter 4.2. However, water traits are the crucial link between in situ and RS approaches for monitoring, assessing and modelling the status, changes, stress, health, disturbances and resource limitations and are crucial for understanding the processes and their diverse interactions with the water ecosystem.

Depending on the respective sensor characteristics (geometric, spectral, radiometric, temporal and angular resolution), RS sensors record the biochemical, physical, optical, morphological, physiological, genesis, structural, textural and functional characteristics (traits) of water. In addition to the sensor traits, the characteristics of the water traits and especially the composition and configuration (e.g., distribution, density, spatio-temporal variability, diversity, etc.) of water traits and their variations are of decisive importance for detectability from RS sensors. If the density is not high enough, it cannot be detected with any sensor if the density is below the detection limit. For example, the detection limit of Sentinel-2 for Chl is around 2 mg-m³ [82].

In the first step, RS records water traits and their variations (depending on RS characteristics and trait distribution). RS can discriminate phytoplankton, algae blooms, aquatic plant species, reef types and waterbody types if they differ from each other in terms of their traits or trait variations (multi-temporal) through process or temporal changes (seasonal changes). Likewise, water traits are the decisive basis for the RS-based quantification of the other four characteristics of water diversity: the genesis diversity, structural diversity, taxonomic diversity and functional diversity of water (see following chapters).

The spectral characteristics of water are recorded by RS either with single traits (chlorophyll-a, phycocyanin, phycoerythrin, salinity, nutrient level and pH value) or as a combination of different spectral traits and their variations (plant strategy types and biomass). For example, the latest generation of hyperspectral satellites (EnMAP, DESIS or multi-source satellite combinations) can be used to estimate the chlorophyll-a concentration in different plant species of water bodies, e.g., for the identification of algal blooms [83,84]. With the use of sensors such as MODIS, MERIS or OLCI (on Sentinel-3), the chlorophyll-a concentration in open marine waters can be estimated with an accuracy of about 10–20% [85]. The pigments phycocyanin and phycoerythrin, which are associated with cyanobacteria and cryptophytes, can be detected very well using RS, allowing an early warning of potentially harmful algal blooms using RS [86]. Furthermore, hyperspectral sensors can be used to estimate turbidity and total suspended solids (TSS) with high accuracy, as they can spectrally separate the effects of TSS from other components [87]. Hyperspectral technology can also be used to differentiate between phytoplankton pigments, phytoplankton functional types (PFTs), including phytoplankton size classes (PSC), phytoplankton taxonomic composition (PTC) and particle size distribution (PSD) [88]. The most recent mission was PACE (Plankton, Aerosol, Cloud, ocean Ecosystem), which was

launched by NASA this year (<https://pace.oceansciences.org/timeline.htm>, accessed on 26 June 2024).

Spectral traits can either be captured by direct indicators (chlorophyll and turbidity) or indirect indicators, i.e., proxies (HAB and ABS indicators) (see Figure 5), which arise from interactions with traits of geodiversity, terrestrial vegetation diversity, LUI, urbanisation or climate change. It should be particularly emphasised that traits and trait variations are filters and proxies for changes and disturbance processes that are triggered by various drivers and stress indicators (e.g., contaminants in water bodies, river straightening, LUI, urbanisation). The sum of the water traits recorded by RS reflects the spectral footprint of the water and its changes or disturbances and is reflected by the water spectranometric approach. This is comparable to the spectrometric approach of terrestrial plants, where the diversity and functionality of plant traits can be quantified and assessed using hyperspectral sensors [89].

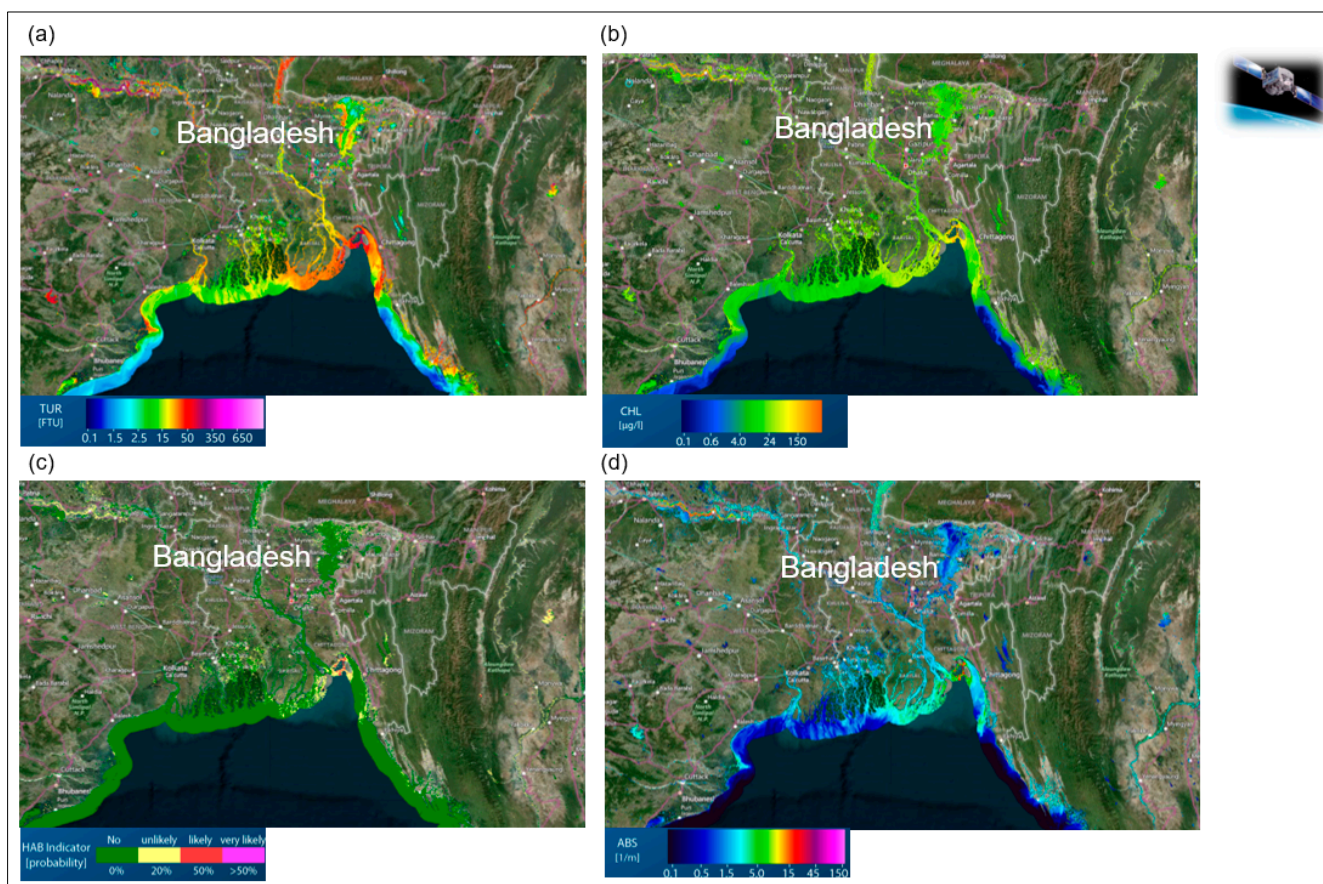


Figure 5. Spectral traits of water diversity monitored with remote sensing approaches, (a) Monitoring of turbidity (TUR), (b) Chlorophyll-a content (CHL), (c) Algal blooms indicator (HAB-Indicator), (d) and the Total absorption (ABS), Bangladesh, India, (online water analysis tool: <https://aqua.eoapp.de>, accessed on 26 June 2024).

RS can detect the five spectral traits of water diversity: the diversity of water traits, the diversity of water genesis, the structural diversity of water, the taxonomic diversity of water and the functional diversity of water. Furthermore, the spectral traits of changes, stress factors and disturbances of water can be monitored using RS (see Table A1 (Appendix A)), which provides an exemplary overview.

4.2.2. Monitoring the Diversity of Water Genese Using Remote Sensing

“The diversity of water genese is the diversity of the length of evolutionary pathways associated with a particular set of water -traits, -taxa, -structures and -functions of water diversity. Therefore, groups of water traits, water taxa, water structures and water functions that maximise the accumulation of the functional diversity of water diversity are identified” (see Chapter 3, modified after Lausch et al. [32]).

The genesis, development and shaping of lake basins and watercourses resulted from various exogenous and endogenous geomorphological developments such as tectonic activity, volcanic activity or glacial erosion. The classification of lakes and watercourses is based on factors such as the genesis of the water body, the organic/inorganic ratio, the nutrient balance, the physiology, the depth, the size, the shape, the sediment types, the morphology of the lake basin and the oxygen content [90]. The presence of aquatic species and the physical and chemical processes taking place in a lake resulting from the influence of geological and terrestrial vegetation diversity and anthropogenic pressures such as LUI and climate change also play a decisive role.

Other factors such as mineral and rock composition, location or physical properties, such as thermal combinations and optical properties, chemical and trophic characteristics and species diversity, therefore lead to the formation of site-specific traits and a characteristic water diversity [91]. As tropical lakes behave differently due to high temperatures, a constant turnover and constant oxygen deficit, they must be monitored and modelled separately [90]. The monitoring of traits of/in and around water bodies is therefore at the forefront if the diversity of water genesis characteristics and water genesis quality is to be recorded with RS.

The following chapter discusses which of these traits can be analysed using RS in order to identify the diversity of water genesis characteristics and water genesis quality. Phylohydrology is a relatively new field that combines phylogenetics, i.e., the study of evolutionary relationships between species, with hydrology, i.e., the study of the characteristics and the distribution of water in the environment. Phylogeogeny, another new field, goes one step further and combines elements of phylogenetics, geology and hydrology.

Until now, RS could not be used directly to measure phylohydrological and phylogeogenic patterns, as its ability to detect individual traits of water or species or to determine their genesis was limited due to RS characteristics (spatial, spectral, temporal and directional resolution). With the increasing development and use of the latest RS technologies, such as hyperspectral RS (EnMAP) and multisensor RS sensors (HyspIRI), important gaps in this monitoring are increasingly being closed. However, RS has long provided important indirectly derived information on the diversity of water genesis. This ensues from monitoring environmental features and processes that are caused or influenced by phylogeogenic and phylohydrological patterns. It can therefore be said that RS can provide holistic monitoring (a combination of water diversity, geodiversity and terrestrial vegetation diversity) to better capture the diversity of water genesis and to better understand natural and anthropogenic causes of water quality and consequently provide better management strategies for its protection. The following exemplary phylogeogenic and phylohydrological traits recorded here have so far been recorded using RS technologies (see Table A1 (Appendix A)):

Structure and patterns of water bodies: RS can be used to record the structural traits of water bodies and their surroundings in great detail. Important indicators here are the area, size, length, shape, density or water level of the water body or river course or the contiguity and connectivity, whereby the water genesis played a decisive role in its formation.

Habitat characteristics: The most recent hyperspectral RS technologies can provide very detailed information on aquatic habitat traits such as the water temperature, depth, substrate type and trophic status [23,92]. These factors influence the processes occurring in water bodies as well as changes to and distributions of species, populations, communities and habitats, i.e., reef habitat structure [93].

Geology and mineralogy: In order to determine the mineralogical composition of the water bed surface, spatial high-resolution airborne hyperspectral RS techniques are used in

particular. In the near future, the use of hyperspectral robots that can record the mineralogical composition of the water bed surface is also planned for water bodies and oceans.

Terrain modelling and hydrological modelling: RS has long been able to use airborne LiDAR, multispectral and hyperspectral RS to measure the topography of the water bed (bathymetry) and create digital elevation models (DEM) for still and flowing waters as well as shallow water in the oceans. These DEMs can be used in hydrological models to model water processes. They thus form a decisive basis for local to global modelling and its process understanding.

Hydrological processes: In addition to the aquatic DEM, RS can provide information on hydrological processes, e.g., changes in water level, flow direction and velocity or connectivity between water bodies. Connectivity provides crucial information on functionality and processes as well as the understanding of species migration and gene flow.

Water quality: Satellite images can be used to monitor water quality parameters such as the chlorophyll-a concentration, water surface temperature, turbidity, water colour, or salinity. For example, the water colour is a current driver of lake and river systems in boreal climate regions such as Scandinavia [75]. They are important indicators of processes of geogenic and/or anthropogenic influences and can be recorded worldwide at a high temporal frequency with remote sensing [76]. RS can therefore be used to map and monitor spatial and temporal changes in aquatic habitats.

The phylogenetic diversity of water promotes the resilience and stability of the entire aquatic ecosystem and is an important indicator of its functionality and response to environmental change [71]. Monitoring the phylogenetic diversity of water using RS is therefore crucial to understanding resilience and the reaction of drivers and changes to water on different scales. Most aquatic plant traits are manifestations of their phylogenetic and geogenic evolution [94]. Thus, the coupling of phenotypical-based taxonomy and the evolutionary history of phytoplankton led to a preliminary scientifically sound categorisation, as a large number of phytoplankton traits are linked to phylogeny [94,95].

In another example, Liu et al. [96] investigated and evaluated the taxonomic, phylogenetic and functional diversity of fish on the alpha and beta dimensions and their environmental drivers at a total of 84 river sites in 3 watersheds. The results showed that local (e.g., nutrients, dissolved oxygen, river width and transparency), regional (e.g., wetland), climatic (e.g., temperature) and spatial variables structured alpha and beta fish diversity. No significant differences in taxonomic and functional alpha diversity were found in the three watersheds, but significantly higher phylogenetic alpha diversity was found in the rivers of other watersheds. In terms of taxonomic and phylogenetic beta diversity, however, total beta diversity and the turnover component were higher in rivers of the same catchment, whereas total beta diversity was significantly lower in functional beta diversity. The analysis of variation partitioning showed that the pure contributions of local and spatial variables, i.e., characteristic genesis streams and catchments, were more important than those of climate and regional variables, suggesting that spatial effects and local environmental filtering are the main drivers of beta diversity of fish communities in these rivers. These studies also emphasise the importance of coupling in situ measurements to monitor local variables with RS-based monitoring to monitor regional variables (Landsat TM).

Figure 6 shows how geological genesis leads to the formation and development of different lakes—glacial erosion lakes, valley lakes and tectonic lakes—and it analyses the development and change characteristics of glacial lakes in the Niangmuco region on the eastern edge of the eastern Himalayas based on Landsat TM/OLI (2000–2021) and classifies the stability of lakes with an area of more than 0.02 km² using the fuzzy matrix method [78]. The results show that the development and change of glacial lakes in this area is primarily controlled by temperature and precipitation and that topography and fault activity have an important influence on the stability of glacial lakes.

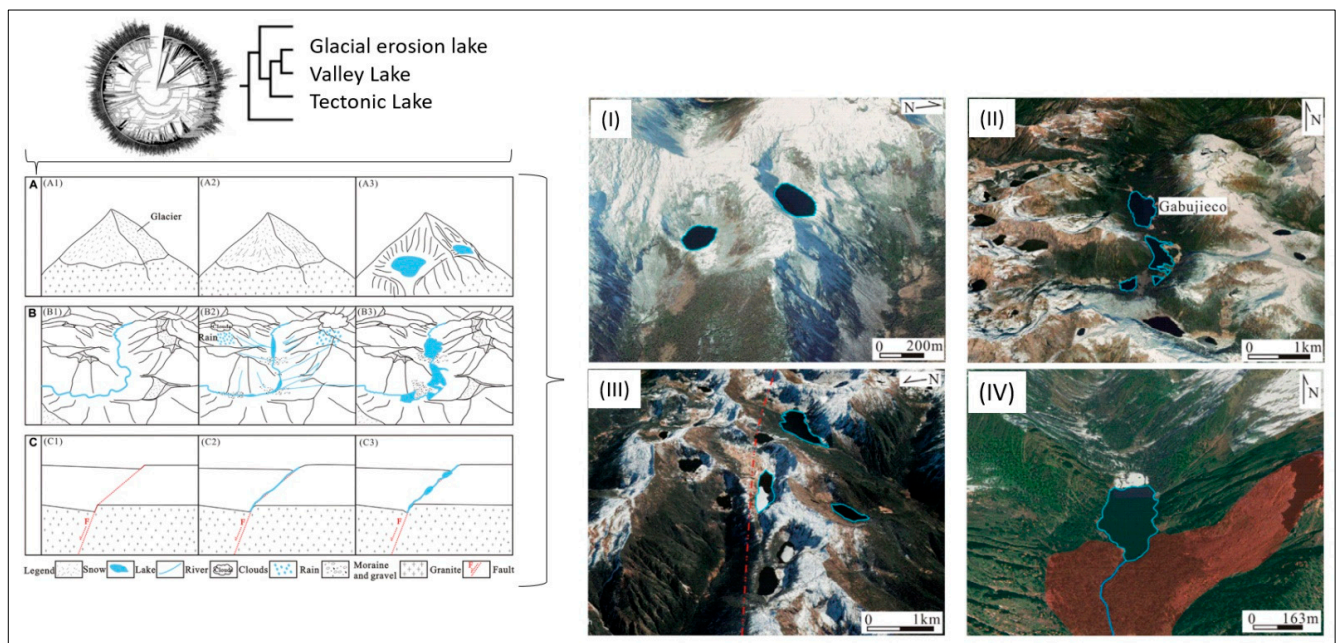


Figure 6. Geological genesis leads to the formation and shaping of different lakes. (A–C) Schematic diagram of the formation mechanism of (A) Glacial erosion lake, (B) Valley lake, and (C) Tectonic lake. Classification of glacial lakes based on Landsat TM/OLI and Aster DGM data. (I) Glacial erosion lakes, (II) Valley lakes (Gabujiéco valley), (III) Tectonic lakes (fault marked by dotted red line), and (IV) Landslide dam lake (red area indicates landslide area) (from Weit et al. [78]).

4.2.3. Monitoring the Structural Diversity of Water Using Remote Sensing

“The structural diversity of water is the diversity of composition and configuration of water characteristics” (see Chapter 3, modified after Lausch et al. [32]).

Exogenous and endogenous processes, genesis, morphometry, morphology, mineral and rock composition, as well as processes of the earth’s formation and evolution, are decisive for the emergence and formation of a characteristic water diversity with site-specific physical properties like thermal combinations and gradients, optical properties, chemical and trophic characteristics and species diversity [91]. Thus, evolutionary characterised structures and patterns of marine and freshwater systems lead to diversity and gradients and niches of species that increase the niche dimensionality of species [97] and consequently promote species richness and overall biodiversity [98]. Numerous marine and freshwater structures and patterns can be captured by different RS technologies, which are discussed in the following chapter (see Figure 1 and Table A1 in Appendix A).

With RS-based approaches, the recording and quantification of the structural diversity of water is more difficult compared to the recording of structural vegetation diversity [53] or geodiversity [32]. In many cases, indirect methods or proxies such as water temperature, salinity or environmental parameters such as light supply and turbulence are used to derive RS-based quantitative structural indicators. Indeed, RS techniques provide an efficient way to monitor indicators such as location, shape, area, size, depth, volume and the water level of various water bodies such as rivers, lakes and oceans. These measurements are useful for a range of applications, such as water resources management, flood forecasts and the monitoring of trophic levels in aquatic ecosystems. Different RS methods and technologies can be applied based on the specific structural and pattern characteristics of the water body and the information needed. Several types of satellites, such as Landsat, MODIS and Sentinel, carry multispectral and hyperspectral sensors that can be used to monitor water bodies. For instance, these can be used to identify changes in water area over time and to distinguish between water and land [99]. RADAR can provide information about the shape and size of water bodies. Synthetic Aperture Radar (SAR) data can detect

water bodies, even in cloudy conditions or during the night. With the use of satellite radar altimetry, the spatial extent, distribution, area or surface water levels of water bodies and their changes can be recorded [100]. Since the 1990s, the water level fluctuations of around 6282 water bodies have been recorded in a permanent water database, and their changes have been monitored [100]. Furthermore, radar altimeters, such as those mounted on the satellites of the Sentinel-3 and Jason series, can measure changes in water level, changes in the extent of water bodies and river flow. In addition, LiDAR can be used to measure the depth of shallow water bodies by calculating the time it takes for the laser pulse to travel to the water surface and back [101]. A wide range of RS-based structural water traits is provided by the ESA Lakes Project (in the Copernicus Essential Climate Variables). These are, e.g., water extent, water level and surface water temperature (see <https://climate.esa.int/en/projects/lakes/>, accessed on 26 June 2024). Thermal Infrared RS (TIR) with, e.g., Landsat TM/ETM+/TIRS thermal infrared data, can be used to measure the temperature of spatially smaller water bodies. The surface temperature of water bodies can be related to their depth, as the water temperature tends to decrease with depth. Thus, the thermal properties of water bodies might be analysed to estimate their depth [102]. Sonar systems (sound navigation and ranging) are an RS technology that can be used to measure the water depth (only for rather shallow water, with ICESat up to approx. 12 m in turbid Baltic Sea water) and volume by sending sound pulses into the water and recording the time it takes for them to return [103]. Furthermore, optical RS technology such as World View, Sentinel-2 MSI or Landsat 8/9 OLI can be used for quantifying the water level, especially in the case of lakes and reservoirs [104].

Hyperspectral RS data like PRISMA and DESIS or multispectral data like Sentinel-2/3, Landsat, MODIS and airborne LiDAR data can estimate the water depth and clarity (highly correlated with Secchi-depth, an indicator of the clarity or turbidity of the water by measuring the visibility depth of a white disc lowered into the water [105–107]). Monitoring water clarity helps to monitor changes in habitat quality and ecosystem health. Information on water depth is obtained by measuring the change in water colour with depth using hyperspectral RS (such as EnMAP, PRISMA or DESIS [108]) and multispectral RS (such as Landsat or Sentinel-2 [109]). Airborne LiDAR, but also increasingly multi- and hyperspectral RS technologies, have been used for bathymetric surveys of the morphology of seabeds, lake beds and riverbeds for some time now [108,110,111]. Furthermore, in clear and shallow waters, information on the substrate type (sandy, muddy and rocky) and its distribution at the bottom of a water body can also be recorded, which provides important information on potential habitats (Niroumand-Jadidi et al. [112,113]). Conclusions can also be drawn about the intensity of matter influx as a cause of intensification or river straightening in reservoirs or dams.

Monitoring hydrological connectivity is important for maintaining the stability and function of wetland ecosystems, streams, riparian zones, floodplains, alluvial aquifers, standing waters and oceans, which are connected by longitudinal, lateral and vertical fluxes of water, matter and energy. This is crucial for understanding, for example, the migration patterns of different species and gene flow, as well as the influence of human activities on this connectivity [114]. With the help of the RS time series, these networks can be recorded, and their changes and effects on biodiversity can be documented [115].

Furthermore, airborne LiDAR can be used to accurately measure the height of the water surface, which allows conclusions to be drawn about the flow characteristics of rivers. In some cases, these data can be used to estimate the discharge of a river, which is an important parameter for water quality modelling [116]. Information on the flow velocity in rivers is crucial for infrastructure planning, the modelling of pollutant and matter flows and habitat assessment. Moving Aircraft River Velocimetry Monitoring can be used to measure the flow velocity effectively and rapidly [117].

Furthermore, high spatial-resolution RS data will be used to determine the complexity, structure, shape and changes in the shoreline of a water body. More complex shorelines can increase habitat diversity and provide niches for different species [118]. However, the

choice of sensor technology with appropriate properties (spectral, radiometric, geometric and temporal resolution) is crucial to capturing accurate geomorphological structures and shorelines. For example, hydrological model predictions are only as good as the quality of the RS-based input data [62]. By capturing detailed terrain structures of coastal regions with airborne LiDAR data, it was shown that more than three times as many people are at risk from climate change and sea level rise than previously calculated with less detailed SRTM-DEM-RS data [119].

By monitoring currents, eddies and ocean circulation patterns, RS helps to understand the movement and transport of water masses. RADAR (Radio Detection and Ranging) data can be used specifically to recognise surface features such as waves and currents that indicate deeper water properties. This information is imperative for studying marine habitats, identifying potential sources of pollution and predicting the spread of pollution or the effects of climate change as a result of changes to natural processes such as El Niño [120]. Furthermore, RS technologies are valuable for estimating water surface roughness and other parameters from a distance using data gathered from aircraft or satellites. Several types of RS techniques are applied for this task, such as optical imaging, thermal infrared and RADAR. Radar RS is commonly used for measuring water surface roughness, whereby radar waves are emitted towards the Earth's surface and then reflected back to the radar system. The degree of backscatter is influenced by the roughness of the water surface. Synthetic Aperture Radar (SAR) is particularly sensitive to surface roughness and has been used in a number of studies to estimate water surface roughness [121] as well as LiDAR [122]. Optical and Infrared RS can monitor the patterns of light reflected off a water body and can provide clues about its roughness. Similarly, rougher surfaces will distribute heat differently compared to smoother ones, leading to detectable differences in thermal infrared data. However, these techniques are generally less accurate than RADAR for this particular application [123,124].

RADAR, microwave radiometer, LiDAR and thermal infrared data provide valuable information on the complex interactions between fresh- and saltwater in coastal areas and estuaries. The sensors can distinguish between different water types and pH values and detect the mixing of freshwater and seawater, which is essential for the study of coastal ecosystems and the management of coastal resources [125,126]. For example, the salinity of the sea surface is indirectly determined using RS by recording the changes in sea surface radiation density caused by changes in salinity. This is conducted using L-band microwave radiometers from the SMOS (Soil Moisture and Ocean Salinity) and Aquarius satellites [127].

Satellites such as Landsat or AVHRR (Advanced Very High-Resolution Radiometer) can collect information on the temperature of the sea surface using TIR sensors. Different temperature regimes can favour different types of organisms, indicating a certain kind of diversity. Water bodies with different thermal properties cause different temperature patterns. Thermal fluctuations and changes provide important insights into phenomena such as the upwelling of nutrient-rich water or currents of colder water rising to the surface. The rise in sea temperature is one of the most important indicators of climate change [128,129]. The surface temperature of water bodies is an outcome variable of energy and mass fluxes in the contact zone between the atmosphere and the water body as a result of interacting environmental processes, whereby the temperature controls the physical, chemical and biological processes in the water [130]. Consequently, the detection of surface temperature using different RS technologies has become one of the key variables for understanding ecological phenomena and processes in marine, coastal and lake environments.

One of the key applications of satellite data is in the use of time series, which now enables almost 40 years of continuous monitoring (e.g., Landsat) of seasonal and annual changes to water extent, water temperature, flow processes and numerous water quality parameters, providing crucial knowledge about spatio-temporal patterns of water diversity and water quality [131].

The composition, dispersion, richness, diversity and homogeneity of phytoplankton [46,132] are good indicators to describe the structural and functional diversity of phytoplankton populations and communities [41,133]. There are numerous environmental factors that shape phytoplankton communities, but also lots of interactions, such as zooplankton grazing. Thus, phylogenetic as well as geogenic factors shape and control the functional traits of phytoplankton structure and their seasonal dynamics in marine and freshwater ecosystems [134]. Traits are crucial for answering the questions of intraspecific and interspecific competition of phytoplankton and thus control not only the composition of the community but also the functioning and processes of ecosystems such as the primary production, the transfer of biomass and the entire nutrient cycle (Abonyi et al. [135]). For example, temperature influences photosynthesis, respiration, growth, resource availability and motility, as well as the dominance of various taxonomic groups of phytoplankton and all aquatic organisms [47]. As the main groups of phytoplankton have different optimum temperatures, the temperature plays a crucial role in the seasonal dynamics and distribution of phytoplankton in both marine and freshwater habitats. The temperature mainly affects heterotrophic organisms and thus plays an indirect role in the seasonal succession of phytoplankton (e.g., [136,137]). Freshwater cyanobacteria have a higher optimum temperature compared to other taxonomic groups, leading to dominance in late summer when water temperatures are higher [138]. Higher optimum temperatures of cyanobacteria are therefore also important indicators of global warming, leading to the spread of harmful toxic algal blooms. However, some other studies have also shown that blooms also like the cold [139].

Initial RS-based surveys of phytoplankton were based on estimates of phytoplankton biomass and its seasonal variation, which can be monitored by chlorophyll concentrations [140]. Recent methods, however, combine RS data with in situ high-performance liquid chromatography (HPLC) measurements of pigments and deep learning-based modelling to estimate the concentrations of different phytoplankton pigments on a global scale [120]. This novel approach enables a global estimate of the concentration of different pigments and thus the dynamics of the phytoplankton community on a large spatio-temporal scale. Vostokov et al. [141] investigated the seasonal and long-term variability of phytoplankton in the ocean based on SeaWiFS and MODIS-Aqua-Scanner RS time series (1998–2021) and in situ data, which allowed them to capture the seasonal variabilities, as well as the main periods for autumn and winter seasons of phytoplankton production [141]. The application of hyperspectral RS technologies (EnMAP, Prisma, DESIS) will greatly improve the monitoring of phytoplankton species composition and configuration as well as influencing factors such as the composition and type of photosynthetic pigments [142], as well as the phytoplankton species composition based on the spaceborne Hyperspectral Imager for the Coastal Ocean (HICO) imagery [143]. Cyanobacterial harmful algal blooms (cyanoHABs) are a progressive problem in freshwater bodies as the growth and decay of cyanoHABs lead to anoxic and hypoxic conditions, which can result in human health impacts, the death of fish and benthic invertebrates, imbalances in the existing food web and loss of biodiversity in the water body [144]. Therefore, monitoring and predicting the distribution and intensity of cyanoHAB in lakes using RS is an approach that has been successfully implemented for some time [145]. In addition to drone-based approaches [146] and airborne hyperspectral RS (AISA) [147], multispectral RS technologies such as Meris (Matthews et al.) [148], Landsat and Sentinel-2 [149], Sentinel-3A and -3B (OLCI) [145]. Matthews [145] was able to predict cyanobacteria and cyanobacterial harmful algal blooms (cyanoHABs) based on Sentinel-3A and -3B (OLCI) satellite data with an accuracy of 80% for one week in advance.

RS can capture the ecological complexity and diversity of aquatic habitats, such as variations in water depth, ecological gradients (thermal gradients and freshwater to saltwater transitions), shoreline complexity or the presence of aquatic and riparian vegetation. These gradients are often areas of high biodiversity [150]. RS is therefore ideal for monitoring aquatic habitats and providing RS-based indicators for habitat modelling. Asner et al. [151]

were able to quantify and assess the live coral cover density, spatial distribution, coral cover of living corals and the relative condition of reefs down to a water depth of 16 m on the main islands of Hawaii using airborne data visible-to-shortwave infrared (VSWIR) imaging spectrometer and a light detection and ranging (LiDAR) scanner. Li and Asner [152] used spectroscopy to determine the three-dimensional complexity of shallow benthos (also referred to as benthic roughness), which reflects the physical conditions of shallow coral reefs and is used to estimate fish biomass and coral cover on the reefs. Figure 7 shows the monitoring of tideways in the Weser River, northeast of Wilhelmshaven in Germany, based on Airborne Laser Scanning (ALS) [62].

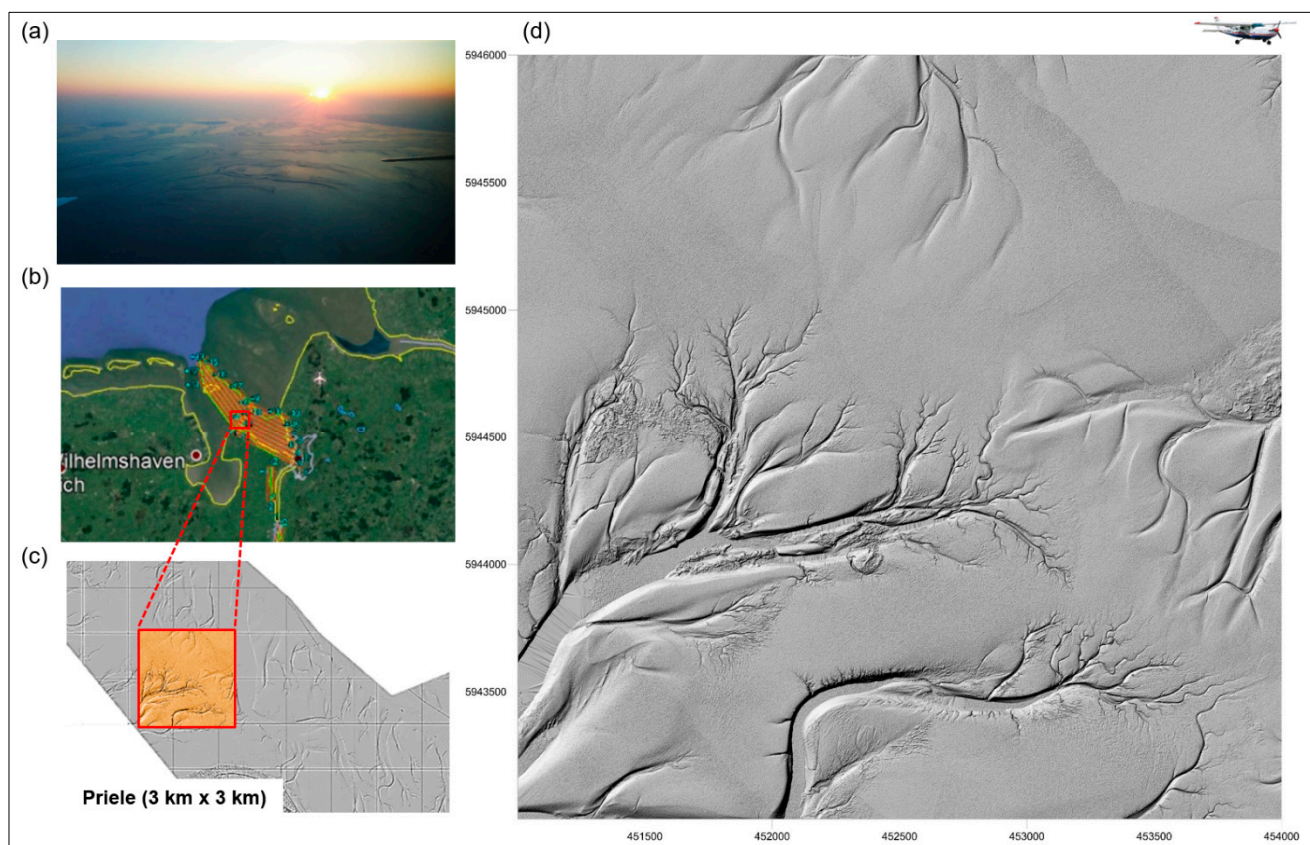


Figure 7. Tideways in the Weser River, northeast of Wilhelmshaven, Germany: (a) Photo of the tideways acquired from the aeroplane. (b) Location (Google Maps) of the monitored area (in orange). (c) Digital Elevation Model (DEM) monitored by Airborne Laser Scanning (ALS) with a blue rectangle (>5 LMW/m²), highlighting the location of the (d) 3×3 km tideways, shown as shaded relief (elevation of the contours $Z = 20$) (from Lausch et al. [62]).

4.2.4. Monitoring the Taxonomic Diversity of Water with Remote Sensing

The “taxonomic diversity of water represents the diversity of water components that differ from a taxonomic perspective” (see Chapter 3, modified after Lausch et al. [32]).

Geogenic factors led to the formation of different types of lakes, such as tectonic and volcanic lakes, dam lakes and erosion lakes [62]. In addition, other factors such as genesis, morphometry, morphology and location; physical properties such as thermal combinations and optical properties; and chemical and trophic status led to the establishment of seas and lakes [91], which exhibit a characteristic aquatic trait diversity.

For example, Reynolds et al. [153] monitored phytoplankton taxa based on their characteristic environmental conditions such as seasons, lake morphology, trophic state of the lake or light availability, as phytoplankton communities are filters of environmental factors such as vertical water dynamics and depth, trophic state, predation and growth [47]. The taxonomic diversity and abundance of different taxonomic phytoplankton groups or

coral communities and their changes are key parameters to describe the status, disturbance, stability, functionality and resilience of aquatic ecosystems [41,154,155].

Specific characteristic aquatic traits can be captured by RS approaches, enabling the determination of taxonomic diversity, e.g., phytoplankton taxonomic groups, coral reef classification or aquatic vegetation taxa or river systems, river network types, coast types, catchment areas, hydrological response units (HRUs) and watersheds (see Figure A1 and Table A1 in Appendix A). Aquatic taxonomic diversity, such as phytoplankton taxonomic groups or coral classification, can be discriminated by RS if species, populations or communities differ in their aquatic traits (e.g., structure, chemical–mineral composition or photosynthetic pigments). Furthermore, the distribution, density, composition and configuration of the aquatic traits of different taxa play a decisive role in RS-based discrimination. For example, the Great Barrier Reef in Australia can be discriminated more easily using RS due to its high density of identical aquatic traits than, for example, reefs in the Red Sea, where traits occur at a lower density. The radiometric, spectral, geometric and temporal resolution of the RS technology also plays a decisive role in discrimination. Only RS sensor technology that can spectrally record these aquatic traits and thus discriminate between taxa will be successful. This is very complex and similar taxa still have different spectral distributions, but in the future, it could work with a high hyperspectral resolution and combinations of validated methods (including optically more complex inland waters).

Airborne LiDAR RS technologies have been successfully used for the taxonomic classification of coral reefs for some time now, providing valuable insights into reef structure, complexity and taxonomy [156,157]. Thus, detailed 3D-LiDAR maps capture complex features of the coral reef, such as the height, 3D complexity and spatial arrangement of corals, which is crucial for the discrimination of different coral species, as each species differs phylogenetically in terms of its unique morphological traits [158]. By integrating RS time series from the same reef, changes in the structure, composition and healthy status of coral reefs are recorded. This is important to understand how reefs respond to environmental changes and to take protective measures [159,160]. Multi-sensor RS approaches can be used to capture a range of aquatic features, e.g., to better distinguish between different reef components such as hard and soft corals and different coral genera or species [161]. In addition, coral reef habitats and their restoration will be monitored using high spatial resolution unmanned aerial systems [162] or satellite imagery from PlanetScope and Sentinel-2 [163].

In order to facilitate the global monitoring of coral reefs, the Millennium Coral Reef Mapping Project was established between 1999 and 2002 by the World Conservation Monitoring Centre of the United Nations Environment Programme in order to use satellite images (IKONOS 2, Landsat, SPOT, High-Resolution Visible (HRV) and the airborne hyperspectral Compact Airborne Spectrographic Imager (CASI)) to understand, classify and map coral reefs, their composition and changes [164]. In 2020, Arizona State University, together with Planet, the Coral Reef Alliance and the University of Queensland, released the world's first high-resolution coral reef monitoring data product (Allen Coral Atlas) [165]. The classification and description of phytoplankton biodiversity was an early area of research, as phenotype-based taxonomy and the phylogeny of phytoplankton are closely linked, and a large number of traits are linked to phylogeny. This ensures the development of different ecological strategies and the occupation of specific niches [94].

Phytoplankton taxonomic classes or groups can be discriminated by different proportions of bio-optical traits using RS, such as, e.g., the Chl-a concentration, accessory pigments (Chl-b, Chl-c, carotenoids and phycobillins) or pigment ratios (TChl-a/AP, TChl-a/TP, PPC/TC) [41]. Furthermore, accurate monitoring of the spatio-temporal distribution, taxonomy and variability of phytoplankton groups using RS approaches is crucial to gain a better understanding of marine ecosystem dynamics and biogeochemical cycles [166]. Li et al. [88] reported on the global satellite observation of the distribution of marine phytoplankton taxonomic groups over the past two decades (2002–2022), with six main taxa globally, namely, chlorophytes (~26%), diatoms (~24%), haptophytes (~15%), cryptophytes

(~10%), cyanobacteria (~8%) and dinoflagellates (~3%), which account for the majority of the variation (~86%) in the phytoplankton communities, compared to diatoms that dominate the spatial distribution. It was further shown that diatoms dominate in high latitudes, marginal seas and coastal upwelling areas, while haptophytes and chlorophytes dominate the open oceans [88]. Due to the increasing free availability of multispectral and hyperspectral RS data, the creation of spectral libraries for green macrophytes for coastal and aquatic biodiversity RS is steadily progressing [167,168]. Similarly, global RS data availability and the use of spaceborne hyperspectral RS (EnMAP and DESIS) facilitates the classification and monitoring of mangrove species as an important part of the global blue carbon pool [169,170].

One of the first applications of RS is the monitoring of the trophic state (eutrophication) of seas, lakes and rivers. Using the RS satellite sensors MODIS MERIS [171], Landsat-8 OLI, Sentinel-2 [172–175] or spaceborne hyperspectral PRISMA data [176]), the trophic state is determined based on different variables of water quality such as chlorophyll-a, total phosphorus and transparency/Secchi disc depth.

The world's rivers are undergoing accelerated change in the Anthropocene and are subject to the increasing influence of human intensification. Based on the geomorphological, structural and trophic state of these rivers, Piégay et al. [177] developed a classification system of rivers that discriminates between rivers whose structure and functions have been characterised by natural and anthropogenic processes.

Another application of taxonomic diversity is the discrimination of water catchment areas as well as river courses. For example, based on the Shuttle Radar Topography Mission (SRTM) DEM with a pixel resolution of 3 arc seconds (~90 m at the equator), Linke et al. [178] calculated, for the first time, globally available hydro-ecological sub-catchment and river section characteristics (HydroATLAS). This provided information on, e.g., runoff accumulation, runoff distances, river orders, catchment boundaries and river networks on a global scale and represents the first standardised classification of water catchment areas (BasinATLAS) and rivers (RiverATLAS) on a global scale [178].

Coastal geomorphology describes the dynamic interface between the ocean and the land surface. Since different coastal types filter water differently, the ecosystem services of the different coastal types can be classified using RS methods, allowing their functionality and resilience to be assessed. Hence, coastlines can be discriminated from each other using RS, as they can be classified into different types based on hydrological, lithological and morphological characteristics, such as small deltas, tidal systems, lagoons, fjords, large rivers, tidal estuaries and karst [179].

Coral reefs are subject to change due to coastal development, resource use and climate change. Using airborne hyperspectral RS data, Asner et al. [80] were able to demonstrate the extent and rate of reef change with robust and spatially explicit monitoring that can support RS-based management and conservation decisions. An airborne approach was developed to plan and optimise field surveys of reef fishes over an ecologically complex reef ecosystem along the islands of Hawaii. Reef habitat variability was best determined by a combination of variables derived from airborne hyperspectral RS data: the water depth, coral and macroalgal cover, fine-scale reef structure, reef curvature and latitude as a proxy for a regional climate–ecosystem gradient. Modelling was used to classify 18 different reef habitats from the combination of these different RS variables. This modelling also required 117 in situ monitoring sites to quantify fish diversity and biomass with minimal uncertainty [80] (see Figure 8).

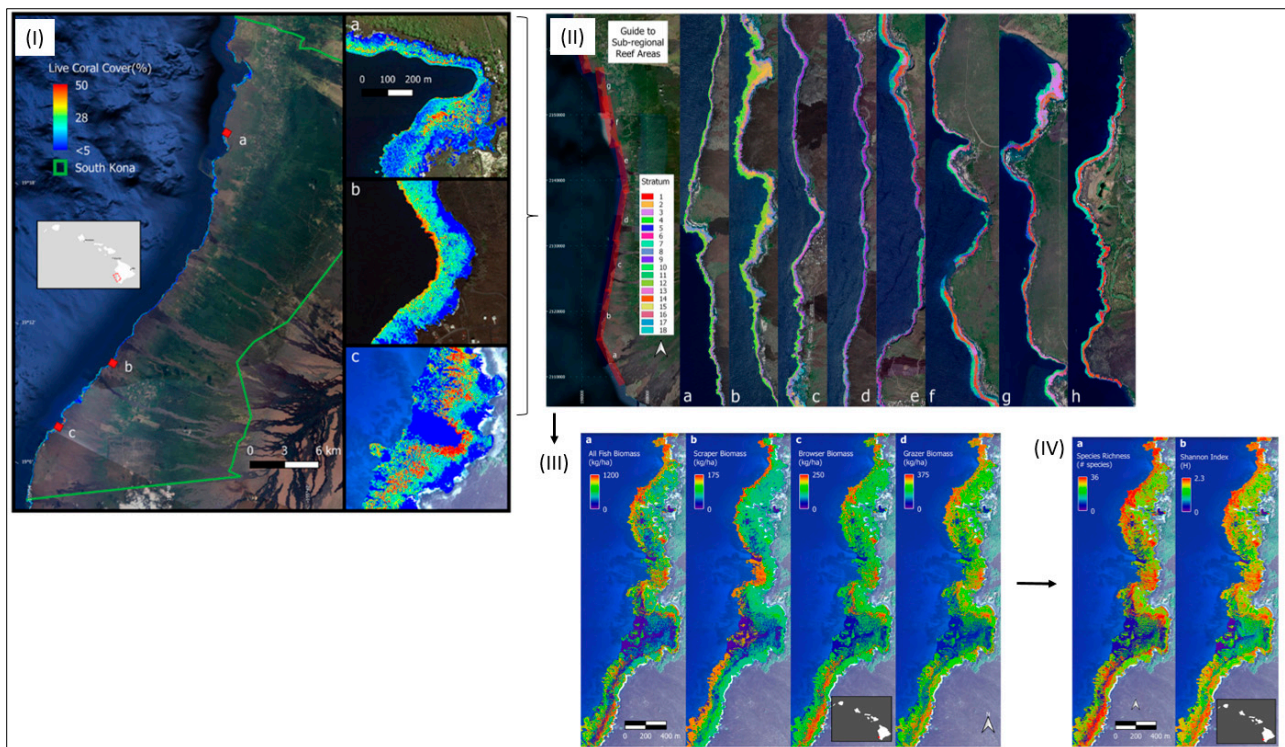


Figure 8. (I) The location of the South Kona District is demarcated by the green lines on the left, with live coral cover mapped along the coast based on airborne hyperspectral data in 2019 and 2020. Example areas of live coral cover are shown at (a) Honaunau Bay, (b) Papa Bay and (c) Okoe-Kapua Bay. (II) The final 18-stratum map of coral reef conditions for the South Kona District coast was derived from the airborne hyperspectral data. The far-left panel indicates the location of each sub-regional zoom image (a–h) shown in the remaining panels. Each colour indicates the location of each ecological layer in the reef system. (III) Ecological modelling was then applied to produce fish biomass maps of Honomalino Bay for (a) all fish and for fish classified as (b) scrapers, (c) browsers and (d) grazers. Differences in distribution patterns between the different trophic groups can be seen, especially across depth gradients. (IV) Finally, upscaled biodiversity maps of Honomalino Bay were generated using (a) species richness and (b) the Shannon diversity index (from Asner et al.) [80].

4.2.5. Monitoring the Functional Diversity of Water with Remote Sensing

The “functional diversity of water is the diversity of water functions and processes, as well as their intra- and interspecific interactions” (see Chapter 3, modified after Lausch et al. [32]).

Monitoring the status and changes of functional diversity in water bodies is crucial for assessing the status, changes and shifts of ecosystem functions such as productivity, nutrient cycling or trophic regulation. In monitoring aquatic functional diversity, the traits approach plays a crucial role with regard to in situ monitoring [41,46] and RS-based monitoring. The traits approach is a proxy and indicator that is crucial for quantifying and assessing the functionality, trade-offs and maintenance of ecosystem services in water bodies [41,154]. On the one hand, the concept of the functional diversity of water refers to the functional diversity of aquatic species such as marine bacteria, macroalgae [180], eutrophication, the composition of freshwater phytoplankton [155] and the changes to the macrosystem community of phytoplankton in lakes, which has an impact on diversity and numerous functions [71,154]. On the other hand, processes and interactions with components of geodiversity, terrestrial vegetation diversity and land use intensification, such as river straightening and urbanisation, influence the functionality and resilience of aquatic diversity. For example, geodiversity influences the functional diversity in freshwater macroinvertebrate systems [181]. In this chapter, the monitoring of functional

diversity using RS can only be discussed as an example. Table A1 (Appendix A) provides an overview of RS-based monitoring of aquatic functional traits.

Plant Functional Types (PFTs) refers to the grouping of plants based on their common functional traits (growth rate, leaf shape, type of photosynthesis or response to stress factors), which is in contrast with the taxonomic classification. PFTs are used to better understand the impact of environmental changes such as climate change or land use intensity on vegetation by focussing on functional traits. The first naming of functional plant types defined the plant strategy types by Grimme [182], where plant characteristics have adapted to stressors and disturbance regimes through structural and functional properties and thus survival strategies over longer periods of time. The term PFTs was coined by Smith [183] and defines groups of plant species that show comparable responses to the environment and the functioning of ecosystems through similar functional characteristics. Reynolds [184] transferred this concept to a functional classification of phytoplankton by assigning 14 phytoplankton associations to specific environmental conditions such as lake size, nutrients, light and carbon availability. This approach was further developed by Reynolds et al. [153], whereby 31 associations of phytoplankton are currently described. The different phytoplankton species that make up a single PFT may have similar morphological characteristics and yet be adapted to similar environmental conditions by implementing different ecological strategies [46].

If aquatic ecosystem functions are to be recorded using RS, the aquatic traits that influence and regulate ecosystem functions must be defined. The traits and trait variations triggered by their processes (e.g., photosynthesis, photosynthetic pathways and carbon sequestration) must be recorded using RS. The RS-based detection of phytoplankton functions in aquatic environments is based on the spectral analysis of light reflected from the surface of a water body, as different PFTs have characteristic optical properties that are reflected in their light spectrum. Most techniques for the detection of phytoplankton with RS focus on the measurement of chlorophyll-a concentration [185,186]. Furthermore, different classes of algae contain different photosynthetic pigments that produce characteristic colour ratios in the reflected light. Optical RS sensors are able to classify different pigments and thus assign them to specific PFTs [120]. By using hyperspectral RS technology (PRISMA, DESIS and EnMAP), much finer discrimination of PFTs is possible compared to multispectral RS data, as spectral information of phytoplankton abundance, particle size distribution (PSD), bio-optical properties, chlorophyll-a and other pigments or spectral features (absorption, backscattering and/or reflectance) of the water in the VIS-NIR range are used [187]. The particle size distribution (PSD) of suspended particles in near-surface seawater is another crucial property that combines biogeochemical and ecosystem characteristics with optical properties and is reflected in the sea colour, which can be detected using RS. For example, small phytoplankton (picoplankton) are found in continuously stratified waters with lots of light at the surface and limited light in deep layers as well as limited nutrients, while large phytoplankton (microplankton) occur in turbulent systems with lots of light and nutrients near the surface [188]. Furthermore, phytoplankton size classes (PSCs) influence the physiological cell properties and, consequently, their biogeochemistry and biological carbon pump, which is crucial for the global carbon cycle and climate [189]. LiDAR technology can also be used to detect the structure of phytoplankton, which is used to distinguish PFTs based on structure and shape [190]. Some studies on RS-based PFT quantification use complex bio-optical models to identify specific phytoplankton species and classes. These models take into account various factors such as water quality, light absorption and scattering [191]. When in situ measurements are combined with RS, it can increase the accuracy of PFT classification, as in situ samples are used to calibrate and validate models [191,192], which is imperative. Furthermore, a tremendous advantage of RS is to use continuous waters using RS time series to capture seasonal and temporal patterns in phytoplankton dynamics, including the dominant occurrence of certain PFTs [186,193,194].

In the 19th–21st century, anthropogenic influences such as river straightening, urbanisation and land use change have increasingly led to irreversible changes and, consequently,

the structural and functional disturbances of watercourses. By using aerial and satellite data, RS is able to monitor these change processes in the morphology, structures and functions of watercourses and their interactions and to assess their impacts on ecosystems and ecosystem functions. Rivers are the result of millions of years of morphogenesis. They are highly dynamic and adapt their course (meanders) according to the temporal changes in their discharge. Their meanders were formed by convergent and divergent flow movements that ran transversely to the general direction of the flow [32] (see Figure 9). The shape and structure of a river's meanders are a proxy of a stable, dynamic equilibrium between the river and the riverbed, leading to the development of a characteristic fluvial biodiversity, resulting in the stability of ecosystem functions such as a high self-purification potential. For example, numerous flood protection measures were implemented on the Upper Rhine in Germany in the 19th century. Areas at risk of flooding were reduced in size; measures were implemented to regulate low water levels, e.g., for year-round navigation, and power stations were built to make use of hydropower. These changes to the natural course of the Rhine in Germany led to strong influences and changes in the erosion and sediment behaviour (strong vertical erosion of up to 7 m) of the river, as well as an increase in flow velocity. The eroded material led to an increased formation of sand and gravel banks, whereby the barrages, in turn, acted as sediment traps, which consequently made further measures for low water regulation necessary [195]. These river regulation measures lead to irreversible changes in the geomorphology as well as the structural, functional and fluvial characteristics of rivers.

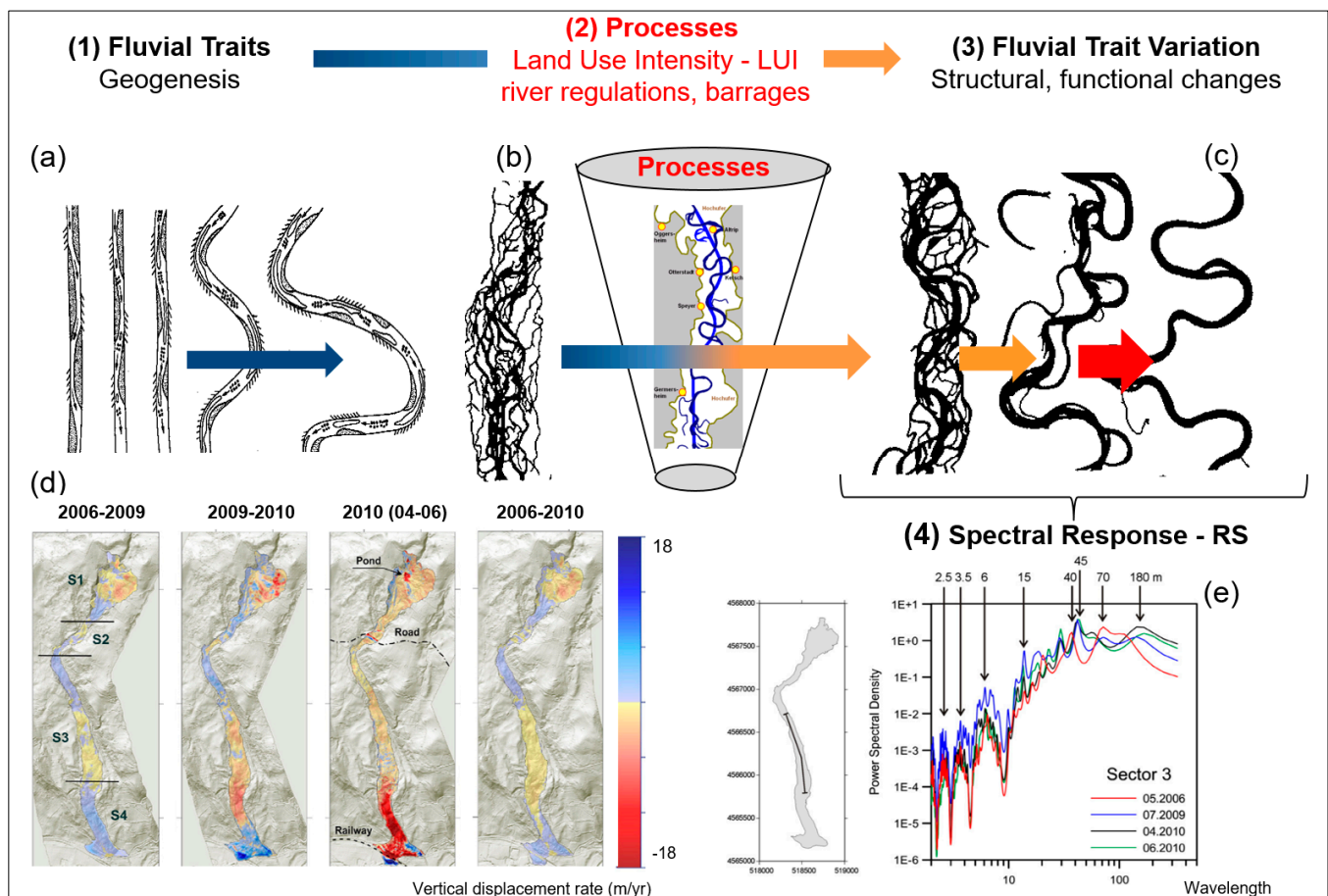


Figure 9. Monitoring status and changes to geomorphic characteristics with RS. (a) Different processes during geogenesis lead to the formation of specific morphometric fluvial traits—the meanders. (b) The entire river system is characterised by these meanders. (2) Processes/drivers such as land use intensity, river regulations and barrages lead to (c) changes in structural and functional fluvial traits

(fluvial trait variations–(3)) (d,e). These fluvial trait variations lead to spectral responses (4) in the remote sensing signal (d,e). An example of monitoring temporal changes to fluvial traits—vertical displacement rate of the river system from 2006 to 2010 with remote sensing technologies (LiDAR) (d,e). From Ventura et al. [81], reprinted with permission from Ventura et al. [81], 2021, Elsevier. License No. 5816961386058 (from Lausch et al. [32]).

RS approaches are able to continuously monitor these structural geomorphological changes of the meanders or sediment displacements over longer periods of time, as these changes to fluvial features lead to spectral responses in the RS signal (see Figure 9e). For example, the temporal changes of fluvial features—the vertical displacement rate of the river system from 2006 to 2010—were recorded using airborne LiDAR technologies (see Figure 9d). In addition to structural changes, the latest hyperspectral sensors, such as HySPEX, AISA, CHIME and EnMAP, can be used to make statements about changes to the functional diversity of water, changes to vegetation diversity (increasing eutrophication, chlorophyll content and turbidity) and the effects of river degradation on the neighbouring terrestrial ecosystem.

5. Conclusions and Further Research

The sea, inland waters and rivers play a central role in our aquatic and other ecosystems and provide the most important ecosystem services that enable and sustain life on Earth. The monitoring of water diversity and quality and their changes are complex, multidimensional and multi-scale in terms of space, time, processes and driving forces.

RS approaches have been successfully used for many years to implement monitoring on local to global scales. The traits approach was already introduced back in the 1980s for aquatic traits, but monitoring was based only on in situ measurements and observations. The aim of this paper was to apply the traits approach to monitoring water diversity and quality using RS approaches, as RS can monitor traits and trait variations for water diversity and quality. Traits form a crucial interface between in situ, airborne and spaceborne RS approaches and are filters or proxies for monitoring status, changes, disturbances and resource limitations on all scales. Therefore, RS approaches and the traits concept can be used to cover water diversity and quality, as well as changes and disturbances to them on all spatio-temporal scales, in a standardised way.

In order to understand how RS approaches monitor water diversity and water quality, five characteristics for the RS-based monitoring of water diversity and water quality were defined in this paper. These five characteristics are (i) the diversity of water traits, (ii) the diversity of water genesis, (iii) the structural diversity of water, (iv) the taxonomic diversity of water and (v) the functional diversity of water. The diversity of water traits is imperative to derive the other four characteristics with RS. The monitoring of the five characteristics of water diversity and water quality using RS technologies is presented in detail in this paper and discussed using numerous examples. Similar to the approach of Diaz (The Global Spectrum of Plant Forms and Functions) and Asner, the “Global Spectrum of Water Diversity and Water Quality” (Spectranometric Approach) can be created based on RS and the traits approach on the basis of traits, genesis, structures, taxonomy and the function of water diversity.

Monitoring water diversity and water quality and their interactions is complex. Therefore, future monitoring requires a holistic and interdisciplinary approach (a combination of water, geological and vegetation diversity) with analytical tools that combine in situ data, RS platforms and databases and integrate ecological modelling (see www.globewq.info). In addition, the traits approach allows the application of semantic data integration methods that enable the monitoring and modelling of ecosystem integrity (see the eReefs Research in Australia, <https://research.csiro.au/ereefs/> accessed on 26 June 2024, Figure 10).

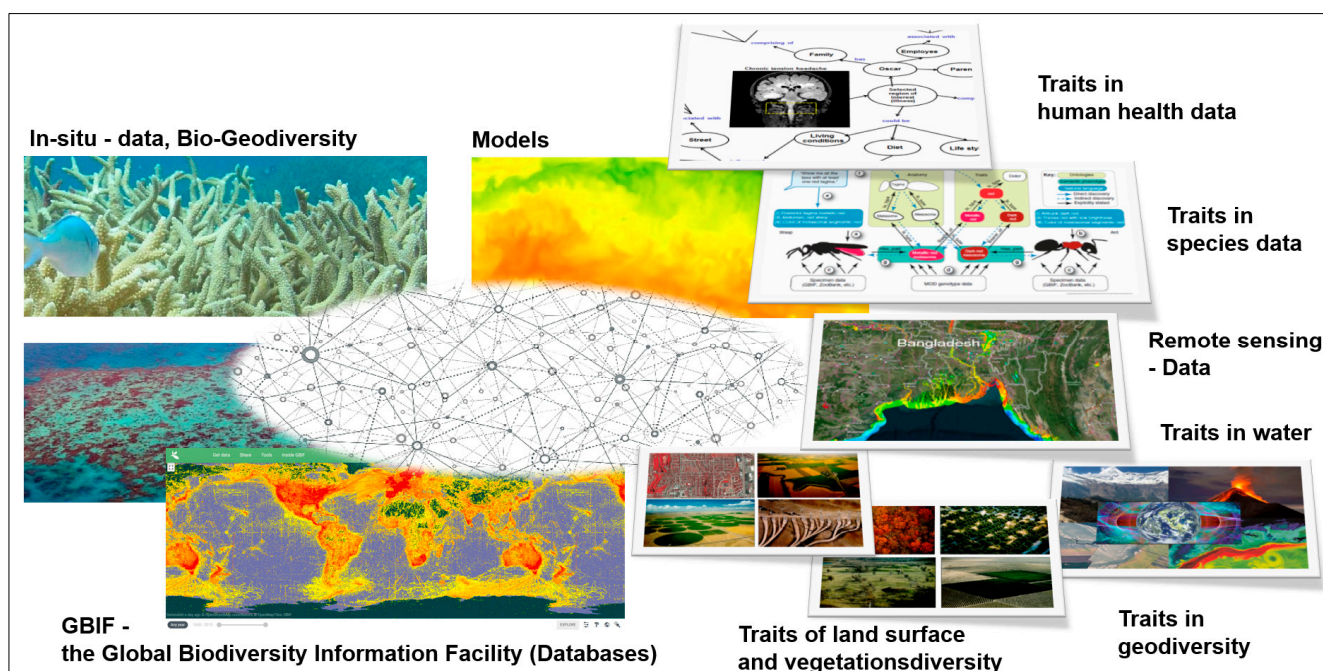


Figure 10. The trait approach allows the application of semantic data integration methods that enable monitoring and modelling of ecosystem integrity (see the eReefs Research in Australia, <https://research.csiro.au/ereefs/> accessed on 26 June 2024).

In addition, the freely available tool (ESIS/Imalys—Ecosystem Integrity Remote Sensing/Modelling Tool and Service) has been developed based on traits and RS data [196]. The tool is under continuous development and can be downloaded from GitLab (<https://doi.org/10.5281/zenodo.8116370>, accessed on 26 June 2024). The tool can therefore be used to support research, application and planning to better classify and model RS data based on the traits approach in order to achieve a better understanding of ecosystems and integrative processes.

Author Contributions: A.L.: conceptualisation, methodology, writing—original draft preparation, writing—review and editing, visualisation, supervision; L.B.: investigation, resources; S.A.B.: investigation, resources, writing—original draft preparation, writing—review and editing, visualisation; E.B.: investigation, resources, writing—review and editing, visualisation; J.B.: investigation, resources; J.M.H.: investigation, resources, visualisation; T.H.: writing—review and editing, visualisation; M.H.: investigation, resources, writing—original draft preparation, writing—review and editing; A.J.: investigation, resources; K.K.: investigation, resources, writing—original draft preparation, writing—review and editing; N.O.: investigation, resources, writing—original draft preparation, writing—review and editing; M.P.: investigation, resources; F.S.: investigation, resources; P.S.: investigation, resources; F.v.T.: writing—review and editing, visualisation; M.V.: investigation, resources; C.G.: investigation, resources. All authors have read and agreed to the published version of the manuscript.

Funding: This research received no external funding.

Data Availability Statement: No data were integrated in this paper.

Acknowledgments: Our special thanks go to the Helmholtz Centre for Environmental Research—UFZ and the TERENO project, funded by the Helmholtz Association and the Federal Ministry of Education and Research, for providing the remote sensing research. The authors gratefully acknowledge the German Helmholtz Association for supporting the activities of research data science approaches and advanced data technologies. András Jung was supported by project No. TKP2021-NVA-29, which was implemented with the support of the Hungarian Ministry of Culture and Innovation from the National Fund for Research, Development and Innovation under the TKP2021-NVA funding programme.

Conflicts of Interest: Author Thomas Heege and Fabian von Trentini were employed by the company EOMAP GmbH & Co KG. The remaining authors declare that the research was conducted in the absence of any commercial or financial relationships that could be construed as a potential conflict of interest.

Appendix A

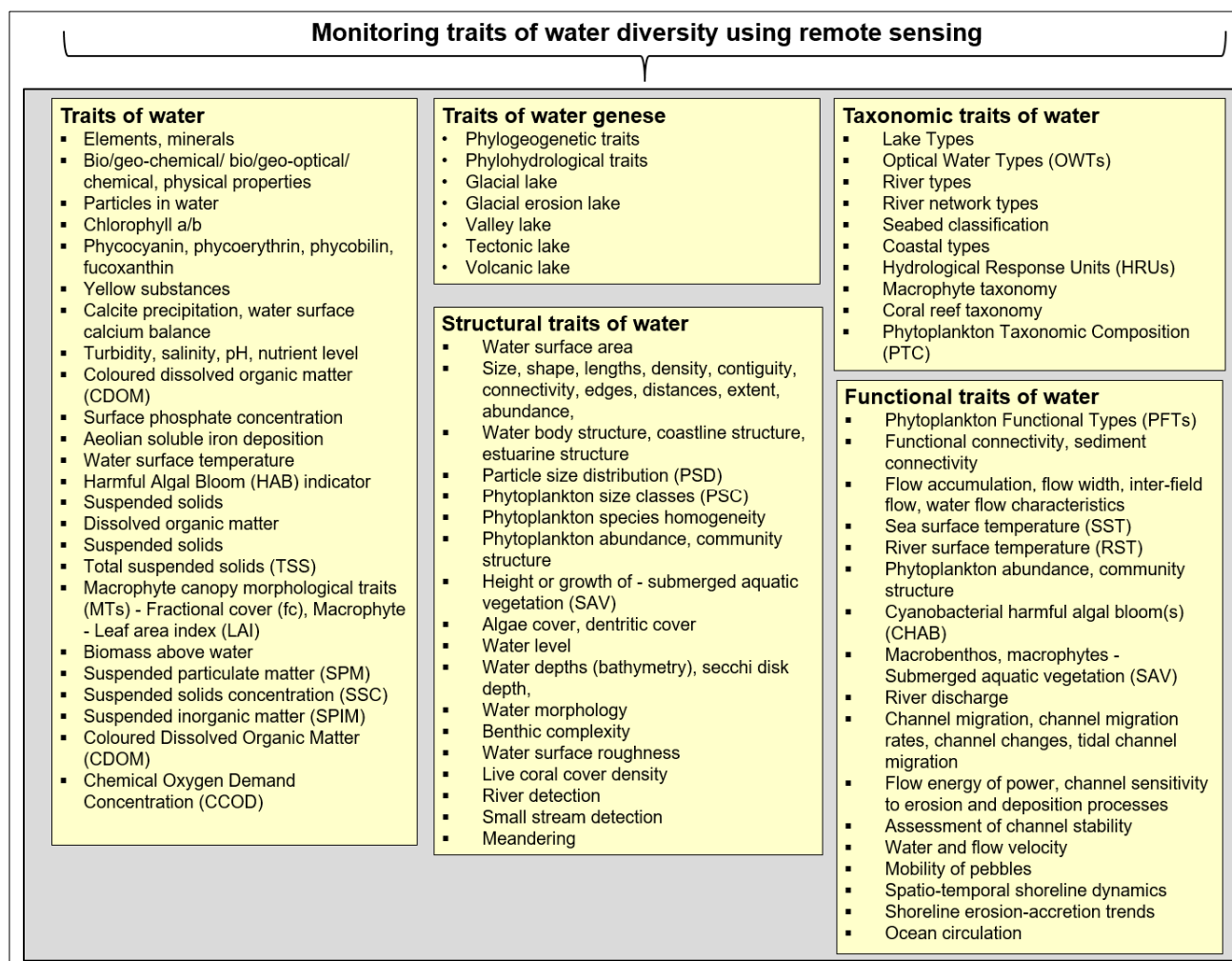


Figure A1. Monitoring traits of water diversity using remote sensing, the traits of water, the traits of water genesis, the structural traits of water, the taxonomic traits of water and the functional traits of water.

Table A1. Remote sensing-aided examples derived in monitoring the characteristics of water diversity (water trait diversity, geogenic water trait diversity, structural water diversity, taxonomic water diversity and functional water diversity) and shifts and disturbances.

Water Traits	Mission/Platform Sensor	References
Sea surface temperature (SST), river surface temperature (RST)	GOES-8 IMAGER ³ , METEOSAT (MSG) SEVIRI ³ , NOAA POES AVHRR ³ , Aqua MODIS ³ , Terra ASTER ³ , Landsat 5 TM ³ , Landsat 7 ETM+ ³ , ERS-1/-2/ ATSR1 ³ , FLIR Tau ²	[197–211]
Chlorophyll-a (CHL)—phytoplankton (large/small phytoplankton)	OrbView-2 SeaWiFS ³ , Terra/Aqua MODIS ³ , Envisat MERIS ³ , Sentinel-3 OLCI ³ , Sentinel-2 ³ , Landsat 8 OLI/TIRS ³ , APEX ² , LiDAR ¹	[23,186,212–231]

Table A1. Cont.

Water Traits	Mission/Platform Sensor	References
Phycocyanin (PC) and phycoerythrin—other photosynthetic and accessory pigments (cyanobacterial blooms indicated by phycocyanin (PC) and phycoerythrin)	Terra/Aqua MODIS ³ , Sentinel-3 OLCI ³ , Landsat 8 OLI/TIRS ³ , NOAA GLERL ² , Sentinel-2 MSI ³	[214,219–221,232,233]
Fluorescence—sun-induced fluorescence emission by phytoplankton/open-ocean phytoplankton chlorophyll fluorescence, (Fsat) distributions	Terra/Aqua MODIS ³	[219,229,234]
Chemical oxygen demand concentration (CCOD) Water pollution	Sentinel ³ A/Ocean ³ , Land Colour Instrument (OLCI) ³	[235]
Algal blooms indicator (HAB)/Cyanobacterial Harmful Algal Bloom(s) (CHAB)	Landsat 8 ³ , Sentinel-2A,2B ³ , Sentinel-3A, 3B, 3C ³ , WorldView-3 ³ , PRISMA ³	[236–239]
Phytoplankton populations, community structures (e.g., phaeocystis and diatoms, phaeocystis globosa spp)	OrbView-2 SeaWiFS ³	[219,240]
Aquatic Phytoplankton Functional Types (A-PFTs)	OrbView-2 SeaWiFS ³ , MERIS ³ , APEX ²	[188,219,241,242]
Macrobenthos, macrophytes—submerged aquatic vegetation (SAV)	QuickBird BGIS2000 ³ , RapidEye REIS ³ , Sentinel-2 ³ , Landsat 8 OLI/TIRS ³ , HJ-WVC ³ , Daedalus MIVIS ² , Ocean Portable Hyperspectral Imager for Low-Light ² , Spectroscopy (Ocean PHILLS) ² , VarioCAM ¹	[82,228,243–250]
Lake-type classification	Landsat TM/ETM +/OLI ³ , ASTER GDEM ³	[78,251]
Optical water types (OWTs)	Sentinel-3 OLCI ³	[214]
Channel landforms, hydrogeomorphic units including coarse woody debris, hydraulic (fluvial) landform classification, hydro-morphological units, riverscape units, river geomorphic units, in-stream mesohabitats, tidal channel characteristics	SAR ³ , aerial images ² , LiDAR ²	[252–255]
Coast taxonomy, coast types (small delta, tidal system, lagoon, fjord and fjärd, large river, tidal estuary, ria, karst, arheic)	Different RADAR sensors ³ , different optical RS sensors ³	[179]
Macrophyte taxonomy/macrophyte taxa/aquatic plant species	Canon Ixus 70 ^{®1} , Sentinel 2 ³ Airborne Hyperspectral ²	[167,256]
Coral classification, coral reef habitat mapping, seagrass, aquatic vegetation community	Landsat 8 OLI/TIRS ³ , RapidEye REIS ³ , Ocean Portable Hyperspectral Imager for Low-Light ³ , Spectroscopy (Ocean PHILLS) ² , Sentinel-2 ³ , QuickBird ³ , WorldView ³ , NOAA ³ Worldview-2 ³ , HyMAP ² , airborne (imaging spectrometer (hyperspectral) ² , Planet Dove satellite imagery ² , Airborne data visible-to-shortwave infrared ² , (VSWIR) imaging spectrometer and a light detection and ranging ² LiDAR ² , CASI ²	[113,151,219,249,257–263]
Coral mortality	Airborne data visible-to-shortwave infrared ² , (VSWIR) imaging spectrometer and a light detection and ranging ² , LiDAR ²	[261]

Table A1. Cont.

Water Traits	Mission/Platform Sensor	References
Live coral cover density	Airborne data visible-to-shortwave infrared ² , VSWIR imaging spectrometer and a light detection and ranging ² , LiDAR ²	[151]
Reef rugosity	LiDAR ² , VSWIR spectrometer Data ²	[264]
Macrophyte canopy morphological traits (MTs)—fractional cover (fc)	APEX ²	[242]
Macrophyte—Leaf Area Index (LAI)	Spot-5 HRG ³ , Sentinel-2 MSI ³ Landsat 7 ETM+ ³ , Landsat 8 OLI/TIRS ³ , APEX ²	[242,245]
Above-water biomass	Landsat 8 OLI/TIRS ³ , Terra/Aqua MODIS ³ , Landsat 8 OLI/TIRS ³ , GaoFen-1 WFV ³ , WorldView-2 WV110 ³ , APEX ²	[242,265,266]
Macrophyte seasonal dynamics (phenology)/spatial distribution patterns/species-dependent variability, interannual changes of aquatic vegetation	Spot-5 HRG ³ , Sentinel-2 MSI ³ , Landsat 7 ETM+ ³ , Landsat 8 OLI/TIRS ³ , HJ-1A/B WVC ³ , Landsat 5 TM ³	[245,267]
Growth height of submerged aquatic vegetation (SAV)	Spot-6 NAOMI ³	[268]
Suspended Particulate Matter (SPM), also referred to as the Total Suspended Matter (TSM)	Envisat MERIS ³ , Terra/Aqua MODIS ³ , Landsat 8 OLI/TIRS ³ , Sentinel 3 OLCI ³ , AHS ²	[23,219,224,265,269–272]
Suspended Sediment Concentration (SSC)	Envisat MERIS ³	[219,273]
Suspended inorganic particulate matter (SPIM)	Sentinel-2 MSI ³ , Daedalus MIVIS ²	[219,248,274]
Coloured Dissolved Organic Matter (CDOM)	OrbView-2 SeaWiFS ³ , Envisat MERIS ³ , Landsat 5 TM ³ < Landsat 7 ETM+ ³ , Landsat 8 OLI/TIRS ³ , Sentinel-2 MSI ³ , Sentinel-3 OLCI ³ , Daedalus MIVIS ²	[23,212,217,219,222,224,248,275,276]
Sediment and sediment dynamic, carbon and nutrient loads, particulate organic carbon (POC)	EO-1 Hyperion ³ , Terra/Aqua MODIS ³ , Landsat 5 TM ³ , Landsat 7 ETM+ ³ , Sentinel-2 MSI ³	[82,269,277,278]
Calcite precipitation, calcium balance in the water surface layer	Landsat 8 OLI/TIRS ³ , Sentinel-2 MSI ³	[279,280]
SEA or ocean water acidification/salinity	SMOS MIRAS ³ , PLMR ² , MODIS-OCGA ³	[281–285]
Surface nitrate concentration	Terra/Aqua MODIS ³	[229]
Surface phosphate concentration	Terra/Aqua MODIS ³	[229]
Aeolian soluble iron deposition	Terra/Aqua MODIS ³	[229]
Secchi disk depth, turbidity	OrbView-2 SeaWiFS ³ , Terra/Aqua MODIS ³ , Landsat 5 TM ³ , Landsat 7 ETM+ ³ , Landsat 8 OLI/TIRS ³ , Sentinel-2 MSI ³ , Sentinel-3 Ocean ³ , Land Colour Instrument (OLCI) ³ , Planet Dove satellites ³	[221,222,270,271,286–291]
Water depth, water transparency	Terra ASTER ³ , Terra/Aqua MODIS ³ , Landsat 8 OLI/TIRS ³ , Sentinel-2 MSI ³ , RapidEye REIS ² RIEGL VQ-820-G ² , Ocean Portable Hyperspectral Imager for Low-Light Spectroscopy (Ocean PHILLS) ² , AISA-EAGLE ²	[82,202,247,249,292–295]
Bathymetry, seabed mapping	Landsat 8 ³ , Sentinel-2 ³ , Multispectral ³ , Hyperspectral Imagery ³ , ICESat-2 ³ , LiDAR ²	[152,296–300]

Table A1. Cont.

Water Traits	Mission/Platform Sensor	References
River bathymetry	CASI 2/H, Daedalus 2/H, aerial images ² , LiDAR ²	[255,301–304]
Water height, water level	ENVISAT ³ , AMSR-E ³ TRMM ³ Daedalus 2/H, aerial images ² , LiDAR ²	[255,304–308]
Water surface roughness	LiDAR ² , RADAR ³	[122]
Water colour	Envisat MERIS ³ , Sentinel-3 OLCI ³	[23,309]
Submarine Groundwater Discharge (SGD)	Landsat 5 TM ³ , Landsat 7 ETM+ ³ Landsat 8 OLI/TIRS ³ , FLIR Systems ² , FLIR Tau ²	[310–315]
Groundwater nutrient fluxes	Landsat 5 TM ³ , Landsat 7 ETM+ ³	[311]
Riverine discharge	Terra/Aqua MODIS ³	[316]
Coastal fronts, plumes, oil slicks	OrbView-2 SeaWiFS ³ , Terra/Aqua MODIS ³ , Landsat 5 TM ³ , Landsat 7 ETM+ ³	[219,317]
Morphology, water level, water surface area, storage variations, extent, size, structure of water bodies, coastline changes	TerraSAR-X/TanDEM-X ³ , SRTM ³ , Landsat 5 TM ³ , Landsat 7 ETM+ ³ , Landsat 8 OLI ³ , Sentinel-2 ³ , WorldView-2 WV110 ³	[219,318–326]
Shallow water inversion	Sentinel-2 ³	[82]
Benthic complexity	Sentinel-2 ³	[152]
Salinity	MODIS-OCGA ³	[285]
River detection, small streams detection	SAR ³ , Landsat-5 TM/-7 ETM+/-8 OLI ³ , aerial images ² , aerial images ¹ , LiDAR ²	[255,327–330]
Channel characteristics, floodplain morphology hydraulic channel morphology, geometries, topography, river width arc length, longitudinal transect (width, depth and longitudinal channel slope, below water line morphology), morphometric patterns of meanders (sinuosity, intrinsic wavelength, curvature and asymmetry), meander dynamics, channel geometry	SAR ³ , ENVISAT ³ , Terra/Aqua MODIS ³ , Landsat-5 TM/-7 ETM+/-8 OLI ³ , Sentinel-2 ³ , aerial images ² , LiDAR ²	[327,331–338]
Channel migration, channel migration rates, channel planform changes and tidal channel migration Channel changes, disturbances, temporal evolution of natural and artificial abandoned channels, canal position, systematic changes of the river banks and canal centre lines	SAR ³ , SRTM ³ , Landsat-5 TM ³ , Landsat-7/8 ETM+ ³ OLI ³ , aerial images ²	[254,339–344]
Flow energy of stream power, channel sensitivity to erosion and deposition processes and channel stability assessment	Landsat-1 MSS/-5 ³ TM/-8 OLI ³ , LiDAR ²	[345,346]
River discharge estimation (river discharge, run-off characteristics)	ENVISAT ³ , Jason-2/-3 ³ , Sentinel-3A ³ OLCI/SLSTR ³ , CryoSat-2 ³ , AltiKa ³ , ENVISAT ³ , Advanced RADAR Altimeter (RA-2) ³ , Terra/Aqua MODIS ³	[308,347]
Water and flow velocity	ENVISAT ³ , Terra/Aqua MODIS ³ , Aerial images ² , LiDAR ²	[255,333,348]

Table A1. Cont.

Water Traits	Mission/Platform Sensor	References
Fluvial sediment transport, sediment budget, channel bank erosion, exposed channel substrates and sediments, suspended soil concentration and bed material, percentage clay, silt and sand in inter-tidal sediments, suspended sediments, flood bank overbank sedimentation, sediment wave and sand mining	LiDAR ² , Radio frequency identification ¹	[337,349–351]
Stream bank retreat	Aerial images ² , LiDAR ²	[352–357]
Grain characteristics, grain size, gravel size, shape, bed and bank sediment size	Daedalus ² , aerial images ² , aerial images ² , LiDAR ²	[177,358–362]
Pebble mobility	Radio frequency identification technologies ¹	[363]
Coastal dynamical and bio-geo-chemical patterns	NOAA/MetOp AVHRR ³ , ERS-1 ³ , TOPEX ³ , Nimbus-7 CZCS ³	[364]
Coastal landforms and coastline and shoreline detection	SRTM ³ , ALOS ³ , NOAA ³ , Landsat-7 ETM+ ³ , Terra ASTER ³ , IKONOS OSA ³ , LiDAR ²	[119,365,366]
Spatio-temporal shoreline dynamic, shoreline erosion–accretion trends, coast changes, cliff retreat and erosion hotspots	SRTM ³ , SAR ³ , Landsat-4 MSS/-5 TM ³ , Landsat-8 OLI ³ , SPOT 5 ³ , Sentinel-2 ² , aerial images ² , LiDAR ²	[367–374]
Different morphometric shoreline indicators: morphological reference lines, vegetation limits, instant tidal levels and wetting limits, tidal datum indicators, virtual reference lines, beach contours and storm lines	Different optical RS sensors ³ , LiDAR ²	[118,375,376]
Coastal dynamical and bio-geo-chemical patterns	NOAA/MetOp AVHRR ³ , ERS-1 ³ , TOPEX ³ , Nimbus-7 CZCS ³	[364]
Trophic state (eutrophication): Chlorophyll-a (CHL-a), total phosphorous and Secchi disk transparency	MODIS ³ , MERIS ³ , Landsat-8 OLI ³ , Sentinel-2B ³ , PRISMA ³	[171–176,377,378]
Phytoplankton Functional Types (PFTs), Chlorophyll-a-Konzentration, different photosynthetic Pigments, Particle Size Distribution (PSD), Phytoplankton Size Classes (PSCs), Bio-Optical Characteristics (BOT)	NOAA ³ , LiDAR ¹ , PRISMA ³ , DESIS ³ , EnMAP ³ , MERIS ³	[120,185,187–189]
Ocean Circulation	SAR Nadir Altimetry ³	[379]

The sensor is used on the RS platform: UAV 1—unmanned aerial vehicles (UAV); airborne 2—airborne RS platform; spaceborne 3—spaceborne RS platform.

References

- Dörnhöfer, K.; Oppelt, N. Remote sensing for lake research and monitoring—Recent advances. *Ecol. Indic.* **2016**, *64*, 105–122. [CrossRef]
- Moss, B. Cogs in the endless machine: Lakes, climate change and nutrient cycles: A review. *Sci. Total Environ.* **2012**, *434*, 130–142. [CrossRef] [PubMed]
- Fabian, P.S.; Kwon, H.-H.; Vithanage, M.; Lee, J.-H. Modeling, challenges, and strategies for understanding impacts of climate extremes (droughts and floods) on water quality in Asia: A review. *Environ. Res.* **2023**, *225*, 115617. [CrossRef] [PubMed]
- Lin, B.; Zeng, Y.; Asner, G.P.; Wilcove, D.S. Coral reefs and coastal tourism in Hawaii. *Nat. Sustain.* **2023**, *6*, 254–258. [CrossRef]
- Carpenter, S.R.; Stanley, E.H.; Vander Zanden, M.J. State of the World’s Freshwater Ecosystems: Physical, Chemical, and Biological Changes. *Annu. Rev. Environ. Resour.* **2011**, *36*, 75–99. [CrossRef]
- Liu, Y.; Jiang, X.; Li, D.; Shen, J.; An, S.; Leng, X. Intensive human land uses cause the biotic homogenization of algae and change their assembly process in a major watershed of China. *Sci. Total Environ.* **2023**, *871*, 162115. [CrossRef]

7. Issac, M.N.; Kandasubramanian, B. Effect of microplastics in water and aquatic systems. *Environ. Sci. Pollut. Res.* **2021**, *28*, 19544–19562. [[CrossRef](#)] [[PubMed](#)]
8. Mukonza, S.S.; Chiang, J.-L. Satellite sensors as an emerging technique for monitoring macro- and microplastics in aquatic ecosystems. *Water Emerg. Contam. Nanoplast.* **2022**, *1*, 17. [[CrossRef](#)]
9. Ding, C.; He, J. Effect of antibiotics in the environment on microbial populations. *Appl. Microbiol. Biotechnol.* **2010**, *87*, 925–941. [[CrossRef](#)]
10. de Wit, H.A.; Valinia, S.; Weyhenmeyer, G.A.; Futter, M.N.; Kortelainen, P.; Austnes, K.; Hessen, D.O.; Räike, A.; Laudon, H.; Vuorenmaa, J. Current Browning of Surface Waters Will Be Further Promoted by Wetter Climate. *Environ. Sci. Technol. Lett.* **2016**, *3*, 430–435. [[CrossRef](#)]
11. Kumar, P.; Lai, S.H.; Wong, J.K.; Mohd, N.S.; Kamal, M.R.; Afan, H.A.; Ahmed, A.N.; Sherif, M.; Sefelnasr, A.; El-Shafie, A. Review of Nitrogen Compounds Prediction in Water Bodies Using Artificial Neural Networks and Other Models. *Sustainability* **2020**, *12*, 4359. [[CrossRef](#)]
12. Nazari Sharabian, M.; Ahmad, S.; Karakouzian, M. Climate Change and Eutrophication: A Short Review. *Eng. Technol. Appl. Sci. Res.* **2018**, *8*, 3668–3672. [[CrossRef](#)]
13. Rodgers, E.M. Adding climate change to the mix: Responses of aquatic ectotherms to the combined effects of eutrophication and warming. *Biol. Lett.* **2021**, *17*. [[CrossRef](#)] [[PubMed](#)]
14. Paerl, H.W.; Huisman, J. Blooms Like It Hot. *Science* **2008**, *320*, 57–58. [[CrossRef](#)] [[PubMed](#)]
15. Kraemer, B.M.; Mehner, T.; Adrian, R. Reconciling the opposing effects of warming on phytoplankton biomass in 188 large lakes. *Sci. Rep.* **2017**, 1–7. [[CrossRef](#)]
16. Paraskevopoulou, S.; Tiedemann, R.; Weithoff, G. Differential response to heat stress among evolutionary lineages of an aquatic invertebrate species complex. *Biol. Lett.* **2018**, *14*. [[CrossRef](#)] [[PubMed](#)]
17. Gray, W.B.; Shimshack, J.P. The Effectiveness of Environmental Monitoring and Enforcement: A Review of the Empirical Evidence. *Rev. Environ. Econ. Policy* **2011**, *5*, 3–24. [[CrossRef](#)]
18. Birk, S.; Bonne, W.; Borja, A.; Brucet, S.; Courrat, A.; Poikane, S.; Solimini, A.; van de Bund, W.; Zampoukas, N.; Hering, D. Three hundred ways to assess Europe’s surface waters: An almost complete overview of biological methods to implement the Water Framework Directive. *Ecol. Indic.* **2012**, *18*, 31–41. [[CrossRef](#)]
19. Warne, M.S.J.; Batley, G.E.; Braga, O.; Chapman, J.C.; Fox, D.R.; Hickey, C.W.; Stauber, J.L.; Van Dam, R. Revisions to the derivation of the Australian and New Zealand guidelines for toxicants in fresh and marine waters. *Environ. Sci. Pollut. Res.* **2014**, *21*, 51–60. [[CrossRef](#)]
20. Luigi Boschetti, M.B. Multi-temporal assessment of bio-physical parameters in lakes Garda and Trasimeno from MODIS and MERIS. *Ital. J. Remote Sens.* **2011**, 49–62. [[CrossRef](#)]
21. van Puijenbroek, P.J.T.M.; Evers, C.H.M.; van Gaalen, F.W. Evaluation of Water Framework Directive metrics to analyse trends in water quality in the Netherlands. *Sustain. Water Qual. Ecol.* **2015**, *6*, 40–47. [[CrossRef](#)]
22. Reyjol, Y.; Argillier, C.; Bonne, W.; Borja, A.; Buijse, A.D.; Cardoso, A.C.; Daufresne, M.; Kernan, M.; Ferreira, M.T.; Poikane, S.; et al. Assessing the ecological status in the context of the European Water Framework Directive: Where do we go now? *Sci. Total Environ.* **2014**, 497–498, 332–344. [[CrossRef](#)] [[PubMed](#)]
23. Dörnhöfer, K.; Scholze, J.; Stelzer, K.; Oppelt, N. Water Colour Analysis of Lake Kummerow Using Time Series of Remote Sensing and In Situ Data. *PFG—J. Photogramm. Remote Sens. Geoinf. Sci.* **2018**, *54*, 2283. [[CrossRef](#)]
24. Williamson, C.E.; Saros, J.E.; Vincent, W.F.; Smol, J.P. Lakes and reservoirs as sentinels, integrators, and regulators of climate change. *Limnol. Oceanogr.* **2009**, *54*, 2273–2282. [[CrossRef](#)]
25. Schmidt, C.; Bärlund, I.; Batool, M.; Buettner, O.; Duerr, H.; Floerke, M.; Heege, T.; Jomaa, S.; Kumar, R.; Paulsen, H.; et al. Improving global water quality information by combining in-situ data, remote sensing and modeling. In Proceedings of the EGU General Assembly 2023, Vienna, Austria, 24–28 April 2023; EGU23-13215. [[CrossRef](#)]
26. Samarinas, N.; Spiliotopoulos, M.; Tziolas, N.; Loukas, A. Synergistic Use of Earth Observation Driven Techniques to Support the Implementation of Water Framework Directive in Europe: A Review. *Remote Sens.* **2023**, *15*, 1983. [[CrossRef](#)]
27. Cavender-Bares, J.; Gamon, J.A.; Townsend, P.A. (Eds.) *Remote Sensing of Plant Biodiversity*; Springer International Publishing: Cham, Switzerland, 2020; ISBN 978-3-030-33156-6.
28. Skidmore, A.K.; Coops, N.C.; Neinavaz, E.; Ali, A.; Schaepman, M.E.; Paganini, M.; Kissling, W.D.; Vihervaara, P.; Darvishzadeh, R.; Feilhauer, H.; et al. Priority list of biodiversity metrics to observe from space. *Nat. Ecol. Evol.* **2021**, *5*, 896–906. [[CrossRef](#)] [[PubMed](#)]
29. Zarnetske, P.; Read, Q.; Record, S.; Gaddis, K.; Pau, S.; Hobi, M.; Malone, S.; Costanza, J.; Dahlin, K.; Latimer, A.; et al. Towards connecting biodiversity and geodiversity across scales with satellite remote sensing. *Glob. Ecol. Biogeogr.* **2019**, *28*, 548–556. [[CrossRef](#)] [[PubMed](#)]
30. Vernham, G.; Bailey, J.J.; Chase, J.M.; Hjort, J.; Field, R.; Schrod, F. Understanding trait diversity: The role of geodiversity. *Trends Ecol. Evol.* **2023**, 1–13. [[CrossRef](#)] [[PubMed](#)]
31. Lausch, A.; Baade, J.; Bannehr, L.; Borg, E.; Bumberger, J.; Chabrilat, S.; Dietrich, P.; Gerighausen, H.; Glässer, C.; Hacker, J.; et al. Linking Remote Sensing and Geodiversity and Their Traits Relevant to Biodiversity—Part I: Soil Characteristics. *Remote Sens.* **2019**, *11*, 2356. [[CrossRef](#)]

32. Lausch, A.; Schaepman, M.E.; Skidmore, A.K.; Catana, E.; Bannehr, L.; Bastian, O.; Borg, E.; Bumberger, J.; Dietrich, P.; Glässer, C.; et al. Remote Sensing of Geomorphodiversity Linked to Biodiversity—Part III: Traits, Processes and Remote Sensing Characteristics. *Remote Sens.* **2022**, *14*, 2279. [[CrossRef](#)]
33. Duan, W.; Maskey, S.; Chaffe, P.L.B.; Luo, P.; He, B.; Wu, Y.; Hou, J. Recent Advancement in Remote Sensing Technology for Hydrology Analysis and Water Resources Management. *Remote Sens.* **2021**, *13*, 1097. [[CrossRef](#)]
34. Kachelriess, D.; Wegmann, M.; Gollock, M.; Pettorelli, N. The application of remote sensing for marine protected area management. *Ecol. Indic.* **2014**, *36*, 169–177. [[CrossRef](#)]
35. Cerra, D.; Marshall, D.; Heiden, U.; Alonso, K.; Bachmann, M.; Burch, K.; Carmona, E.; Dietrich, D.; Lester, H.; Knodt, U.; et al. The Spaceborne Imaging Spectrometer Desis: Data Access, Outreach Activities, and Scientific Applications. In Proceedings of the IGARSS 2022—2022 IEEE International Geoscience and Remote Sensing Symposium, Kuala Lumpur, Malaysia, 17–22 July 2022; pp. 5395–5398.
36. Chabrilat, S.; Segl, K.; Foerster, S.; Brell, M.; Guanter, L.; Schickling, A.; Storch, T.; Honold, H.-P.; Fischer, S. EnMAP Pre-Launch and Start Phase: Mission Update. In Proceedings of the IGARSS 2022—2022 IEEE International Geoscience and Remote Sensing Symposium, Kuala Lumpur, Malaysia, 17–22 July 2022; pp. 5000–5003.
37. Torresani, M.; Rocchini, D.; Alberti, A.; Moudry, V.; Heym, M.; Thouverai, E.; Kacic, P.; Tomelleri, E. LiDAR GEDI derived tree canopy height heterogeneity reveals patterns of biodiversity in forest ecosystems. *Ecol. Inform.* **2023**, *76*, 102082. [[CrossRef](#)] [[PubMed](#)]
38. Le Quilleuc, A.; Collin, A.; Jasinski, M.F.; Devillers, R. Very high-resolution satellite-derived bathymetry and habitat mapping using pleiades-1 and icesat-2. *Remote Sens.* **2022**, *14*, 133. [[CrossRef](#)]
39. Cawse-Nicholson, K.; Townsend, P.A.; Schimel, D.; Assiri, A.M.; Blake, P.L.; Buongiorno, M.F.; Campbell, P.; Carmon, N.; Casey, K.A.; Correa-Pabón, R.E.; et al. NASA's surface biology and geology designated observable: A perspective on surface imaging algorithms. *Remote Sens. Environ.* **2021**, *257*. [[CrossRef](#)]
40. Pahlevan, N.; Smith, B.; Schalles, J.; Binding, C.; Cao, Z.; Ma, R.; Alikas, K.; Kangro, K.; Gurlin, D.; Hà, N.; et al. Seamless retrievals of chlorophyll-a from Sentinel-2 (MSI) and Sentinel-3 (OLCI) in inland and coastal waters: A machine-learning approach. *Remote Sens. Environ.* **2020**, *240*, 111604. [[CrossRef](#)]
41. Weithoff, G.; Beisner, B.E. Measures and Approaches in Trait-Based Phytoplankton Community Ecology—From Freshwater to Marine Ecosystems. *Front. Mar. Sci.* **2019**, *6*, 1–11. [[CrossRef](#)]
42. Rocchini, D.; Santos, M.J.; Ustin, S.L.; Féret, J.; Asner, G.P.; Beierkuhnlein, C.; Dalponte, M.; Feilhauer, H.; Foody, G.M.; Geller, G.N.; et al. The Spectral Species Concept in Living Color. *J. Geophys. Res. Biogeosci.* **2022**, *127*, 1–13. [[CrossRef](#)]
43. Le Provost, G.; Thiele, J.; Westphal, C.; Penone, C.; Allan, E.; Neyret, M.; van der Plas, F.; Ayasse, M.; Bardgett, R.D.; Birkhofer, K.; et al. Contrasting responses of above- and belowground diversity to multiple components of land-use intensity. *Nat. Commun.* **2021**, *12*, 3918. [[CrossRef](#)]
44. Palmer, M.W.; Earls, P.G.; Hoagland, B.W.; White, P.S.; Wohlgemuth, T. Quantitative tools for perfecting species lists. *Environmetrics* **2002**, *13*, 121–137. [[CrossRef](#)]
45. Lausch, A.; Selsam, P.; Pause, M.; Bumberger, J. Monitoring vegetation- and geodiversity with remote sensing and traits. *Philos. Trans. R. Soc. A Math. Phys. Eng. Sci.* **2024**, *382*. [[CrossRef](#)]
46. Weithoff, G. The concepts of 'plant functional types' and 'functional diversity' in lake phytoplankton - a new understanding of phytoplankton ecology? *Freshw. Biol.* **2003**, *48*, 1669–1675. [[CrossRef](#)]
47. Litchman, E.; Klausmeier, C.A. Trait-Based Community Ecology of Phytoplankton. *Annu. Rev. Ecol. Evol. Syst.* **2008**, *39*, 615–639. [[CrossRef](#)]
48. Lange, K.; Townsend, C.R.; Matthaei, C.D. A trait-based framework for stream algal communities. *Ecol. Evol.* **2016**, *6*, 23–36. [[CrossRef](#)]
49. Bolius, S.; Wiedner, C.; Weithoff, G. High local trait variability in a globally invasive cyanobacterium. *Freshw. Biol.* **2017**, *62*, 1879–1890. [[CrossRef](#)]
50. Weithoff, G.; Gaedke, U. Mean functional traits of lake phytoplankton reflect seasonal and inter-annual changes in nutrients, climate and herbivory. *J. Plankton Res.* **2017**, *39*, 509–517. [[CrossRef](#)]
51. Hardikar, R.; Haridevi, C.K.; Deshbhratar, S. Trait-based classification and environmental drivers of phytoplankton functional structure from anthropogenically altered tropical creek, Thane Creek India. *Mar. Pollut. Bull.* **2024**, *198*, 115767. [[CrossRef](#)]
52. Green, J.L.; Bohannan, J.M.; Whitaker, R.J. Microbial biogeography: From taxonomy to traits. *Science* **2008**, *320*, 1039–1043. [[CrossRef](#)]
53. Lausch, A.; Bastian, O.; Klotz, S.; Leitão, P.J.; Jung, A.; Rocchini, D.; Schaepman, M.E.; Skidmore, A.K.; Tischendorf, L.; Knapp, S. Understanding and assessing vegetation health by in situ species and remote-sensing approaches. *Methods Ecol. Evol.* **2018**, *9*, 1799–1809. [[CrossRef](#)]
54. Lausch, A.; Bannehr, L.; Beckmann, M.; Boehm, C.; Feilhauer, H.; Hacker, J.M.; Heurich, M.; Jung, A.; Klenke, R.; Neumann, C.; et al. Linking Earth Observation and taxonomic, structural and functional biodiversity: Local to ecosystem perspectives. *Ecol. Indic.* **2016**, *70*, 317–339. [[CrossRef](#)]
55. Lausch, A.; Erasmí, S.; King, D.; Magdon, P.; Heurich, M. Understanding Forest Health with Remote Sensing -Part I—A Review of Spectral Traits, Processes and Remote-Sensing Characteristics. *Remote Sens.* **2016**, *8*, 1029. [[CrossRef](#)]

56. Lausch, A.; Borg, E.; Bumberger, J.; Dietrich, P.; Heurich, M.; Huth, A.; Jung, A.; Klenke, R.; Knapp, S.; Mollenhauer, H.; et al. Understanding Forest Health with Remote Sensing, Part III: Requirements for a Scalable Multi-Source Forest Health Monitoring Network Based on Data Science Approaches. *Remote Sens.* **2018**, *10*, 1120. [CrossRef]
57. Lausch, A.; Erasmi, S.; King, D.J.; Magdon, P.; Heurich, M. Understanding forest health with Remote sensing-Part II—A review of approaches and data models. *Remote Sens.* **2017**, *9*, 129. [CrossRef]
58. Wellmann, T.; Haase, D.; Knapp, S.; Salbach, C.; Selsam, P.; Lausch, A. Urban land use intensity assessment: The potential of spatio-temporal spectral traits with remote sensing. *Ecol. Indic.* **2018**, *85*, 190–203. [CrossRef]
59. Andersson, E.; Haase, D.; Anderson, P.; Cortinovis, C.; Goodness, J.; Kendal, D.; Lausch, A.; McPhearson, T.; Sikorska, D.; Wellmann, T. What are the traits of a social-ecological system: Towards a framework in support of urban sustainability. *npj Urban Sustain.* **2021**, *1*, 14. [CrossRef]
60. EEA. *European Waters—Assessment of Status and Pressures 2018, Publications Office EEA Report No. 7/2018*; 2018; ISSN 1725-9177. Available online: <https://data.europa.eu/doi/10.2800/303664> (accessed on 26 June 2024).
61. Schultz, G.A. Remote sensing in hydrology. *J. Hydrol.* **1988**, *100*, 239–265. [CrossRef]
62. Lausch, A.; Schaepman, M.E.; Skidmore, A.K.; Truckenbrodt, S.C.; Hacker, J.M.; Baade, J.; Bannehr, L.; Borg, E.; Bumberger, J.; Dietrich, P.; et al. Linking the Remote Sensing of Geodiversity and Traits Relevant to Biodiversity—Part II: Geomorphology, Terrain and Surfaces. *Remote Sens.* **2020**, *12*, 3690. [CrossRef]
63. McGraw, D.; Ohren, M. Humboldt River Basin Water Quality Standards Review. 2007. Available online: <https://citeseerx.ist.psu.edu/document?repid=rep1&type=pdf&doi=daecb67625801043034135d3af6c0546073da247> (accessed on 26 June 2024).
64. Schrodt, F.; Santos, M.J.; Bailey, J.J.; Field, R. Challenges and opportunities for biogeography—What can we still learn from von Humboldt? *J. Biogeogr.* **2019**, *46*, 1631–1642. [CrossRef]
65. Curtis, J.A.; Thorne, K.M.; Freeman, C.M.; Buffington, K.J. *A Summary of Water-Quality and Salt Marsh Monitoring, Humboldt Bay, California: U.S. Geological Survey Open-File Report 2022–1076*; USGS Publications Warehouse: Reston, VA, USA, 2022; 30p. [CrossRef]
66. Kruse, P. Review on water quality sensors. *J. Phys. D Appl. Phys.* **2018**, *51*, 203002. [CrossRef]
67. Yaroshenko, I.; Kirsanov, D.; Marjanovic, M.; Lieberzeit, P.A.; Korostynska, O.; Mason, A.; Frau, I.; Legin, A. Real-time water quality monitoring with chemical sensors. *Sensors* **2020**, *20*, 3432. [CrossRef]
68. Winston, M.; Oliver, T.; Couch, C.; Donovan, M.K.; Asner, G.P.; Conklin, E.; Fuller, K.; Grady, B.W.; Huntington, B.; Kageyama, K.; et al. Coral taxonomy and local stressors drive bleaching prevalence across the Hawaiian Archipelago in 2019. *PLoS ONE* **2022**, *17*, e0269068. [CrossRef] [PubMed]
69. Blanco-Gómez, P.; Luis Jiménez-García, J.; Cecilia, J.M. Low-cost automated GPS, electrical conductivity and temperature sensing device (EC + T Track) and Android platform for water quality monitoring campaigns. *HardwareX* **2023**, *13*, e00381. [CrossRef] [PubMed]
70. Trejo, D.S.; Bandera, A.; González, M. *Vision—Based Techniques for Automatic Marine Plankton Classification*; Springer: Dordrecht, The Netherlands, 2023; Volume 56, ISBN 0123456789.
71. Alahuhta, J.; Erős, T.; Kärnä, O.-M.; Soininen, J.; Wang, J.; Heino, J. Understanding environmental change through the lens of trait-based, functional, and phylogenetic biodiversity in freshwater ecosystems. *Environ. Rev.* **2019**, *27*, 263–273. [CrossRef]
72. Lehmann, M.K.; Gurlin, D.; Pahlevan, N.; Alikas, K.; Conroy, T.; Anstee, J.; Balasubramanian, S.V.; Barbosa, C.C.F.; Binding, C.; Bracher, A.; et al. GLORIA—A globally representative hyperspectral in situ dataset for optical sensing of water quality. *Sci. Data* **2023**, *10*, 100. [CrossRef] [PubMed]
73. Xi, H.; Hieronymi, M.; Krasemann, H.; Röttgers, R. Phytoplankton Group Identification Using Simulated and In situ Hyperspectral Remote Sensing Reflectance. *Front. Mar. Sci.* **2017**, *4*, 1–13. [CrossRef]
74. Fonvielle, J.A.; Giling, D.P.; Dittmar, T.; Berger, S.A.; Nejtgaard, J.C.; Lyche Solheim, A.; Gessner, M.O.; Grossart, H.; Singer, G. Exploring the Suitability of Ecosystem Metabolomes to Assess Imprints of Brownification and Nutrient Enrichment on Lakes. *J. Geophys. Res. Biogeosci.* **2021**, *126*, 1–19. [CrossRef]
75. Lyche Solheim, A.; Gundersen, H.; Mischke, U.; Skjelbred, B.; Nejtgaard, J.C.; Guislain, A.L.N.; Sperfeld, E.; Giling, D.P.; Haande, S.; Ballot, A.; et al. Lake browning counteracts cyanobacteria responses to nutrients: Evidence from phytoplankton dynamics in large enclosure experiments and comprehensive observational data. *Glob. Change Biol.* **2024**, *30*, 1–23. [CrossRef]
76. Chawla, I.; Karthikeyan, L.; Mishra, A.K. A review of remote sensing applications for water security: Quantity, quality, and extremes. *J. Hydrol.* **2020**, *585*, 124826. [CrossRef]
77. Foo, S.A.; Asner, G.P. Scaling up coral reef restoration using remote sensing technology. *Front. Mar. Sci.* **2019**, *6*. [CrossRef]
78. Wei, Y.; Jia, L.; Ma, X.; Lei, Z. Development genetic and stability classification of seasonal glacial lakes in a tectonically active area—A case study in Niangmuco, east margin of the Eastern Himalayan Syntaxis. *Front. Earth Sci.* **2024**, *12*, 1–13. [CrossRef]
79. Harris, D.L.; Webster, J.M.; Vila-Concejo, A.; Duce, S.; Leon, J.X.; Hacker, J. Defining multi-scale surface roughness of a coral reef using a high-resolution LiDAR digital elevation model. *Geomorphology* **2023**, *439*, 108852. [CrossRef]
80. Asner, G.P.; Vaughn, N.; Grady, B.W.; Foo, S.A.; Anand, H.; Carlson, R.R.; Shafron, E.; Teague, C.; Martin, R.E. Regional Reef Fish Survey Design and Scaling Using High-Resolution Mapping and Analysis. *Front. Mar. Sci.* **2021**, *8*, 1–17. [CrossRef]
81. Ventura, G.; Vilardo, G.; Terranova, C.; Sessa, E.B. Tracking and evolution of complex active landslides by multi-temporal airborne LiDAR data: The Montaguto landslide (Southern Italy). *Remote Sens. Environ.* **2011**, *115*, 3237–3248. [CrossRef]

82. Dörnhöfer, K.; Göritz, A.; Gege, P.; Pflug, B.; Oppelt, N. Water Constituents and Water Depth Retrieval from Sentinel-2A—A First Evaluation in an Oligotrophic Lake. *Remote Sens.* **2016**, *8*, 941. [[CrossRef](#)]
83. Wang, J.; Chen, X. A new approach to quantify chlorophyll-a over inland water targets based on multi-source remote sensing data. *Sci. Total Environ.* **2024**, *906*, 167631. [[CrossRef](#)] [[PubMed](#)]
84. Kim, J.; Seo, D. Three-dimensional augmentation for hyperspectral image data of water quality: An Integrated approach using machine learning and numerical models. *Water Res.* **2024**, *251*, 121125. [[CrossRef](#)] [[PubMed](#)]
85. Zhang, M.; Ibrahim, A.; Franz, B.A.; Sayer, A.M.; Werdell, P.J.; McKinna, L.I. Spectral correlation in MODIS water-leaving reflectance retrieval uncertainty. *Opt. Express* **2024**, *32*, 2490. [[CrossRef](#)] [[PubMed](#)]
86. Schaeffer, B.A.; Reynolds, N.; Ferriby, H.; Salls, W.; Smith, D.; Johnston, J.M.; Myer, M. Forecasting freshwater cyanobacterial harmful algal blooms for Sentinel-3 satellite resolved U.S. lakes and reservoirs. *J. Environ. Manag.* **2024**, *349*, 119518. [[CrossRef](#)]
87. Ulrich, C.; Hupfer, M.; Schwefel, R.; Bannehr, L.; Lausch, A. Mapping Specific Constituents of an Ochre-Coloured Watercourse Based on In Situ and Airborne Hyperspectral Remote Sensing Data. *Water* **2023**, *15*, 1532. [[CrossRef](#)]
88. Li, Z.; Sun, D.; Wang, S.; Huan, Y.; Zhang, H.; Liu, J.; He, Y. A global satellite observation of phytoplankton taxonomic groups over the past two decades. *Glob. Change Biol.* **2023**, *29*, 4511–4529. [[CrossRef](#)]
89. Asner, G.P.; Martin, R.E. Airborne spectranomics: Mapping canopy chemical and taxonomic diversity in tropical forests. *Front. Ecol. Environ.* **2009**, *7*, 269–276. [[CrossRef](#)]
90. Schwoerbel, J.; Brendelberger, H. *Einführung in die Limnologie*; 11. Auflag.; Springer: Berlin/Heidelberg, Germany, 2022; ISBN 978-3-662-63333-5.
91. Dieter, W.; Buch, N.; Sly, P.G. *The Development of an Aquatic Habitat Classification System of Lakes*; CRC Press, Taylor & Francis Group: Boca Raton, FL, USA, 2018; ISBN 13-978-1-315-89904-9.
92. Meyer, M.F.; Topp, S.N.; King, T.V.; Ladwig, R.; Pilla, R.M.; Dugan, H.A.; Eggleston, J.R.; Hampton, S.E.; Leech, D.M.; Oleksy, I.A.; et al. National-scale remotely sensed lake trophic state from 1984 through 2020. *Sci. Data* **2024**, *11*, 77. [[CrossRef](#)] [[PubMed](#)]
93. Asbury, M.; Schiettekatte, N.M.D.; Couch, C.S.; Oliver, T.; Burns, J.H.R.; Madin, J.S. Geological age and environments shape reef habitat structure. *Glob. Ecol. Biogeogr.* **2023**, *32*, 1230–1240. [[CrossRef](#)]
94. Bruggeman, J. A Phylogenetic Approach to the Estimation of Phytoplankton Traits 1. *J. Phycol.* **2011**, *47*, 52–65. [[CrossRef](#)] [[PubMed](#)]
95. Narwani, A.; Alexandrou, M.A.; Herrin, J.; Vouaux, A.; Zhou, C.; Oakley, T.H.; Cardinale, B.J. Common Ancestry Is a Poor Predictor of Competitive Traits in Freshwater Green Algae. *PLoS ONE* **2015**, *10*, e0137085. [[CrossRef](#)] [[PubMed](#)]
96. Liu, H.; Qu, X.; Xia, W.; Chen, Y. Taxonomic, functional, and phylogenetic diversity patterns reveal different processes shaping river fish assemblages in the Eastern Huai River Basin, China. *Water Biol. Secur.* **2023**, *2*, 100078. [[CrossRef](#)]
97. Grossart, H.-P.; Van den Wyngaert, S.; Kagami, M.; Wurzbacher, C.; Cunliffe, M.; Rojas-Jimenez, K. Fungi in aquatic ecosystems. *Nat. Rev. Microbiol.* **2019**, *17*, 339–354. [[CrossRef](#)]
98. Stein, A.; Gerstner, K.; Kreft, H. Environmental heterogeneity as a universal driver of species richness across taxa, biomes and spatial scales. *Ecol. Lett.* **2014**, *17*, 866–880. [[CrossRef](#)]
99. Li, J.; Ma, R.; Cao, Z.; Xue, K.; Xiong, J.; Hu, M.; Feng, X. Satellite Detection of Surface Water Extent: A Review of Methodology. *Water* **2022**, *14*, 1148. [[CrossRef](#)]
100. Birkett, C.M.; O'Brien, K.; Kinsey, S.; Ricko, M.; Li, Y. Enhancement of a global lake and reservoir database to aid climate studies and resource monitoring utilizing satellite radar altimetry. *J. Great Lakes Res.* **2022**, *48*, 37–51. [[CrossRef](#)]
101. Zhou, G.; Wu, G.; Zhou, X.; Xu, C.; Zhao, D.; Lin, J.; Liu, Z.; Zhang, H.; Wang, Q.; Xu, J.; et al. Adaptive model for the water depth bias correction of bathymetric LiDAR point cloud data. *Int. J. Appl. Earth Obs. Geoinf.* **2023**, *118*, 103253. [[CrossRef](#)]
102. Harvey, A.H.; Hrubý, J.; Meier, K. Improved and Always Improving: Reference Formulations for Thermophysical Properties of Water. *J. Phys. Chem. Ref. Data* **2023**, *52*, 011501. [[CrossRef](#)]
103. Bradbury, G.; Puttock, A.; Coxon, G.; Clarke, S.; Brazier, R.E. Testing a novel sonar-based approach for measuring water depth and monitoring sediment storage in beaver ponds. *River Res. Appl.* **2023**, *39*, 266–273. [[CrossRef](#)]
104. Jean Milien, E.; Nunes, G.M.; Pierre, G.; Hamilton, S.K.; Da Cunha, C.N. Hydrological Dynamics of the Pantanal, a Large Tropical Floodplain in Brazil, Revealed by Analysis of Sentinel-2 Satellite Imagery. *Water* **2023**, *15*, 2180. [[CrossRef](#)]
105. Karle, N.; Wolf, T.; Heege, T.; Schenk, K.; Klinger, P.; Schulz, K. Satellite remote sensing of chlorophyll and Secchi depth for monitoring lake water quality: A validation study. In *Earth Resources and Environmental Remote Sensing/GIS Applications X*; Schulz, K., Nikolakopoulos, K.G., Michel, U., Eds.; SPIE: Bellingham, WA, USA, 2019; p. 61.
106. Bresciani, M.; Giardino, C.; Fabbretto, A.; Pellegrino, A.; Mangano, S.; Free, G.; Pinardi, M. Application of New Hyperspectral Sensors in the Remote Sensing of Aquatic Ecosystem Health: Exploiting PRISMA and DESIS for Four Italian Lakes. *Resources* **2022**, *11*, 8. [[CrossRef](#)]
107. Wang, D.; Xing, S.; He, Y.; Yu, J.; Xu, Q.; Li, P. Evaluation of a New Lightweight UAV-Borne Topo-Bathymetric LiDAR for Shallow Water Bathymetry and Object Detection. *Sensors* **2022**, *22*, 1379. [[CrossRef](#)]
108. Gwon, Y.; Kwon, S.; Kim, D.; Seo, I.W.; You, H. Estimation of shallow stream bathymetry under varying suspended sediment concentrations and compositions using hyperspectral imagery. *Geomorphology* **2023**, *433*, 108722. [[CrossRef](#)]
109. Ji, X.; Ma, Y.; Zhang, J.; Xu, W.; Wang, Y. A Sub-Bottom Type Adaption-Based Empirical Approach for Coastal Bathymetry Mapping Using Multispectral Satellite Imagery. *Remote Sens.* **2023**, *15*, 3570. [[CrossRef](#)]

110. MacDonell, C.J.; Williams, R.D.; Maniatis, G.; Roberts, K.; Naylor, M. Consumer-grade UAV solid-state LiDAR accurately quantifies topography in a vegetated fluvial environment. *Earth Surf. Processes Landf.* **2023**, 1–19. [[CrossRef](#)]
111. Wang, Y.; Chen, Y.; Feng, Y.; Dong, Z.; Liu, X. Multispectral Satellite-Derived Bathymetry Based on Sparse Prior Measured Data. *Mar. Geod.* **2023**, 1–15. [[CrossRef](#)]
112. Niroumand-Jadidi, M.; Bovolo, F.; Vitti, A.; Bruzzone, L. A novel approach for bathymetry of shallow rivers based on spectral magnitude and shape predictors using stepwise regression. In *Image and Signal Processing for Remote Sensing XXIV*; Bruzzone, L., Bovolo, F., Benediktsson, J.A., Eds.; SPIE: Bellingham, WA, USA, 2018; p. 23.
113. Kuhwald, K.; Schneider von Deimling, J.; Schubert, P.; Oppelt, N. How can Sentinel-2 contribute to seagrass mapping in shallow, turbid Baltic Sea waters? *Remote Sens. Ecol. Conserv.* **2022**, *8*, 328–346. [[CrossRef](#)]
114. Fritz, K.M.; Schofield, K.A.; Alexander, L.C.; McManus, M.G.; Golden, H.E.; Lane, C.R.; Kepner, W.G.; LeDuc, S.D.; DeMeester, J.E.; Pollard, A.I. Physical and Chemical Connectivity of Streams and Riparian Wetlands to Downstream Waters: A Synthesis. *JAWRA J. Am. Water Resour. Assoc.* **2018**, *54*, 323–345. [[CrossRef](#)] [[PubMed](#)]
115. Xia, Y.; Fang, C.; Lin, H.; Li, H.; Wu, B. Spatiotemporal Evolution of Wetland Eco-Hydrological Connectivity in the Poyang Lake Area Based on Long Time-Series Remote Sensing Images. *Remote Sens.* **2021**, *13*, 4812. [[CrossRef](#)]
116. Dillon, J.W.; Lawrence, R.L.; Hammonds, K.D. Determining the Flow State of Channels Under Vegetation with Airborne Lidar. *Water Resour. Res.* **2023**, *59*. [[CrossRef](#)]
117. Legleiter, C.J.; Kinzel, P.J.; Laker, M.; Conaway, J.S. Moving Aircraft River Velocimetry (MARV): Framework and Proof-of-Concept on the Tanana River. *Water Resour. Res.* **2023**, *59*, 1–29. [[CrossRef](#)]
118. Toure, S.; Diop, O.; Kpalma, K.; Maiga, A. Shoreline Detection using Optical Remote Sensing: A Review. *ISPRS Int. J. Geo-Inf.* **2019**, *8*, 75. [[CrossRef](#)]
119. Kulp, S.A.; Strauss, B.H. New elevation data triple estimates of global vulnerability to sea-level rise and coastal flooding. *Nat. Commun.* **2019**, *10*, 4844. [[CrossRef](#)] [[PubMed](#)]
120. Li, X.; Yang, Y.; Ishizaka, J.; Li, X. Global estimation of phytoplankton pigment concentrations from satellite data using a deep-learning-based model. *Remote Sens. Environ.* **2023**, *294*, 113628. [[CrossRef](#)]
121. Wu, H. Journal of Geophysical Research: Oceans. *J. Geophys. Res. Ocean.* **2015**, 2813–2825.
122. Tomsett, C.; Leyland, J. Remote sensing of river corridors: A review of current trends and future directions. *River Res. Appl.* **2019**, *35*, 779–803. [[CrossRef](#)]
123. Zhang, H.; Yang, K.; Lou, X.; Li, Y.; Zheng, G.; Wang, J.; Wang, X.; Ren, L.; Li, D.; Shi, A. Observation of sea surface roughness at a pixel scale using multi-angle sun glitter images acquired by the ASTER sensor. *Remote Sens. Environ.* **2018**, *208*, 97–108. [[CrossRef](#)]
124. Kramer, G.; Filho, W.P.; de Carvalho, L.A.S.; Trindade, P.M.P.; da Rosa, C.N.; Dezordi, R. Performance and validation of water surface temperature estimates from Landsat 8 of the Itaipu Reservoir, State of Paraná, Brazil. *Environ. Monit. Assess.* **2023**, *195*, 137. [[CrossRef](#)] [[PubMed](#)]
125. Kottmeier, C.; Agnon, A.; Al-Halbouni, D.; Alpert, P.; Corsmeier, U.; Dahm, T.; Eshel, A.; Geyer, S.; Haas, M.; Holohan, E.; et al. New perspectives on interdisciplinary earth science at the Dead Sea: The DESERVE project. *Sci. Total Environ.* **2016**, *544*, 1045–1058. [[CrossRef](#)] [[PubMed](#)]
126. Taillade, T.; Engdahl, M.; Fernandez, D. Can We Retrieve Sea Surface Salinity with Polarimetric Radar Measurements? *IEEE Geosci. Remote Sens. Lett.* **2023**, *20*, 1–5. [[CrossRef](#)]
127. Dumas, J.; Gilbert, D. Comparison of SMOS, SMAP and In Situ Sea Surface Salinity in the Gulf of St. Lawrence. *Atmosphere-Ocean* **2023**, *61*, 148–161. [[CrossRef](#)]
128. Whitehead, P.G.; Wilby, R.L.; Battarbee, R.W.; Kernan, M.; Wade, A.J. A review of the potential impacts of climate change on surface water quality. *Hydrol. Sci. J.* **2009**, *54*, 101–123. [[CrossRef](#)]
129. Meyssignac, B.; Boyer, T.; Zhao, Z.; Hakuba, M.Z.; Landerer, F.W.; Stammer, D.; Köhl, A.; Kato, S.; L'Ecuyer, T.; Ablain, M.; et al. Measuring Global Ocean Heat Content to Estimate the Earth Energy Imbalance. *Front. Mar. Sci.* **2019**, *6*, 1–31. [[CrossRef](#)]
130. Gholizadeh, M.; Melesse, A.; Reddi, L. A Comprehensive Review on Water Quality Parameters Estimation Using Remote Sensing Techniques. *Sensors* **2016**, *16*, 1298. [[CrossRef](#)]
131. Lim, J.; Choi, M. Assessment of water quality based on Landsat 8 operational land imager associated with human activities in Korea. *Environ. Monit. Assess.* **2015**, *187*, 384. [[CrossRef](#)]
132. Laliberte, E.; Legendre, P. A distance-based framework for measuring functional diversity from multiple traits. *Ecology* **2010**, *91*, 299–305. [[CrossRef](#)]
133. Moser, G.A.O.; Piedras, F.R.; Oaquim, A.B.J.; Souza, D.S.; Leles, S.G.; de Lima, D.T.; Ramos, A.B.A.; Farias, C.d.O.; Fernandes, A.M. Tidal effects on phytoplankton assemblages in a near-pristine estuary: A trait-based approach for the case of a shallow tropical ecosystem in Brazil. *Mar. Ecol.* **2017**, *38*, e12450. [[CrossRef](#)]
134. Edwards, K.F.; Litchman, E.; Klausmeier, C.A. Functional traits explain phytoplankton community structure and seasonal dynamics in a marine ecosystem. *Ecol. Lett.* **2013**, *16*, 56–63. [[CrossRef](#)] [[PubMed](#)]
135. Abonyi, A.; Horváth, Z.; Ptačnik, R. Functional richness outperforms taxonomic richness in predicting ecosystem functioning in natural phytoplankton communities. *Freshw. Biol.* **2018**, *63*, 178–186. [[CrossRef](#)]
136. Berger, S.A.; Diehl, S.; Stibor, H.; Trommer, G.; Ruhlenstroth, M.; Wild, A.; Weigert, A.; Jäger, C.G.; Striebel, M. Water temperature and mixing depth affect timing and magnitude of events during spring succession of the plankton. *Oecologia* **2006**, *150*, 643–654. [[CrossRef](#)]

137. BERGER, S.A.; DIEHL, S.; STIBOR, H.; TROMMER, G.; RUHENSTROTH, M. Water temperature and stratification depth independently shift cardinal events during plankton spring succession. *Glob. Change Biol.* **2010**, *16*, 1954–1965. [[CrossRef](#)]
138. Aberle, N.; Malzahn, A.; Lewandowska, A.; Sommer, U. Some like it hot: The protozooplankton-copepod link in a warming ocean. *Mar. Ecol. Prog. Ser.* **2015**, *519*, 103–113. [[CrossRef](#)]
139. Reinl, K.L.; Harris, T.D.; North, R.L.; Almela, P.; Berger, S.A.; Bizic, M.; Burnet, S.H.; Grossart, H.; Ibelings, B.W.; Jakobsson, E.; et al. Blooms also like it cold. *Limnol. Oceanogr. Lett.* **2023**, *8*, 546–564. [[CrossRef](#)]
140. Joint, I.; Groom, S.B. Estimation of phytoplankton production from space: Current status and future potential of satellite remote sensing. *J. Exp. Mar. Biol. Ecol.* **2000**, *250*, 233–255. [[CrossRef](#)] [[PubMed](#)]
141. Vostokov, S.V.; Pautova, L.A.; Sahling, I.V.; Vostokova, A.S.; Gadzhiev, A.A.; Petherbridge, G.; Lobachev, E.N.; Abtahi, B.; Shojaei, M.G. Seasonal and Long-Term Phytoplankton Dynamics in the Middle Caspian According to Satellite Data and In Situ Observations in the First Decades of the 21st Century. *J. Mar. Sci. Eng.* **2023**, *11*, 957. [[CrossRef](#)]
142. Pahlevan, N.; Smith, B.; Binding, C.; Gurlin, D.; Li, L.; Bresciani, M.; Giardino, C. Hyperspectral retrievals of phytoplankton absorption and chlorophyll-a in inland and nearshore coastal waters. *Remote Sens. Environ.* **2021**, *253*, 112200. [[CrossRef](#)]
143. Zhu, Q.; Shen, F.; Shang, P.; Pan, Y.; Li, M. Hyperspectral Remote Sensing of Phytoplankton Species Composition Based on Transfer Learning. *Remote Sens.* **2019**, *11*, 2001. [[CrossRef](#)]
144. Burkholder, J.M.; Shumway, S.E.; Glibert, P.M. Food Web and Ecosystem Impacts of Harmful Algae. In *Harmful Algal Blooms*; Wiley: Hoboken, NJ, USA, 2018; pp. 243–336.
145. Matthews, M.W. Near-term forecasting of cyanobacteria and harmful algal blooms in lakes using simple univariate methods with satellite remote sensing data. *Int. Waters* **2023**, *13*, 62–73. [[CrossRef](#)]
146. Bunyon, C.L.; Fraser, B.T.; McQuaid, A.; Congalton, R.G. Using Imagery Collected by an Unmanned Aerial System to Monitor Cyanobacteria in New Hampshire, USA, Lakes. *Remote Sens.* **2023**, *15*, 2839. [[CrossRef](#)]
147. Hong, S.M.; Cho, K.H.; Park, S.; Kang, T.; Kim, M.S.; Nam, G.; Pyo, J. Estimation of cyanobacteria pigments in the main rivers of South Korea using spatial attention convolutional neural network with hyperspectral imagery. *GIScience Remote Sens.* **2022**, *59*, 547–567. [[CrossRef](#)]
148. Matthews, M.W.; Bernard, S.; Winter, K. Remote sensing of cyanobacteria-dominant algal blooms and water quality parameters in Zeekoevlei, a small hypertrophic lake, using MERIS. *Remote Sens. Environ.* **2010**, *114*, 2070–2087. [[CrossRef](#)]
149. Niroumand-Jadidi, M.; Bovolo, F. Deep-Learning-Based Retrieval of an Orange Band Sensitive to Cyanobacteria for Landsat-8/9 and Sentinel-2. *IEEE J. Sel. Top. Appl. Earth Obs. Remote Sens.* **2023**, *16*, 3929–3937. [[CrossRef](#)]
150. Hart, J.D.; Jenkins, D.G. Experimental disturbance and productivity gradients drive community diversity in aquatic mesocosms. *Ecol. Evol.* **2023**, *13*, 1–10. [[CrossRef](#)] [[PubMed](#)]
151. Asner, G.P.; Vaughn, N.R.; Heckler, J.; Knapp, D.E.; Balzotti, C.; Shafron, E.; Martin, R.E.; Neilson, B.J.; Gove, J.M. Large-scale mapping of live corals to guide reef conservation. *Proc. Natl. Acad. Sci. USA* **2020**, *117*, 33711–33718. [[CrossRef](#)] [[PubMed](#)]
152. Li, J.; Asner, G.P. Global analysis of benthic complexity in shallow coral reefs. *Environ. Res. Lett.* **2023**, *18*, 024038. [[CrossRef](#)]
153. Reynolds, C.S.; Huszar, V.; Kruk, C.; Naselli-Flores, L.; Melo, S. Towards a functional classification of the freshwater phytoplankton. *J. Plankton Res.* **2002**, *24*, 417–428. [[CrossRef](#)]
154. Weigel, B.; Kotamäki, N.; Malve, O.; Vuorio, K.; Ovaskainen, O. Macrosystem community change in lake phytoplankton and its implications for diversity and function. *Glob. Ecol. Biogeogr.* **2023**, *32*, 295–309. [[CrossRef](#)]
155. Machado, K.B.; Bini, L.M.; Melo, A.S.; Andrade, A.T.d.; Almeida, M.F.d.; Carvalho, P.; Teresa, F.B.; Roque, F.d.O.; Bortolini, J.C.; Padial, A.A.; et al. Functional and taxonomic diversities are better early indicators of eutrophication than composition of freshwater phytoplankton. *Hydrobiologia* **2023**, *850*, 1393–1411. [[CrossRef](#)]
156. Hedley, J.; Roelfsema, C.; Chollett, I.; Harborne, A.; Heron, S.; Weeks, S.; Skirving, W.; Strong, A.; Eakin, C.; Christensen, T.; et al. Remote Sensing of Coral Reefs for Monitoring and Management: A Review. *Remote Sens.* **2016**, *8*, 118. [[CrossRef](#)]
157. Collin, A.; Ramambason, C.; Pastol, Y.; Casella, E.; Rovere, A.; Thiault, L.; Espiau, B.; Siu, G.; Lerouvreur, F.; Nakamura, N.; et al. Very high resolution mapping of coral reef state using airborne bathymetric LiDAR surface-intensity and drone imagery. *Int. J. Remote Sens.* **2018**, *39*, 5676–5688. [[CrossRef](#)]
158. Zhong, J.; Li, M.; Zhang, H.; Qin, J. Fine-Grained 3D Modeling and Semantic Mapping of Coral Reefs Using Photogrammetric Computer Vision and Machine Learning. *Sensors* **2023**, *23*, 6753. [[CrossRef](#)] [[PubMed](#)]
159. Eakin, C.M.; Nim, C.; Brainard, R.; Aubrecht, C.; Elvidge, C.; Gledhill, D.; Muller-Karger, F.; Mumby, P.; Skirving, W.; Strong, A.; et al. Monitoring Coral Reefs from Space. *Oceanography* **2010**, *23*, 118–133. [[CrossRef](#)]
160. Dong, Y.; Liu, Y.; Hu, C.; Xu, B. Coral reef geomorphology of the Spratly Islands: A simple method based on time-series of Landsat-8 multi-band inundation maps. *ISPRS J. Photogramm. Remote Sens.* **2019**, *157*, 137–154. [[CrossRef](#)]
161. Chen, H.; Chu, S.; Zhuang, Q.; Duan, Z.; Cheng, J.; Li, J.; Ye, L.; Yu, J.; Cheng, L. FSPN: End-to-end full-space pooling weakly supervised network for benthic habitat mapping using remote sensing images. *Int. J. Appl. Earth Obs. Geoinf.* **2023**, *118*. [[CrossRef](#)]
162. Peterson, E.A.; Carne, L.; Balderamos, J.; Faux, V.; Gleason, A.; Schill, S.R. The Use of Unoccupied Aerial Systems (UASs) for Quantifying Shallow Coral Reef Restoration Success in Belize. *Drones* **2023**, *7*, 221. [[CrossRef](#)]
163. Barve, S.; Webster, J.M.; Chandra, R. Reef-Insight: A Framework for Reef Habitat Mapping with Clustering Methods Using Remote Sensing. *Information* **2023**, *14*, 373. [[CrossRef](#)]
164. Mumby, P.J.; Edwards, A.J. Mapping marine environments with IKONOS imagery: Enhanced spatial resolution can deliver greater thematic accuracy. *Remote Sens. Environ.* **2002**, *82*, 248–257. [[CrossRef](#)]

165. Li, A.S.; Chirayath, V.; Segal-Rozenhaimer, M.; Torres-Perez, J.L.; Van Den Bergh, J. NASA NeMO-Net's Convolutional Neural Network: Mapping Marine Habitats with Spectrally Heterogeneous Remote Sensing Imagery. *IEEE J. Sel. Top. Appl. Earth Obs. Remote Sens.* **2020**, *13*, 5115–5133. [[CrossRef](#)]
166. Zhang, Y.; Shen, F.; Sun, X.; Tan, K. Marine big data-driven ensemble learning for estimating global phytoplankton group composition over two decades (1997–2020). *Remote Sens. Environ.* **2023**, *294*, 113596. [[CrossRef](#)]
167. Ghirardi, N.; Bresciani, M.; Free, G.; Pinardi, M.; Bolpagni, R.; Giardino, C. Evaluation of Macrophyte Community Dynamics (2015–2020) in Southern Lake Garda (Italy) from Sentinel-2 Data. *Appl. Sci.* **2022**, *12*, 2693. [[CrossRef](#)]
168. Davies, B.F.R.; Gernez, P.; Geraud, A.; Oiry, S.; Rosa, P.; Zoffoli, M.L.; Barillé, L. Multi- and hyperspectral classification of soft-bottom intertidal vegetation using a spectral library for coastal biodiversity remote sensing. *Remote Sens. Environ.* **2023**, *290*, 113554. [[CrossRef](#)]
169. Lassalle, G.; Ferreira, M.P.; Cué La Rosa, L.E.; Del’Papa Moreira Scafutto, R.; de Souza Filho, C.R. Advances in multi- and hyperspectral remote sensing of mangrove species: A synthesis and study case on airborne and multisource spaceborne imagery. *ISPRS J. Photogramm. Remote Sens.* **2023**, *195*, 298–312. [[CrossRef](#)]
170. Pillodar, F.; Suson, P.; Aguilos, M.; Amparado, R. Mangrove Resource Mapping Using Remote Sensing in the Philippines: A Systematic Review and Meta-Analysis. *Forests* **2023**, *14*, 1080. [[CrossRef](#)]
171. Aranha, T.R.B.T.; Martinez, J.-M.; Souza, E.P.; Barros, M.U.G.; Martins, E.S.P.R. Remote Analysis of the Chlorophyll-a Concentration Using Sentinel-2 MSI Images in a Semiarid Environment in Northeastern Brazil. *Water* **2022**, *14*, 451. [[CrossRef](#)]
172. Loge, P.; Fonseca, E.; Silveira, A. Revista Brasileira de Geografia Física. *Rev. Bras. Geogr.* **2021**, *1*, 758–769.
173. Ogashawara, I.; Kiel, C.; Jechow, A.; Kohnert, K.; Ruhtz, T.; Grossart, H.P.; Hölker, F.; Nejtgaard, J.C.; Berger, S.A.; Wollrab, S. The use of sentinel-2 for chlorophyll-A spatial dynamics assessment: A comparative study on different lakes in northern Germany. *Remote Sens.* **2021**, *13*, 1542. [[CrossRef](#)]
174. Mohamed, H.M.; Khalil, M.T.; El-Zeiny, A.M.; Khalifa, N.; Kafrawy, S.B.E.; Emam, W.W.M. Trophic state and potential productivity assessment for Qaroun Lake using spatial techniques. *Environ. Monit. Assess.* **2023**, *195*, 987. [[CrossRef](#)] [[PubMed](#)]
175. Hu, M.; Ma, R.; Cao, Z.; Xiong, J.; Xue, K. Remote Estimation of Trophic State Index for Inland Waters Using Landsat-8 OLI Imagery. *Remote Sens.* **2021**, *13*, 1988. [[CrossRef](#)]
176. Pellegrino, A.; Fabbretto, A.; Bresciani, M.; de Lima, T.M.A.; Braga, F.; Pahlevan, N.; Brando, V.E.; Kratzer, S.; Gianinetto, M.; Giardino, C. Assessing the Accuracy of PRISMA Standard Reflectance Products in Globally Distributed Aquatic Sites. *Remote Sens.* **2023**, *15*, 2163. [[CrossRef](#)]
177. Piégay, H.; Arnaud, F.; Belletti, B.; Bertrand, M.; Bizzi, S.; Carbonneau, P.; Dufour, S.; Liébault, F.; Ruiz-Villanueva, V.; Slater, L. Remotely sensed rivers in the Anthropocene: State of the art and prospects. *Earth Surf. Processes Landf.* **2020**, *45*, 157–188. [[CrossRef](#)]
178. Linke, S.; Lehner, B.; Ouellet Dallaire, C.; Ariwi, J.; Grill, G.; Anand, M.; Beames, P.; Burchard-Levine, V.; Maxwell, S.; Moidu, H.; et al. Global hydro-environmental sub-basin and river reach characteristics at high spatial resolution. *Sci. Data* **2019**, *6*, 1–15. [[CrossRef](#)] [[PubMed](#)]
179. Dürr, H.H.; Laruelle, G.G.; van Kempen, C.M.; Slomp, C.P.; Meybeck, M.; Middelkoop, H. Worldwide Typology of Nearshore Coastal Systems: Defining the Estuarine Filter of River Inputs to the Oceans. *Estuaries Coasts* **2011**, *34*, 441–458. [[CrossRef](#)]
180. Ryznar, E.R.; Smith, L.L.; Hà, B.A.; Grier, S.R.; Fong, P. Functional trait variability supports the use of mean trait values and identifies resistance trade-offs for marine macroalgae. *J. Ecol.* **2023**, 1–15. [[CrossRef](#)]
181. Ao, S.; Chiu, M.-C.; Lin, X.; Cai, Q. Trait selection strategy for functional diversity in freshwater systems: A case framework of macroinvertebrates. *Ecol. Indic.* **2023**, *153*, 110450. [[CrossRef](#)]
182. Grime, J.P. Vegetation classification by reference to strategies. *Nature* **1974**, *250*, 26–31. [[CrossRef](#)]
183. Smith, T.M.; Shugart, H.H.; Woodward, F.I.; Burton, P.J. Plant Functional Types. In *Vegetation Dynamics & Global Change*; Springer: Boston, MA, USA, 1993; pp. 272–292.
184. Reynolds, C.S. Phytoplankton assemblages and their periodicity in stratifying lake systems. *Ecography* **1980**, *3*, 141–159. [[CrossRef](#)]
185. Hirata, T.; Hardman-Mountford, N.J.; Brewin, R.J.W.; Aiken, J.; Barlow, R.; Suzuki, K.; Isada, T.; Howell, E.; Hashioka, T.; Noguchi-Aita, M.; et al. Synoptic relationships quantified between surface Chlorophyll- a and diagnostic pigments specific to phytoplankton functional types. *Biogeosci. Discuss.* **2010**, *7*, 6675–6704.
186. Deng, L.; Zhao, J.; Zeng, X.; Cao, W. Evaluation of Satellite-Derived Size-Fractionated Phytoplankton Primary Production in the South China Sea. *IEEE Trans. Geosci. Remote Sens.* **2023**, *61*, 1–17. [[CrossRef](#)]
187. Ruescas, A.B.; Garcia-Jimenez, J.; Mueller, D.; Brockmann, C.; Amoros, J.; Stelzer, K. Study of ENMAP imagery for the application of methods for Phytoplankton Functional Types determination in coastal waters. In Proceedings of the EGU General Assembly 2023, Vienna, Austria, 24–28 April 2023; EGU23-8662. [[CrossRef](#)]
188. Aiken, J.; Hardman-Mountford, N.J.; Barlow, R.; Fishwick, J.; Hirata, T.; Smyth, T. Functional links between bioenergetics and bio-optical traits of phytoplankton taxonomic groups: An overarching hypothesis with applications for ocean colour remote sensing. *J. Plankton Res.* **2008**, *30*, 165–181. [[CrossRef](#)]
189. Kostadinov, T.S.; Robertson Lain, L.; Kong, C.E.; Zhang, X.; Maritorea, S.; Bernard, S.; Loisel, H.; Jorge, D.S.F.; Kochetkova, E.; Roy, S.; et al. Ocean color algorithm for the retrieval of the particle size distribution and carbon-based phytoplankton size classes using a two-component coated-sphere backscattering model. *Ocean Sci.* **2023**, *19*, 703–727. [[CrossRef](#)]

190. Schulien, J.A.; Della Penna, A.; Gaube, P.; Chase, A.P.; Haëntjens, N.; Graff, J.R.; Hair, J.W.; Hostetler, C.A.; Scarino, A.J.; Boss, E.S.; et al. Shifts in Phytoplankton Community Structure Across an Anticyclonic Eddy Revealed From High Spectral Resolution Lidar Scattering Measurements. *Front. Mar. Sci.* **2020**, *7*, 1–13. [[CrossRef](#)]
191. Mouw, C.B.; Hardman-Mountford, N.J.; Alvain, S.; Bracher, A.; Brewin, R.J.W.; Bricaud, A.; Ciotti, A.M.; Devred, E.; Fujiwara, A.; Hirata, T.; et al. A Consumer's Guide to Satellite Remote Sensing of Multiple Phytoplankton Groups in the Global Ocean. *Front. Mar. Sci.* **2017**, *4*. [[CrossRef](#)]
192. Lain, L.R.; Kravitz, J.; Matthews, M.; Bernard, S. Simulated Inherent Optical Properties of Aquatic Particles using The Equivalent Algal Populations (EAP) model. *Sci. Data* **2023**, *10*, 412. [[CrossRef](#)] [[PubMed](#)]
193. Kostadinov, T.S.; Cabré, A.; Vedantham, H.; Marinov, I.; Bracher, A.; Brewin, R.J.W.; Bricaud, A.; Hirata, T.; Hirawake, T.; Hardman-Mountford, N.J.; et al. Inter-comparison of phytoplankton functional type phenology metrics derived from ocean color algorithms and Earth System Models. *Remote Sens. Environ.* **2017**, *190*, 162–177. [[CrossRef](#)]
194. Haëntjens, N.; Boss, E.S.; Graff, J.R.; Chase, A.P.; Karp-Boss, L. Phytoplankton size distributions in the western North Atlantic and their seasonal variability. *Limnol. Oceanogr.* **2022**, *67*, 1865–1878. [[CrossRef](#)]
195. Mock, J. Auswirkungen des Hochwasserschutzes. In *Eine Einführung in die Umweltwissenschaften*; Böhm, H.R., Deneke, M., Eds.; Wissenschaftliche Buchgesellschaft: Darmstadt, Germany, 1992; pp. 176–196.
196. Selsam, P.; Bumberger, J.; Wellmann, T.; Pause, M.; Gey, R.; Borg, E.; Lausch, A. Ecosystem Integrity Remote Sensing—Modelling and Service Tool—ESIS/Imalys. *Remote Sens.* **2024**, *16*, 1139. [[CrossRef](#)]
197. Sun, D.; Pinker, R.T. Estimation of land surface temperature from a Geostationary Operational Environmental Satellite (GOES-8). *J. Geophys. Res.* **2003**, *108*. [[CrossRef](#)]
198. Sun, D.; Pinker, R.T. Retrieval of surface temperature from the MSG-SEVIRI observations: Part I. Methodology. *Int. J. Remote Sens.* **2007**, *28*, 5255–5272. [[CrossRef](#)]
199. Ling, F.; Foody, G.; Du, H.; Ban, X.; Li, X.; Zhang, Y.; Du, Y. Monitoring Thermal Pollution in Rivers Downstream of Dams with Landsat ETM+ Thermal Infrared Images. *Remote Sens.* **2017**, *9*, 1175. [[CrossRef](#)]
200. Tavares, M.H.; Cunha, A.H.F.; Motta-Marques, D.; Ruhoff, A.L.; Cavalcanti, J.R.; Fragoso, C.R.; Bravo, J.M.; Munar, A.M.; Fan, F.M.; Rodrigues, L.H.R. Comparison of methods to estimate lake-surface-water temperature using landsat 7 ETM+ and MODIS imagery: Case study of a large shallow subtropical lake in Southern Brazil. *Water* **2019**, *11*, 168. [[CrossRef](#)]
201. Dugdale, S.J.; Hannah, D.M.; Kelleher, C.A.; Malcolm, I.A.; Caldwell, S. Assessing the potential of drone - based thermal infrared imagery for quantifying river temperature heterogeneity. *Hydrol. Process.* **2019**, *33*, 1152–1163. [[CrossRef](#)]
202. Matsui, K.; Shirai, H.; Kageyama, Y.; Yokoyama, H.; Asano, M. Estimating water quality through neural networks using Terra ASTER data, water depth, and temperature of Lake Hachiroko, Japan. *Environ. Model. Softw.* **2023**, *159*, 105584. [[CrossRef](#)]
203. Fukushima, T.; Setiawan, F.; Subehi, L.; Jiang, D.; Matsushita, B. Water temperature and some water quality in Lake Toba, a tropical volcanic lake. *Limnology* **2023**, *24*, 61–69. [[CrossRef](#)]
204. Politi, E.; Cutler, M.E.J.; Rowan, J.S. Using the NOAA Advanced Very High Resolution Radiometer to characterise temporal and spatial trends in water temperature of large European lakes. *Remote Sens. Environ.* **2012**, *126*, 1–11. [[CrossRef](#)]
205. Pareeth, S.; Salmaso, N.; Adrian, R.; Neteler, M. Homogenised daily lake surface water temperature data generated from multiple satellite sensors: A long-term case study of a large sub-Alpine lake. *Sci. Rep.* **2016**, *6*, 31251. [[CrossRef](#)]
206. Stark, J.D.; Donlon, C.J.; Martin, M.J.; McCulloch, M.E. OSTIA: An operational, high resolution, real time, global sea surface temperature analysis system. In Proceedings of the OCEANS 2007-Europe, Aberdeen, UK, 18–21 June 2007; pp. 1–4.
207. Sima, S.; Ahmadalipour, A.; Tajrishy, M. Mapping surface temperature in a hyper-saline lake and investigating the effect of temperature distribution on the lake evaporation. *Remote Sens. Environ.* **2013**, *136*, 374–385. [[CrossRef](#)]
208. Eleveld, M.A.; Van der Wal, D.; Van Kessel, T. Estuarine suspended particulate matter concentrations from sun-synchronous satellite remote sensing: Tidal and meteorological effects and biases. *Remote Sens. Environ.* **2014**, *143*, 204–215. [[CrossRef](#)]
209. Gaube, P.; Chickadel, C.C.; Branch, R.; Jessup, A. Satellite Observations of SST-Induced Wind Speed Perturbation at the Oceanic Submesoscale. *Geophys. Res. Lett.* **2019**. [[CrossRef](#)]
210. Allan, M.G.; Hamilton, D.P.; Trolle, D.; Muraoka, K.; McBride, C. Spatial heterogeneity in geothermally-influenced lakes derived from atmospherically corrected Landsat thermal imagery and three-dimensional hydrodynamic modelling. *Int. J. Appl. Earth Obs. Geoinf.* **2016**, *50*, 106–116. [[CrossRef](#)]
211. Fricke, K.; Baschek, B. Water surface temperature profiles for the Rhine River derived from Landsat ETM+ data. In *Remote Sensing for Agriculture, Ecosystems, and Hydrology XV*; SPIE: Bellingham, WA, USA, 2013; Volume 8887.
212. Toming, K.; Kutser, T.; Uiboupin, R.; Arikas, A.; Vahter, K.; Paavel, B. Mapping Water Quality Parameters with Sentinel-3 Ocean and Land Colour Instrument imagery in the Baltic Sea. *Remote Sens.* **2017**, *9*, 1070. [[CrossRef](#)]
213. Shen, M.; Duan, H.; Cao, Z.; Xue, K.; Loisselle, S.; Yesou, H. Determination of the Downwelling Diffuse Attenuation Coefficient of Lake Water with the Sentinel-3A OLCI. *Remote Sens.* **2017**, *9*, 1246. [[CrossRef](#)]
214. Xue, K.; Ma, R.; Wang, D.; Shen, M. Optical Classification of the Remote Sensing Reflectance and Its Application in Deriving the Specific Phytoplankton Absorption in Optically Complex Lakes. *Remote Sens.* **2019**, *11*, 184. [[CrossRef](#)]
215. Bresciani, M.; Cazzaniga, I.; Austoni, M.; Sforzi, T.; Buzzi, F.; Morabito, G.; Giardino, C. Mapping phytoplankton blooms in deep subalpine lakes from Sentinel-2A and Landsat-8. *Hydrobiologia* **2018**, *3*, 31. [[CrossRef](#)]

216. Ha, N.T.T.; Thao, N.T.P.; Koike, K.; Nhuan, M.T. Selecting the Best Band Ratio to Estimate Chlorophyll-a Concentration in a Tropical Freshwater Lake Using Sentinel 2A Images from a Case Study of Lake Ba Be (Northern Vietnam). *ISPRS Int. J. Geo-Inf.* **2017**, *6*, 290. [[CrossRef](#)]
217. Toming, K.; Kutser, T.; Laas, A.; Sepp, M.; Paavel, B.; Nöges, T. First Experiences in Mapping Lake Water Quality Parameters with Sentinel-2 MSI Imagery. *Remote Sens.* **2016**, *8*, 640. [[CrossRef](#)]
218. Dörnhöfer, K.; Klinger, P.; Heege, T.; Oppelt, N. Multi-sensor satellite and in situ monitoring of phytoplankton development in a eutrophic-mesotrophic lake. *Sci. Total Environ.* **2018**, *612*, 1200–1214. [[CrossRef](#)]
219. Devred, E.; Turpie, K.R.; Moses, W.; Klemas, V.V.; Moisan, T.; Babin, M.; Toro-Farmer, G.; Forget, M.H.; Jo, Y.H. Future retrievals of water column bio-optical properties using the hyperspectral infrared imager (hyspirci). *Remote Sens.* **2013**, *5*, 6812–6837. [[CrossRef](#)]
220. Bresciani, M.; Giardino, C.; Lauceri, R.; Matta, E.; Cazzaniga, I.; Pinardi, M.; Lami, A.; Austoni, M.; Viaggiu, E.; Congestri, R.; et al. Earth observation for monitoring and mapping of cyanobacteria blooms. Case studies on five Italian lakes. *J. Limnol.* **2016**. [[CrossRef](#)]
221. Pamula, A.S.P.; Gholizadeh, H.; Krzmarzick, M.J.; Mausbach, W.E.; Lampert, D.J. A remote sensing tool for near real-time monitoring of harmful algal blooms and turbidity in reservoirs. *JAWRA J. Am. Water Resour. Assoc.* **2023**, 1–21. [[CrossRef](#)]
222. Pozdnyakov, D.; Shuchman, R.; Korosov, A.; Hatt, C. Operational algorithm for the retrieval of water quality in the Great Lakes. *Remote Sens. Environ.* **2005**, *97*, 352–370. [[CrossRef](#)]
223. Fiorani, L.; Angelini, F.; Artuso, F.; Cataldi, D.; Colao, F. Lidar Monitoring of Chlorophyll a During the XXIX and XXXI Italian Antarctic Expeditions. *Int. J. Environ. Res.* **2019**, *13*, 253–263. [[CrossRef](#)]
224. Giannini, F.; Hunt, B.P.V.; Jacoby, D.; Costa, M. Performance of OLCI Sentinel-3A satellite in the Northeast Pacific coastal waters. *Remote Sens. Environ.* **2021**, *256*, 112317. [[CrossRef](#)]
225. Moisan, J.R.; Moisan, T.A.H.; Linkswiler, M.A. An inverse modeling approach to estimating phytoplankton pigment concentrations from phytoplankton absorption spectra. *J. Geophys. Res. Ocean.* **2011**, *116*, 1–16. [[CrossRef](#)]
226. Yuras, G.; Ulloa, O.; Hormazabal, S. On the annual cycle of coastal and open ocean satellite chlorophyll off Chile (18°–40°s). *Geophys. Res. Lett.* **2005**, *32*, 1–4. [[CrossRef](#)]
227. Fahnenstiel, G.L.; Sayers, M.J.; Shuchman, R.A.; Yousef, F.; Pothoven, S.A. Lake-wide phytoplankton production and abundance in the Upper Great Lakes. *J. Great Lakes Res.* **2016**, *42*, 619–629. [[CrossRef](#)]
228. Luo, J.; Duan, H.; Ma, R.; Jin, X.; Li, F.; Hu, W.; Shi, K.; Huang, W. Mapping species of submerged aquatic vegetation with multi-seasonal satellite images and considering life history information. *Int. J. Appl. Earth Obs. Geoinf.* **2017**, *57*, 154–165. [[CrossRef](#)]
229. Behrenfeld, M.J.; Dall’Olmo, G.; Moore, J.K.; McClain, C.R.; Mahowald, N.; Milligan, A.J.; Doney, S.C.; O’Malley, R.T.; Boss, E.S.; Wiggert, J.D.; et al. Satellite-detected fluorescence reveals global physiology of ocean phytoplankton. *Biogeosciences* **2010**, *6*, 779–794. [[CrossRef](#)]
230. Philipson, P.; Kratzer, S.; Ben Mustapha, S.; Strömbeck, N.; Stelzer, K. Satellite-based water quality monitoring in Lake Vänern, Sweden. *Int. J. Remote Sens.* **2016**, *37*, 3938–3960. [[CrossRef](#)]
231. Palmer, S.C.J.; Odermatt, D.; Hunter, P.D.; Brockmann, C.; Présing, M.; Balzter, H.; Tóth, V.R. Satellite remote sensing of phytoplankton phenology in Lake Balaton using 10 years of MERIS observations. *Remote Sens. Environ.* **2015**, *158*, 441–452. [[CrossRef](#)]
232. Vander Woude, A.; Ruberg, S.; Johengen, T.; Miller, R.; Stuart, D. Spatial and temporal scales of variability of cyanobacteria harmful algal blooms from NOAA GLERL airborne hyperspectral imagery. *J. Great Lakes Res.* **2019**. [[CrossRef](#)]
233. Sharaf, N.; Bresciani, M.; Giardino, C.; Faour, G.; Slim, K.; Fadel, A. Using Landsat and in situ data to map turbidity as a proxy of cyanobacteria in a hypereutrophic Mediterranean reservoir. *Ecol. Inform.* **2019**, *50*, 197–206. [[CrossRef](#)]
234. Hoge, F.E.; Lyon, P.E.; Swift, R.N.; Yungel, J.K.; Abbott, M.R.; Letelier, R.M.; Esaias, W.E. Validation of Terra-MODIS phytoplankton chlorophyll fluorescence line height I Initial airborne lidar results. *Appl. Opt.* **2007**, *42*, 2767. [[CrossRef](#)] [[PubMed](#)]
235. Cai, X.; Li, Y.; Lei, S.; Zeng, S.; Zhao, Z.; Lyu, H.; Dong, X.; Li, J.; Wang, H.; Xu, J.; et al. A hybrid remote sensing approach for estimating chemical oxygen demand concentration in optically complex waters: A case study in inland lake waters in eastern China. *Sci. Total Environ.* **2023**, *856*, 158869. [[CrossRef](#)]
236. O’Shea, R.E.; Pahlevan, N.; Smith, B.; Bresciani, M.; Egerton, T.; Giardino, C.; Li, L.; Moore, T.; Ruiz-Verdu, A.; Ruberg, S.; et al. Advancing cyanobacteria biomass estimation from hyperspectral observations: Demonstrations with HICO and PRISMA imagery. *Remote Sens. Environ.* **2021**, *266*, 112693. [[CrossRef](#)]
237. Gray, A.; Krolkowski, M.; Fretwell, P.; Convey, P.; Peck, L.S.; Mendelova, M.; Smith, A.G.; Davey, M.P. Remote Sensing Phenology of Antarctic Green and Red Snow Algae Using WorldView Satellites. *Front. Plant Sci.* **2021**, *12*, 1–16. [[CrossRef](#)]
238. Ogashawara, I. The Use of Sentinel-3 Imagery to Monitor Cyanobacterial Blooms. *Environments* **2019**, *6*, 60. [[CrossRef](#)]
239. Alarcon, A.G.; German, A.; Aleksinko, A.; Ferreyra, M.F.G.; Scavuzzo, C.M.; Ferral, A. Spatial Algal Bloom Characterization by Landsat 8-Oli and Field Data Analysis. In Proceedings of the IGARSS 2018—2018 IEEE International Geoscience and Remote Sensing Symposium, Valencia, Spain, 22–27 July 2018; pp. 929–9295.
240. Bricaud, A.; Claustre, H.; Ras, J.; Oubelkheir, K. Natural variability of phytoplanktonic absorption in oceanic waters: Influence of the size structure of algal populations. *J. Geophys. Res. Oceans* **2004**, *109*, 1–12. [[CrossRef](#)]
241. Aiken, J.; Fishwick, J.R.; Lavender, S.; Barlow, R.; Moore, G.F.; Sessions, H.; Bernard, S.; Ras, J.; Hardman-Mountford, N.J. Validation of MERIS reflectance and chlorophyll during the BENCAL cruise October 2002: Preliminary validation of new

- demonstration products for phytoplankton functional types and photosynthetic parameters. *Int. J. Remote Sens.* **2007**, *28*, 497–516. [[CrossRef](#)]
242. Villa, P.; Pinardi, M.; Bresciani, M. Remote sensing of macrophyte morphological traits: Implications for the management of shallow lakes. *J. Limnol.* **2017**, *76*, 109–126. [[CrossRef](#)]
243. Heblinski, J.; Schmieder, K.; Heege, T.; Agyemang, T.K.; Sayadyan, H.; Vardanyan, L. High-resolution satellite remote sensing of littoral vegetation of Lake Sevan (Armenia) as a basis for monitoring and assessment. *Hydrobiologia* **2011**, *661*, 97–111. [[CrossRef](#)]
244. Fritz, C.; Dörnhöfer, K.; Schneider, T.; Geist, J.; Oppelt, N. Mapping Submerged Aquatic Vegetation Using RapidEye Satellite Data. *Water* **2017**, *9*, 510. [[CrossRef](#)]
245. Villa, P.; Pinardi, M.; Bolpagni, R.; Gillier, J.-M.; Zinke, P.; Nedelcuț, F.; Bresciani, M. Assessing macrophyte seasonal dynamics using dense time series of medium resolution satellite data. *Remote Sens. Environ.* **2018**, *216*, 230–244. [[CrossRef](#)]
246. Villa, P.; Bresciani, M.; Bolpagni, R.; Pinardi, M.; Giardino, C. A rule-based approach for mapping macrophyte communities using multi-temporal aquatic vegetation indices. *Remote Sens. Environ.* **2015**, *171*, 218–233. [[CrossRef](#)]
247. Yadav, S.; Yoneda, M.; Tamura, M.; Susaki, J.; Ishikawa, K.; Yamashiki, Y. A Satellite-Based Assessment of the Distribution and Biomass of Submerged Aquatic Vegetation in the Optically Shallow Basin of Lake Biwa. *Remote Sens.* **2017**, *9*, 966. [[CrossRef](#)]
248. Giardino, C.; Bresciani, M.; Valentini, E.; Gasperini, L.; Bolpagni, R.; Brando, V.E. Airborne hyperspectral data to assess suspended particulate matter and aquatic vegetation in a shallow and turbid lake. *Remote Sens. Environ.* **2015**, *157*, 48–57. [[CrossRef](#)]
249. Lesser, M.P.; Mobley, C.D. Bathymetry, water optical properties, and benthic classification of coral reefs using hyperspectral remote sensing imagery. *Coral Reefs* **2007**, *26*, 819–829. [[CrossRef](#)]
250. Wawrzyniak, V.; Piégay, H.; Allemand, P.; Vaudor, L. Prediction of water temperature heterogeneity of braided rivers using very high resolution thermal infrared (TIR) images. *Int. J. Remote Sens.* **2013**, *34*, 4812–4831. [[CrossRef](#)]
251. Wang, Y.; Wang, K.; Bai, Y.; Wu, D.; Zheng, H. Research progress in calculating net community production of marine ecosystem by remote sensing. *Front. Mar. Sci.* **2023**, *10*, 1–11. [[CrossRef](#)]
252. Wheaton, J.M.; Fryirs, K.A.; Brierley, G.; Bangen, S.G.; Bouwes, N.; O'Brien, G. Geomorphic mapping and taxonomy of fluvial landforms. *Geomorphology* **2015**, *248*, 273–295. [[CrossRef](#)]
253. Demarchi, L.; Bizzi, S.; Piégay, H. Regional hydromorphological characterization with continuous and automated remote sensing analysis based on VHR imagery and low-resolution LiDAR data. *Earth Surf. Processes Landf.* **2017**, *42*, 531–551. [[CrossRef](#)]
254. Pinheiro, M.; Amao-Oliva, J.; Scheiber, R.; Jaeger, M.; Horn, R.; Keller, M.; Fischer, J.; Reigber, A. Dual-frequency airborne SAR for large scale mapping of tidal flats. *Remote Sens.* **2020**, *12*, 1827. [[CrossRef](#)]
255. Mandlbürger, G.; Hauer, C.; Wieser, M.; Pfeifer, N. Topo-Bathymetric LiDAR for Monitoring River Morphodynamics and Instream Habitats—A Case Study at the Pielach River. *Remote Sens.* **2015**, *7*, 6160–6195. [[CrossRef](#)]
256. Husson, E.; Hagner, O.; Ecke, F. Unmanned aircraft systems help to map aquatic vegetation. *Appl. Veg. Sci.* **2014**, *17*, 567–577.
257. Hestir, E.L.; Brando, V.E.; Bresciani, M.; Giardino, C.; Matta, E.; Villa, P.; Dekker, A.G. Measuring freshwater aquatic ecosystems: The need for a hyperspectral global mapping satellite mission. *Remote Sens. Environ.* **2015**, *167*, 181–195. [[CrossRef](#)]
258. Kennedy, E.V.; Roelfsema, C.M.; Lyons, M.B.; Kovacs, E.M.; Borrego-Acevedo, R.; Roe, M.; Phinn, S.R.; Larsen, K.; Murray, N.J.; Yuwono, D.; et al. Reef Cover, a coral reef classification for global habitat mapping from remote sensing. *Sci. Data* **2021**, *8*, 1–20.
259. Traganos, D.; Reinartz, P. Interannual Change Detection of Mediterranean Seagrasses Using RapidEye Image Time Series. *Front. Plant Sci.* **2018**, *9*, 96. [[CrossRef](#)]
260. Kobryn, H.T.; Wouters, K.; Beckley, L.E.; Heege, T. Ningaloo Reef: Shallow Marine Habitats Mapped Using a Hyperspectral Sensor. *PLoS ONE* **2013**, *8*. [[CrossRef](#)]
261. Asner, G.P.; Vaughn, N.R.; Martin, R.E.; Foo, S.A.; Heckler, J.; Neilson, B.J.; Gove, J.M. Mapped coral mortality and refugia in an archipelago-scale marine heat wave. *Proc. Natl. Acad. Sci. USA* **2022**, *119*, 1–6. [[CrossRef](#)]
262. Li, J.; Knapp, D.E.; Fabina, N.S.; Kennedy, E.V.; Larsen, K.; Lyons, M.B.; Murray, N.J.; Phinn, S.R.; Roelfsema, C.M.; Asner, G.P. A global coral reef probability map generated using convolutional neural networks. *Coral Reefs* **2020**, *39*, 1805–1815. [[CrossRef](#)]
263. Lyons, M.B.; Roelfsema, C.M.; Kennedy, E.V.; Kovacs, E.M.; Borrego-Acevedo, R.; Markey, K.; Roe, M.; Yuwono, D.M.; Harris, D.L.; Phinn, S.R.; et al. Mapping the world's coral reefs using a global multiscale earth observation framework. *Remote Sens. Ecol. Conserv.* **2020**, *6*, 557–568.
264. Asner, G.P.; Vaughn, N.R.; Balzotti, C.; Brodrick, P.G.; Heckler, J. High-Resolution Reef Bathymetry and Coral Habitat Complexity from Airborne Imaging Spectroscopy. *Remote Sens.* **2020**, *12*, 310. [[CrossRef](#)]
265. Zhang, Y.; Zhang, Y.; Shi, K.; Zha, Y.; Zhou, Y.; Liu, M. A Landsat 8 OLI-Based, Semianalytical Model for Estimating the Total Suspended Matter Concentration in the Slightly Turbid Xin'anjiang Reservoir (China). *IEEE J. Sel. Top. Appl. Earth Obs. Remote Sens.* **2016**, *9*, 398–413. [[CrossRef](#)]
266. Hu, L.; Zeng, K.; Hu, C.; He, M. Remote Sensing of Environment On the remote estimation of *Ulva prolifera* areal coverage and biomass. *Remote Sens. Environ.* **2019**, *223*, 194–207. [[CrossRef](#)]
267. Luo, J.; Li, X.; Ma, R.; Li, F.; Duan, H.; Hu, W. Applying remote sensing techniques to monitoring seasonal and interannual changes of aquatic vegetation in Taihu Lake, China. *Ecol. Indic.* **2016**, *60*, 503–513. [[CrossRef](#)]
268. Rotta, L.H.S.; Mishra, D.R.; Watanabe, F.S.Y.; Rodrigues, T.W.; Alcântara, E.H.; Imai, N.N. Analyzing the feasibility of a spaceborne sensor (SPOT-6) to estimate the height of submerged aquatic vegetation (SAV) in inland waters. *ISPRS J. Photogramm. Remote Sens.* **2018**, *144*, 341–356. [[CrossRef](#)]

269. Doxaran, D.; Ehn, J.; Bélanger, S.; Matsuoaka, A.; Hooker, S.; Babin, M. Optical characterisation of suspended particles in the Mackenzie River plume (Canadian Arctic Ocean) and implications for ocean colour remote sensing. *Biogeosciences* **2012**, *9*, 3213–3229. [[CrossRef](#)]
270. Manzo, C.; Federica, B.; Luca, Z.; Ernesto, B.V.; Claudia, G.; Mariano, B.; Cristiana, B. Spatio-temporal analysis of prodelta dynamics by means of new satellite generation. *Int. J. Appl. Earth Obs. Geoinf.* **2018**, *66*, 210–225.
271. Lymburner, L.; Botha, E.; Hestir, E.; Anstee, J.; Sagar, S.; Dekker, A.; Malthus, T. Landsat 8: Providing continuity and increased precision for measuring multi-decadal time series of total suspended matter. *Remote Sens. Environ.* **2016**, *185*, 108–118. [[CrossRef](#)]
272. Sterckx, S.; Knaeps, E.; Bollen, M.; Trouw, K.; Houthuys, R. Retrieval of Suspended Sediment from Advanced Hyperspectral Sensor Data in the Scheldt Estuary at Different Stages in the Tidal Cycle. *Mar. Geod.* **2007**, *30*, 97–108. [[CrossRef](#)]
273. Shen, F.; Verhoef, W.; Zhou, Y.; Salama, M.S.; Liu, X. Satellite Estimates of Wide-Range Suspended Sediment Concentrations in Changjiang (Yangtze) Estuary Using MERIS Data. *Estuaries Coasts* **2010**, *33*, 1420–1429. [[CrossRef](#)]
274. Liu, H.; Li, Q.; Shi, T.; Hu, S.; Wu, G.; Zhou, Q. Application of Sentinel 2 MSI Images to Retrieve Suspended Particulate Matter Concentrations in Poyang Lake. *Remote Sens.* **2017**, *9*, 761. [[CrossRef](#)]
275. Kutser, T. The possibility of using the Landsat image archive for monitoring long time trends in coloured dissolved organic matter concentration in lake waters. *Remote Sens. Environ.* **2012**, *123*, 334–338. [[CrossRef](#)]
276. Li, J.; Yu, Q.; Tian, Y.Q.; Becker, B.L.; Siqueira, P.; Torbick, N. Spatio-temporal variations of CDOM in shallow inland waters from a semi-analytical inversion of Landsat-8. *Remote Sens. Environ.* **2018**, *218*, 189–200. [[CrossRef](#)]
277. Milewski, R.; Chabrilat, S.; Behling, R. Analyses of Recent Sediment Surface Dynamic of a Namibian Kalahari Salt Pan Based on Multitemporal Landsat and Hyperspectral Hyperion Data. *Remote Sens.* **2017**, *9*, 170. [[CrossRef](#)]
278. Fassoni-andrade, A.C.; Cauduro, R.; Paiva, D. De Remote Sensing of Environment Mapping spatial-temporal sediment dynamics of river-floodplains in the Amazon. *Remote Sens. Environ.* **2019**, *221*, 94–107. [[CrossRef](#)]
279. Nouchi, V.; Kutser, T.; Wüest, A.; Müller, B.; Odermatt, D.; Baracchini, T.; Bouffard, D. Resolving biogeochemical processes in lakes using remote sensing. *Aquat. Sci.* **2019**, *81*, 1–13. [[CrossRef](#)]
280. Heine, I.; Brauer, A.; Heim, B.; Itzerott, S.; Kasprzak, P.; Kienel, U.; Kleinschmit, B. Monitoring of calcite precipitation in hardwater lakes with multi-spectral remote sensing archives. *Water* **2017**, *9*, 15. [[CrossRef](#)]
281. Mu, Z.; Zhang, W.; Wang, P.; Wang, H.; Yang, X. Assimilation of SMOS Sea Surface Salinity in the Regional Ocean Model for South China Sea. *Remote Sens.* **2019**, *11*, 919. [[CrossRef](#)]
282. Dinnat, E.P.; Vine, D.M.L.; Boutin, J.; Meissner, T.; Lagerloef, G. Remote Sensing of Sea Surface Salinity: Comparison of Satellite and In Situ Observations and Impact of Retrieval Parameters. *Remote Sens.* **2019**, *11*, 750.
283. Wang, Y.; Heron, M.L.; Prytz, A.; Ridd, P.V.; Steinberg, C.R.; Hacker, J.M. Evaluation of a new airborne microwave remote sensing radiometer by measuring the salinity gradients across the shelf of the great barrier reef lagoon. *IEEE Trans. Geosci. Remote Sens.* **2007**, *45*, 3701–3710. [[CrossRef](#)]
284. Heron, M.L.; Ridd, P.V.; Prytz, A.; Wang, Y.; Hacker, J.M. Salinity gradients in coastal waters by airborne microwave radiometer remote sensing. In Proceedings of the Ocean 2006-Asia Pacific, Singapore, 16–19 May 2006. [[CrossRef](#)]
285. Liu, C.; Zhu, L.; Wang, J.; Ju, J.; Ma, Q.; Kou, Q. The decrease of salinity in lakes on the Tibetan Plateau between 2000 and 2019 based on remote sensing model inversions. *Int. J. Digit. Earth* **2023**, *16*, 2644–2659. [[CrossRef](#)]
286. Horion, S.; Bergamino, N.; Stenuite, S.; Descy, J.-P.; Plisnier, P.-D.; Loisele, S.A.; Cornet, Y. Optimized extraction of daily bio-optical time series derived from MODIS/Aqua imagery for Lake Tanganyika, Africa. *Remote Sens. Environ.* **2010**, *114*, 781–791. [[CrossRef](#)]
287. Binding, C.E.; Jerome, J.H.; Booty, W.G. Suspended particulate matter in Lake Erie derived from MODIS aquatic colour imagery. *Int. J. Remote Sens.* **2010**, *31*, 5239–5255. [[CrossRef](#)]
288. Heege, T.; Kiselev, V.; Wettle, M.; Hung, N.N. Operational multi-sensor monitoring of turbidity for the entire Mekong Delta. *Int. J. Remote Sens.* **2014**, *35*, 2910–2926. [[CrossRef](#)]
289. Braga, F.; Zaggia, L.; Bellafiore, D.; Bresciani, M.; Giardino, C.; Lorenzetti, G.; Maicu, F.; Manzo, C.; Riminucci, F.; Ravaioli, M.; et al. Mapping turbidity patterns in the Po river prodelta using multi-temporal Landsat 8 imagery. *Estuar. Coast. Shelf Sci.* **2017**, *198*, 555–567. [[CrossRef](#)]
290. Jiang, D.; Scholze, J.; Liu, X.; Simis, S.G.H.; Stelzer, K.; Müller, D.; Hunter, P.; Tyler, A.; Spyrakos, E. A data-driven approach to flag land-affected signals in satellite derived water quality from small lakes. *Int. J. Appl. Earth Obs. Geoinf.* **2023**, *117*, 103188. [[CrossRef](#)]
291. Grady, B.W.; Kittle, R.P.; Pugh, A.; Lamson, M.R.; Richards, J.L.; Fredericq, S.; McDermid, K.J.; Allen, Q.; Asner, G.P. Long-term ecological monitoring of reefs on Hawai'i Island (2003–2020): Characterization of a common cryptic crust, *Ramicrusta hawaiiensis* (Peyssonneliales, Rhodophyta). *Front. Mar. Sci.* **2022**, *9*, 1–16. [[CrossRef](#)]
292. Giardino, C.; Bresciani, M.; Cazzaniga, I.; Schenk, K.; Rieger, P.; Braga, F.; Matta, E.; Brando, V.E. Evaluation of Multi-Resolution Satellite Sensors for Assessing Water Quality and Bottom Depth of Lake Garda. *Sensors* **2014**, *14*, 24116–24131.
293. Hacker, J.M.; Pfennigbauer, M. Pushing Lidar to the Limits: High-resolution Bathymetric Lidar from Slow-flying Aircraft. *GIM Int.* **2017**, *31*, 29–31.
294. Uhl, F.; Bartsch, I.; Oppelt, N. Submerged Kelp Detection with Hyperspectral Data. *Remote Sens.* **2016**, *8*, 487. [[CrossRef](#)]
295. Legleiter, C.J.; Roberts, D.A.; Lawrence, R.L. Spectrally based remote sensing of river bathymetry. *EARTH Surf. Processes Landf.* **2009**, *1059*, 1039–1059. [[CrossRef](#)]

296. Li, J.; Knapp, D.E.; Lyons, M.; Roelfsema, C.; Phinn, S.; Schill, S.R.; Asner, G.P. Automated global shallowwater bathymetry mapping using google earth engine. *Remote Sens.* **2021**, *13*.
297. Xu, Y.; Cao, B.; Deng, R.; Cao, B.; Liu, H.; Li, J. Bathymetry over broad geographic areas using optical high-spatial-resolution satellite remote sensing without in-situ data. *Int. J. Appl. Earth Obs. Geoinf.* **2023**, *119*, 103308. [CrossRef]
298. Zhou, W.; Tang, Y.; Jing, W.; Li, Y.; Yang, J.; Deng, Y.; Zhang, Y. A Comparison of Machine Learning and Empirical Approaches for Deriving Bathymetry from Multispectral Imagery. *Remote Sens.* **2023**, *15*, 393. [CrossRef]
299. Li, S.; Wang, X.H.; Ma, Y.; Yang, F. Satellite-Derived Bathymetry with Sediment Classification Using ICESat-2 and Multispectral Imagery: Case Studies in the South China Sea and Australia. *Remote Sens.* **2023**, *15*, 1026. [CrossRef]
300. Marcello, J.; Eugenio, F.; Martín, J.; Marqués, F. Seabed Mapping in Coastal Shallow Waters Using High Resolution Multispectral and Hyperspectral Imagery. *Remote Sens.* **2018**, *10*, 1208. [CrossRef]
301. Dietrich, J.T. Bathymetric Structure-from-Motion: Extracting shallow stream bathymetry from multi-view stereo photogrammetry. *Earth Surf. Processes Landf.* **2017**, *42*, 355–364. [CrossRef]
302. Legleiter, C.J. Remote measurement of river morphology via fusion of LiDAR topography and spectrally based bathymetry. *Earth Surf. Processes Landf.* **2012**, *37*, 499–518. [CrossRef]
303. Legleiter, C.J.; Overstreet, B.T.; Glennie, C.L.; Pan, Z.; Fernandez-Diaz, J.C.; Singhania, A. Evaluating the capabilities of the CASI hyperspectral imaging system and Aquarius bathymetric LiDAR for measuring channel morphology in two distinct river environments. *Earth Surf. Processes Landf.* **2016**, *41*, 344–363. [CrossRef]
304. Gilvear, D.J.; Davids, C.; Tyler, A.N. The use of remotely sensed data to detect channel hydromorphology; River Tummel, Scotland. *River Res. Appl.* **2004**, *20*, 795–811. [CrossRef]
305. Emery, C.M.; Paris, A.; Biancamaria, S.; Boone, A.; Calmant, S.; Garambois, P.-A.; Santos da Silva, J. Large-scale hydrological model river storage and discharge correction using a satellite altimetry-based discharge product. *Hydrol. Earth Syst. Sci.* **2018**, *22*, 2135–2162. [CrossRef]
306. Ridolf, E.; Manciola, P. Water Level Measurements from Drones: A Pilot Case Study at a Dam Site. *Water* **2018**, *10*, 297. [CrossRef]
307. Hirpa, F.A.; Hopson, T.M.; De Groeve, T.; Brakenridge, G.R.; Gebremichael, M.; Restrepo, P.J. Upstream satellite remote sensing for river discharge forecasting: Application to major rivers in South Asia. *Remote Sens. Environ.* **2013**, *131*, 140–151. [CrossRef]
308. Tourian, M.J.; Sneeuw, N.; Bárdossy, A. A quantile function approach to discharge estimation from satellite altimetry (ENVISAT). *Water Resour. Res.* **2013**, *49*, 4174–4186. [CrossRef]
309. Donlon, C.; Berruti, B.; Buongiorno, A.; Ferreira, M.H.; Féménias, P.; Frerick, J.; Goryl, P.; Klein, U.; Laur, H.; Mavrocordatos, C.; et al. The Global Monitoring for Environment and Security (GMES) Sentinel-3 mission. *Remote Sens. Environ.* **2012**, *120*, 37–57. [CrossRef]
310. Schubert, M.; Scholten, J.; Schmidt, A.; Comanducci, J.F.; Pham, M.K.; Mallast, U.; Knoeller, K. Submarine groundwater discharge at a single spot location: Evaluation of different detection approaches. *Water* **2014**, *6*, 584–601. [CrossRef]
311. Oehler, T.; Eiche, E.; Putra, D.; Adyasari, D.; Hennig, H.; Mallast, U.; Moosdorf, N. Seasonal variability of land-ocean groundwater nutrient fluxes from a tropical karstic region (southern Java, Indonesia). *J. Hydrol.* **2018**, *565*. [CrossRef]
312. Kelly, J.L. Integration of aerial infrared thermography and in situ radon-222 to investigate submarine groundwater discharge to Pearl Harbor. *Limnol. Oceanogr.* **2019**, *238*–257. [CrossRef]
313. Tamborski, J.J.; Rogers, A.D.; Bokuniewicz, H.J.; Cochran, J.K.; Young, C.R. Identification and quantification of diffuse fresh submarine groundwater discharge via airborne thermal infrared remote sensing. *Remote Sens. Environ.* **2015**, *171*, 202–217. [CrossRef]
314. Lee, E.; Yoon, H.; Hyun, S.P.; Burnett, W.C.; Koh, D.C.; Ha, K.; Kim, D.J.; Kim, Y.; Kang, K.M. Unmanned aerial vehicles (UAVs)-based thermal infrared (TIR) mapping, a novel approach to assess groundwater discharge into the coastal zone. *Limnol. Oceanogr. Methods* **2016**, *14*, 725–735. [CrossRef]
315. Mallast, U.; Siebert, C. Combining continuous spatial and temporal scales for SGD investigations using UAV-based thermal infrared measurements. *Hydrol. Earth Syst. Sci.* **2019**, *23*, 1375–1392. [CrossRef]
316. Kang, Y.; Pan, D.; Bai, Y.; He, X.; Chen, X.; Chen, C.T.A.; Wang, D. Areas of the global major river plumes. *Acta Oceanol. Sin.* **2013**, *32*, 79–88. [CrossRef]
317. Purkis, S.J.; Klemas, V.V. *Remote Sensing and Global Environmental Change*; John Wiley & Sons: Hoboken, NJ, USA, 2013; ISBN 9781118687659.
318. Du, Y.; Feng, G.; Li, Z.; Peng, X.; Ren, Z.; Zhu, J. A Method for Surface Water Body Detection and DEM Generation with Multigeometry TanDEM-X Data. *IEEE J. Sel. Top. Appl. Earth Obs. Remote Sens.* **2018**, *12*, 1–11. [CrossRef]
319. Heine, I.; Francke, T.; Rogass, C.; Medeiros, P.H.A.; Bronstert, A.; Foerster, S. Monitoring seasonal changes in the water surface areas of reservoirs using terrasAR-X time series data in semiarid northeastern Brazil. *IEEE J. Sel. Top. Appl. Earth Obs. Remote Sens.* **2014**, *7*, 3190–3199. [CrossRef]
320. NASA/NGA SRTM Water Body Data Product Specific Guidance, Version 2.0. 2003. Available online: https://library.mcmaster.ca/maps/SWDB_Product_Specific_Guidance.pdf (accessed on 20 February 2019).
321. Yamazaki, D.; Trigg, M.A.; Ikeshima, D. Development of a global ~90m water body map using multi-temporal Landsat images. *Remote Sens. Environ.* **2015**, *171*, 337–351. [CrossRef]
322. Pekel, J.-F.; Cottam, A.; Gorelick, N.; Belward, A.S. High-resolution mapping of global surface water and its long-term changes. *Nature* **2016**, *540*, 418–422. [CrossRef] [PubMed]

323. Palmer, S.C.J.; Kutser, T.; Hunter, P.D. Remote sensing of inland waters: Challenges, progress and future directions. *Remote Sens. Environ.* **2015**, *157*, 1–8. [[CrossRef](#)]
324. Du, Y.; Zhang, Y.; Ling, F.; Wang, Q.; Li, W.; Li, X. Water Bodies' Mapping from Sentinel-2 Imagery with Modified Normalized Difference Water Index at 10-m Spatial Resolution Produced by Sharpening the SWIR Band. *Remote Sens.* **2016**, *8*, 354. [[CrossRef](#)]
325. Heine, I.; Stüve, P.; Kleinschmit, B.; Itzerott, S. Reconstruction of lake level changes of groundwater-fed lakes in Northeastern Germany using rapideye time series. *Water* **2015**, *7*, 4175–4199. [[CrossRef](#)]
326. Jawak, S.D.; Luis, A.J. Improved land cover mapping using high resolution multiangle 8-band WorldView-2 satellite remote sensing data. *J. Appl. Remote Sens.* **2013**, *7*, 73573. [[CrossRef](#)]
327. Liu, Y.; Zhang, P.; He, Y.; Peng, Z. River detection based on feature fusion from synthetic aperture radar images. *J. Appl. Remote Sens.* **2020**, *14*, 1. [[CrossRef](#)]
328. Allen, G.H.; Pavelsky, T. Global extent of rivers and streams. *Science* **2018**, *361*, 585–588. [[CrossRef](#)]
329. Bird, S.; Hogan, D.; Schwab, J. Photogrammetric monitoring of small streams under a riparian forest canopy. *Earth Surf. Processes Landf.* **2010**, *970*, 952–970. [[CrossRef](#)]
330. Bizzi, S.; Demarchi, L.; Grabowski, R.C.; Weissteiner, C.J. The use of remote sensing to characterise hydromorphological properties of European rivers. *Aquat. Sci.* **2016**, *78*, 57–70. [[CrossRef](#)]
331. Lorenz, R.D.; Lopes, R.M.; Paganelli, F.; Lunine, J.I.; Kirk, R.L.; Mitchell, K.L.; Soderblom, L.A.; Stofan, E.R.; Ori, G.; Myers, M.; et al. Fluvial channels on Titan: Initial Cassini RADAR observations. *Planet. Space Sci.* **2008**, *56*, 1132–1144. [[CrossRef](#)]
332. Smith, L.C.; Pavelsky, T.M. Estimation of river discharge, propagation speed, and hydraulic geometry from space: Lena River, Siberia. *Water Resour. Res.* **2008**, *44*, 1–11. [[CrossRef](#)]
333. Tarpanelli, A.; Brocca, L.; Barbetta, S.; Faruolo, M.; Lacava, T.; Moramarco, T. Coupling MODIS and Radar Altimetry Data for Discharge Estimation in Poorly Gauged River Basins. *IEEE J. Sel. Top. Appl. Earth Obs. Remote Sens.* **2015**, *8*, 141–148. [[CrossRef](#)]
334. Belletti, B.; Dufour, S.; Piégay, H. What is the Relative Effect of Space and Time to Explain the Braided River Width and Island Patterns at a Regional Scale? *River Res. Appl.* **2015**, *31*, 1–15. [[CrossRef](#)]
335. Finotello, A.; D'Alpaos, A.; Bogoni, M.; Ghinassi, M.; Lanzoni, S. Remotely-sensed planform morphologies reveal fluvial and tidal nature of meandering channels. *Sci. Rep.* **2020**, *10*, 1–13.
336. Naito, K.; Parker, G. Can Bankfull Discharge and Bankfull Channel Characteristics of an Alluvial Meandering River be Cospecified From a Flow Duration Curve? *J. Geophys. Res. Earth Surf.* **2019**, *124*, 2381–2401. [[CrossRef](#)]
337. Lallias-Tacon, S.; Liébault, F.; Piégay, H. Step by step error assessment in braided river sediment budget using airborne LiDAR data. *Geomorphology* **2014**, *214*, 307–323. [[CrossRef](#)]
338. Houser, C.; Hamilton, S. Morphodynamics of a 1000-year flood in the Kamp River, Austria, and impacts on floodplain morphology. *Earth Surf. Processes Landf.* **2009**, *34*, 613–628. [[CrossRef](#)]
339. Yang, C.; Cai, X.; Wang, X.; Yan, R.; Zhang, T.; Zhang, Q.; Lu, X. Remotely sensed trajectory analysis of channel migration in Lower Jingjiang Reach during the period of 1983–2013. *Remote Sens.* **2015**, *7*, 16241–16256. [[CrossRef](#)]
340. Peixoto, J.M.A.; Nelson, B.W.; Wittmann, F. Spatial and temporal dynamics of river channel migration and vegetation in central Amazonian white-water floodplains by remote-sensing techniques. *Remote Sens. Environ.* **2009**, *113*, 2258–2266. [[CrossRef](#)]
341. Dépret, T.; Riquier, J.; Piégay, H. Evolution of abandoned channels: Insights on controlling factors in a multi-pressure river system. *Geomorphology* **2017**, *294*, 99–118. [[CrossRef](#)]
342. Yang, X.; Damen, M.C.J.; Van Zuidam, R.A. Satellite remote sensing and GIS for the analysis of channel migration changes in the active Yellow River Delta, China. *ITC J.* **1999**, *1*, 146–157. [[CrossRef](#)]
343. Wen; Yang; Zhang; Shao; Wu Remotely Sensed Mid-Channel Bar Dynamics in Downstream of the Three Gorges Dam, China. *Remote Sens.* **2020**, *12*, 409. [[CrossRef](#)]
344. Garofalo, D. The Influence of Wetland Vegetation on Tidal Stream Channel Migration and Morphology. *Estuaries* **1980**, *3*, 258. [[CrossRef](#)]
345. Thomas, J.; Kumar, S.; Sudheer, K.P. Channel stability assessment in the lower reaches of the Krishna River (India) using multi-temporal satellite data during 1973–2015. *Remote Sens. Appl. Soc. Environ.* **2020**, *17*, 100274. [[CrossRef](#)]
346. Biron, P.M.; Choné, G.; Buffin-Bélanger, T.; Demers, S.; Olsen, T. Improvement of streams hydro-geomorphological assessment using LiDAR DEMs. *Earth Surf. Processes Landf.* **2013**, *38*, 1808–1821. [[CrossRef](#)]
347. Zakharova, E.; Nielsen, K.; Kamenev, G.; Kouraev, A. River discharge estimation from radar altimetry: Assessment of satellite performance, river scales and methods. *J. Hydrol.* **2020**, 124561. [[CrossRef](#)]
348. Perks, M.T.; Russell, A.J.; Large, A.R.G. Technical Note: Advances in flash flood monitoring using UAVs. *Hydrol. Earth Syst. Sci. Discuss.* **2016**, 1–18.
349. Wyrick, J.R.; Senter, A.E.; Pasternack, G.B. Revealing the natural complexity of fluvial morphology through 2D hydrodynamic delineation of river landforms. *Geomorphology* **2014**, *210*, 14–22. [[CrossRef](#)]
350. Brousse, G.; Arnaud-Fassetta, G.; Liébault, F.; Bertrand, M.; Melun, G.; Loire, R.; Malavoi, J.; Fantino, G.; Borgniet, L. Channel response to sediment replenishment in a large gravel-bed river: The case of the Saint-Sauveur dam in the Buëch River (Southern Alps, France). *River Res. Appl.* **2020**, *36*, 880–893. [[CrossRef](#)]
351. Bhattacharya, R.K.; Das Chatterjee, N.; Das, K. Impact of instream sand mining on habitat destruction or transformation using coupling models of HSI and MLR. *Spat. Inf. Res.* **2020**, *28*, 67–85. [[CrossRef](#)]

352. Heeren, D.M.; Mittelstet, A.R.; Fox, G.A.; Storm, D.E.; Al-Madhhachi, A.T.; Midgley, T.L.; Stringer, A.F.; Stunkel, K.B.; Tejral, R.D. Using Rapid Geomorphic Assessments to Assess Streambank Stability in Oklahoma Ozark Streams. *Trans. ASABE* **2012**, *55*, 957–968. [[CrossRef](#)]
353. Hamshaw, S.D.; Bryce, T.; Rizzo, D.M.; O’Neil-Dunne, J.; Frolik, J.; Dewoolkar, M.M. Quantifying streambank movement and topography using unmanned aircraft system photogrammetry with comparison to terrestrial laser scanning. *River Res. Appl.* **2017**, *33*, 1354–1367. [[CrossRef](#)]
354. Johansen, K.; Grove, J.; Denham, R.; Phinn, S. Assessing stream bank condition using airborne LiDAR and high spatial resolution image data in temperate semirural areas in Victoria, Australia. *J. Appl. Remote Sens.* **2013**, *7*, 073492. [[CrossRef](#)]
355. Resop, J.P.; Lehmann, L.; Hession, W.C. Drone Laser Scanning for Modeling Riverscape Topography and Vegetation: Comparison with Traditional Aerial Lidar. *Drones* **2019**, *3*, 35. [[CrossRef](#)]
356. Meinen, B.U.; Robinson, D.T. Streambank topography: An accuracy assessment of UAV-based and traditional 3D reconstructions. *Int. J. Remote Sens.* **2020**, *41*, 1–18. [[CrossRef](#)]
357. Micheli, E.R.; Kirchner, J.W. Effects of wet meadow riparian vegetation on streambank erosion. 1. Remote sensing measurements of streambank migration and erodibility. *Earth Surf. Processes Landf.* **2002**, *27*, 627–639. [[CrossRef](#)]
358. Vázquez-Tarrió, D.; Borgniet, L.; Liébault, F.; Recking, A. Using UAS optical imagery and SfM photogrammetry to characterize the surface grain size of gravel bars in a braided river (Vénéon River, French Alps). *Geomorphology* **2017**, *285*, 94–105. [[CrossRef](#)]
359. Carbonneau, P.E.; Bizzi, S.; Marchetti, G. Robotic photosieving from low-cost multirotor sUAS: A proof-of-concept. *Earth Surf. Process. Landforms* **2018**, *43*, 1160–1166. [[CrossRef](#)]
360. Carbonneau, P.E.; Dugdale, S.J.; Breckon, T.P.; Dietrich, J.D.; Fonstad, M.A.; Miyamoto, H.; Woodget, A.S. Generalised classification of hyperspatial resolution airborne imagery of fluvial scenes with deep convolutional neural networks. *Geophys. Res. Abstr.* **2019**, *21*, 1.
361. Carbonneau, P.E.; Lane, S.N.; Bergeron, N.E. Catchment-scale mapping of surface grain size in gravel bed rivers using airborne digital imagery. *Water Resour. Res.* **2004**, *40*. [[CrossRef](#)]
362. Rainey, M.; Tyler, A.; Gilvear, D.; Bryant, R.; McDonald, P. Mapping intertidal estuarine sediment grain size distributions through airborne remote sensing. *Remote Sens. Environ.* **2003**, *86*, 480–490. [[CrossRef](#)]
363. Cassel, M.; Piégay, H.; Fantino, G.; Lejot, J.; Bultingaire, L.; Michel, K.; Perret, F. Comparison of ground-based and UAV a-UHF artificial tracer mobility monitoring methods on a braided river. *Earth Surf. Processes Landf.* **2020**, *45*, 1123–1140. [[CrossRef](#)]
364. Barale, V. Environmental Remote Sensing of the Mediterranean Sea. *J. Environ. Sci. Health Part A* **2003**, *38*, 1681–1688. [[CrossRef](#)] [[PubMed](#)]
365. Kaliraj, S.; Chandrasekar, N.; Ramachandran, K.K. Mapping of coastal landforms and volumetric change analysis in the south west coast of Kanyakumari, South India using remote sensing and GIS techniques. *Egypt. J. Remote Sens. Space Sci.* **2017**, *20*, 265–282. [[CrossRef](#)]
366. Dang, K.B.; Dang, V.B.; Bui, Q.T.; Nguyen, V.V.; Pham, T.P.N.; Ngo, V.L. A Convolutional Neural Network for Coastal Classification Based on ALOS and NOAA Satellite Data. *IEEE Access* **2020**, *8*, 11824–11839. [[CrossRef](#)]
367. Boak, E.H.; Turner, I.L. Shoreline Definition and Detection: A Review. *J. Coast. Res.* **2005**, *214*, 688–703. [[CrossRef](#)]
368. Moore, L.J.; Griggs, G.B. Long-term cliff retreat and erosion hotspots along the central shores of the Monterey Bay National Marine Sanctuary. *Mar. Geol.* **2002**, *181*, 265–283. [[CrossRef](#)]
369. Valderrama-Landeros, L.; Blanco y Correa, M.; Flores-Verdugo, F.; Álvarez-Sánchez, L.F.; Flores-de-Santiago, F. Spatiotemporal shoreline dynamics of Marismas Nacionales, Pacific coast of Mexico, based on a remote sensing and GIS mapping approach. *Environ. Monit. Assess.* **2020**, *192*. [[CrossRef](#)] [[PubMed](#)]
370. Kanwal, S.; Ding, X.; Sajjad, M.; Abbas, S. Three Decades of Coastal Changes in Sindh, Pakistan (1989–2018): A Geospatial Assessment. *Remote Sens.* **2019**, *12*, 8. [[CrossRef](#)]
371. Ford, M.R.; Dickson, M.E. Detecting ebb-tidal delta migration using Landsat imagery. *Mar. Geol.* **2018**, *405*, 38–46. [[CrossRef](#)]
372. Marghany, M.; Sabu, Z.; Hashim, M. Mapping coastal geomorphology changes using synthetic aperture radar data. *Int. J. Phys. Sci.* **2010**, *5*, 1890–1896.
373. Shu, Y.; Li, J.; Gomes, G. Shoreline Extraction from RADARSAT-2 Intensity Imagery Using a Narrow Band Level Set Segmentation Approach. *Mar. Geod.* **2010**, *33*, 187–203. [[CrossRef](#)]
374. Elnabwy, M.T.; Elbeltagi, E.; El Banna, M.M.; Elshikh, M.M.Y.; Motawa, I.; Kaloop, M.R. An approach based on landsat images for shoreline monitoring to support integrated coastal management—A case study, ezbet elborg, nile delta, Egypt. *ISPRS Int. J. Geo-Inf.* **2020**, *9*, 199. [[CrossRef](#)]
375. Dong, P.; Chen, Q. *LiDAR Remote Sensing and Its Applications*; CRC Press, Taylor & Francis Group: Boca Raton, FL, USA, 2018; ISBN 978-1-4822-4301-7.
376. Voudoukas, M.I.; Ranasinghe, R.; Mentaschi, L.; Plomaritis, T.A.; Athanasiou, P.; Luijendijk, A.; Feyen, L. Sandy coastlines under threat of erosion. *Nat. Clim. Change* **2020**, *10*, 260–263. [[CrossRef](#)]
377. Seidel, M.; Hutengs, C.; Oertel, F.; Schwefel, D.; Jung, A.; Vohland, M. Underwater Use of a Hyperspectral Camera to Estimate Optically Active Substances in the Water Column of Freshwater Lakes. *Remote Sens.* **2020**, *12*, 1745. [[CrossRef](#)]

-
378. Lyu, L.; Song, K.; Wen, Z.; Liu, G.; Shang, Y.; Li, S.; Tao, H.; Wang, X.; Hou, J. Estimation of the lake trophic state index (TSI) using hyperspectral remote sensing in Northeast China. *Opt. Express* **2022**, *30*, 10329. [[CrossRef](#)] [[PubMed](#)]
379. Morrow, R.; Fu, L.-L.; Rio, M.-H.; Ray, R.; Prandi, P.; Le Traon, P.-Y.; Benveniste, J. Ocean Circulation from Space. *Surv. Geophys.* **2023**, *44*, 1243–1286. [[CrossRef](#)]

Disclaimer/Publisher’s Note: The statements, opinions and data contained in all publications are solely those of the individual author(s) and contributor(s) and not of MDPI and/or the editor(s). MDPI and/or the editor(s) disclaim responsibility for any injury to people or property resulting from any ideas, methods, instructions or products referred to in the content.